

**SUPRAMOLECULAR STRUCTURES OF
FOUR-COORDINATE NICKEL NITROSYL
BIS(TRIPHENYLPHOSPHINE) COMPLEXES**

Miss Angkana Kiatpichitpong

**A Thesis Submitted in Partial Fulfillment of the Requirements
for the Degree of Master of Science in Chemistry
Suranaree University of Technology
Academic Year 2002
ISBN 974-533-170-8**

โครงสร้างซูปรามอเลกุลาร์ของสารประกอบเชิงซ้อน
สี่โคออร์ดิเนตนิเกิลในโตรซิดบิสไตรฟีนิลฟอสฟีน

นางสาวอังคณา เกียรติพิชิตพงษ์

วิทยานิพนธ์นี้เป็นส่วนหนึ่งของการศึกษาตามหลักสูตรปริญญาวิทยาศาสตรมหาบัณฑิต

สาขาวิชาเคมี

มหาวิทยาลัยเทคโนโลยีสุรนารี

ปีการศึกษา 2545

ISBN 974-533-170-8

**SUPRAMOLECULAR STRUCTURES OF FOUR-COORDINATE NICKEL
NITROSYL BIS(TRIPHENYLPHOSPHINE) COMPLEXES**

**Suranaree University of Technology Council has approved this thesis,
submitted in partial fulfillment of the requirements for a Master's Degree.**

Thesis Examining Committee

.....
(Asst. Prof. Dr. Malee Tangsathitkulchai)
Chairman

.....
(Assoc. Prof. Dr. Kenneth J. Haller)
Thesis Advisor

.....
(Asst. Prof. Dr. Kunwadee Rangsiwatananon)
Member

.....
(Assoc. Prof. Dr. Tawit Chitsomboon)
Vice Rector for Academic Affairs

.....
(Assoc. Prof. Dr. Prasart Suebka)
Dean of the Institute of Science

อังคณา เกียรติพิชิตพงษ์: โครงสร้างซูปราโมเลคิวลาร์ของสารประกอบเชิงซ้อน ลิโคออร์ดินเตนิกไนโตรซิลบิสไตรฟีนิลฟอสฟีน

(SUPRAMOLECULAR STRUCTURES OF FOUR-COORDINATE NICKEL NITROSYL
BIS(TRIPHENYLPHOSPHINE) COMPLEXES)

อาจารย์ที่ปรึกษา : รศ. ดร. เค็นเนท เจ. แสลดอร์, 102 หน้า. ISBN 974-533-170-8

โครงสร้างผลึกของ $Ni(X)(NO)(P(C_6H_5)_3)_2$ ได้ถูกวิเคราะห์ในเทอมของอันตรกิริยาของซูปราโมเลคิวลาร์ของการเกาะกันของฟีนิลจำนวนมาก ทำให้เพิ่มความเข้าใจโครงสร้างทางเคมีของผลึกนี้ ซึ่งส่วนหนึ่งของกลุ่มซูปราโมเลคิวลาร์เกี่ยวข้องกับอันตรกิริยาการแบบคิงคูดระหว่างฟีนิลซึ่งสามารถเกิดอันตรกิริยารวมกันแบบ face-to-face (*off*) stacking ระหว่างไฮโดรเจนอะตอมและระบบ π ของวงอะโรเมติกข้างเคียง และแบบ edge-to-edge (*ef*) เป็น “herringbone” stacking ระหว่างไฮโดรเจนอะตอมของกลุ่ม C-H ของวงฟีนิลหนึ่งและระบบ π ของวงฟีนิลอีกวงหนึ่ง อันตรกิริยาแบบ *off* หรือ *ef* มีพลังงานเพียง 2-3 kcal/mole โดยทั่วไปฟีนิล 6 วงของไตรฟีนิลฟอสฟีน (TPP) ลิแกนด์ที่อยู่ใกล้กันสามารถที่จะจัดตัวโดยเกิดอันตรกิริยาแบบ *ef* มีจำนวน 6 ลักษณะโดยสลับกันไปจากลิแกนด์ A ไปลิแกนด์ B, จาก B ไป A, จาก A ไป B สลับกันไป การเกาะรวมกันของวงฟีนิลจำนวน 6 วง six fold phenyl embrace (6PE) เป็นรูปแบบที่มีแนวโน้มทำให้อันตรกิริยาระหว่างโมเลกุลแข็งแรงที่สุดในโมเลกุลผลึก เมื่อบางฟีนิลจาก TPP ของ 2 ลิแกนด์มีการจัดโครงสร้างแบบ C_3 ซึ่งสัมพันธ์กับ inversion center ทำให้เกิด 6PE ซึ่งอันตรกิริยาของโครงสร้างซูปราโมเลคิวลาร์ถูกพิสูจน์โดยการคำนวณระยะทางและมุมพร้อมทั้งทำการตรวจสอบด้วยกราฟิกของทั้งโมเลกุลและส่วนต่างๆของโมเลกุล สำหรับ 6PE พิสูจน์จากระยะทางระหว่างอะตอมของฟอสฟอรัสแต่ละโมเลกุลโดยที่ $d[P \cdots P] < 8 \text{ \AA}$ และ $\angle[M-P \cdots P-M]$ อยู่ในแนวเดียวกันในช่วง $160-180^\circ$

อันตรกิริยาเพิ่มเติมระหว่างโมเลกุลที่อาจจะเกิดขึ้นได้ถูกพิสูจน์โดยการคำนวณระยะทางระหว่างโมเลกุลไปยังตำแหน่งของไฮโดรเจนอะตอม (edge-to-face contacts) คาร์บอนอะตอมของฟีนิล (face-to-face contacts) และ hydrogen bond acceptors สำหรับ nonbonded อื่น ๆ เมื่อพิจารณาถึงระยะสัมผัสของวง $C \cdots H < 3.4 \text{ \AA}$ ได้ถูกตรวจสอบด้วยกราฟิกเพื่อที่จะบ่งบอกถึงการสัมผัสแบบ face-to-face ส่วนระยะสัมผัสของวง $C \cdots H < 3.2 \text{ \AA}$ ที่เหลือก็จะถูกตรวจสอบเพื่อบ่งชี้ว่าเป็นการสัมผัสแบบ edge-to-face contacts หรือแบบ van der Waals edge-to-edge contacts

อันตรกิริยาแบบคิงคูดของ $C-H \cdots \pi$ แบบ *ef* ของ ฟีนิล-ฟีนิลที่เกี่ยวข้องกับ 6PE มีพลังงานอันตรกิริยาที่มากเพียงพอที่ทำให้เกิดเป็นกลุ่มซูปราโมเลคิวลาร์หลักสำหรับสารประกอบเชิงซ้อน TPP ในสารประกอบเชิงซ้อน $Ni(X)(NO)(P(C_6H_5)_3)_2$ ซึ่ง X เป็น NCS^- , N_3^- หรือ Cl^- ที่ต้องการศึกษามีความคล้ายคลึงกันแต่มีโครงสร้างซูปราโมเลคิวลาร์ที่มีความแตกต่างกัน

สำหรับสารประกอบเชิงซ้อน isothiocyanato คาดว่ามีอันตรกิริยาที่ต่อเนื่อง 6PE ระหว่างลิแกนด์ TPP ข้างเคียงซึ่งเกิดขึ้นภายในแถวเดียวกันสลับกันไปโดยมี $d[P \cdots P] = 7.087 \text{ \AA}$, colinearity = 176.9° และ $d[P \cdots P] = 7.246 \text{ \AA}$, colinearity = 173° ของ 6PE ในระหว่างแถวเชื่อมกัน

ด้วยอันตรกิริยาของวงฟีนิลจำนวน 4 วงที่อยู่ในบริเวณใกล้เคียงกันทำให้เกิดเป็นชั้นของสารประกอบโดยอันตรกิริยาของ C-H... π แบบ *ef* และในระหว่างชั้นเชื่อมกันด้วยอันตรกิริยาของไนโตรซิล-ฟีนิลและฟีนิล-ฟีนิล

สารประกอบเชิงซ้อน chloro ประกอบด้วยเบนซีนโซเวตซึ่งสามารถเห็นได้ว่าเบนซีนวางอยู่ในโพรง ด้วยปลายข้างหนึ่งสอดเข้าไปในรอยแยกของ bis-TPP nickel fragment ที่ตั้งอยู่บน pseudo two-fold axis ทำให้เกิดอันตรกิริยาแบบ *ef* จากเบนซีนไปสารประกอบและจากสารประกอบไปเบนซีนในแต่ละ TPP ลิแกนด์ และที่บริเวณตรงกลางของโพรงจะถูกยึดไว้ด้วยอันตรกิริยาของ *ef* จำนวน 6 อันตรกิริยา และมีการเกิดโพรงอย่างสมบูรณ์โดยลิแกนด์ของคลอโรและไนโตรซิลของอีกโมเลกุลหนึ่ง ดังนั้นเบนซีนสามารถที่จะเกิดอันตรกิริยาของ C-H... π ได้มากกว่าจึงเป็นอันตรกิริยาหลักในการเชื่อมระหว่างโมเลกุลรอบๆรวมทั้งอันตรกิริยาของ 6PE ของโครงสร้างซูปราโมเลคิวลาร์ของสารประกอบเชิงซ้อน chloro

สารประกอบเชิงซ้อน azido มีระยะของ P...P ที่สั้นที่สุดเป็น 7.411 และ 7.825 Å, colinearity 86.9 และ 117° แต่ไม่เกิดอันตรกิริยาของ 6PE ซึ่งอันตรกิริยาของ nonbonded ที่แข็งแรงที่สุดเป็นอันตรกิริยา ภายในโมเลกุลของ C-H... π ที่ lone pair ของไนโตรเจนที่เกาะกับนิเกิลเป็นการทำลาย pseudo three-fold symmetry ของ TPP ลิแกนด์ของอีกลิแกนด์หนึ่งขณะที่อันตรกิริยา C-H... π ของ TPP ลิแกนด์อื่นกับ π cloud ของ azido ก็เกิดเป็นอันตรกิริยาที่แข็งแรงแบบภายในโมเลกุลด้วย ดังนั้นทั้งสองอันตรกิริยาจึงเป็นไปได้ที่จะรบกวนการเกิด 6PE และความแข็งแรงที่สุดของ hydrogen bond acceptor ของ azido ลิแกนด์กลายเป็นส่วนที่สำคัญที่กำหนดโครงสร้างซูปราโมเลคิวลาร์ของสารประกอบเชิงซ้อน azido

สาขาวิชาเคมี
ปีการศึกษา 2545

ลายมือชื่อนักศึกษา
ลายมือชื่ออาจารย์ที่ปรึกษา
ลายมือชื่ออาจารย์ที่ปรึกษาร่วม
ลายมือชื่ออาจารย์ที่ปรึกษาร่วม

ANGKANA KIATPICHITPONG: SUPRAMOLECULAR STRUCTURES OF FOUR-COORDINATE NICKEL NITROSYL BIS(TRIPHENYLPHOSPHINE) COMPLEXES

THESIS ADVISOR: ASSOCIATE PROFESSOR KENNETH J. HALLER, Ph.D.,
102 PP. ISBN 974-533-170-8

Crystal structures of $\text{Ni}(\text{X})(\text{NO})(\text{P}(\text{C}_6\text{H}_5)_3)_2$ have been analyzed in terms of the supramolecular interaction of multiphenyl embraces to increase understanding of their structural chemistry. One type of supramolecular motif is the concerted attractive directional interaction between phenyl rings which are able to engage in offset face-to-face (*off*) stacking interactions between ring hydrogen atoms and the π system of the adjacent aromatic ring and in the edge-to-face (*ef*) “herringbone” stacking interactions between hydrogen atoms of the C–H groups of one ring and the π system of another. An individual *off* or *ef* interaction is only a few kcal/mole. In the most common motif the six phenyl groups of two adjacent triphenylphosphine (TPP) ligands can arrange such that there are six concerted *ef* interactions alternating from ligand A to ligand B, B to A, A to B, *etc.* The concerted six fold phenyl embrace (6PE) thus formed will often be the strongest intermolecular interaction in a molecular crystal. Sextuple phenyl embraces result when the phenyl rings of two TPP ligands are arranged in interlocking C_3 propeller configurations, usually related by an inversion center. The supramolecular structure interactions were identified by a combination of distance and angle calculations along with examination of graphical images of molecules and fragments of molecules. Six-fold phenyl embraces are characterized by intermolecular $d[\text{P}\cdots\text{P}] < 8 \text{ \AA}$ and $\angle[\text{M}-\text{P}\cdots\text{P}-\text{M}]$ colinearity in the range $160-180^\circ$.

Additional potential intermolecular contacts were identified by calculating contact distances to the idealized hydrogen atom positions (edge-to-face contacts), to the phenyl carbon atoms (face-to-face contacts), and to the hydrogen bond acceptors for other nonbonded contacts. Ring $\text{C}\cdots\text{H}$ contact distances less than 3.4 \AA were examined graphically to determine if they were face-to-face contacts. Remaining ring $\text{C}\cdots\text{H}$ contact distances less than 3.2 \AA were examined to determine if they were edge-to-face contacts or van der Waals edge-to-edge contacts.

The multiple phenyl-phenyl edge-to-face (*ef*) $\text{C}-\text{H}\cdots\pi$ attractive interactions of the concerted 6PE give a sum of interaction energy sufficient to make it a dominant supramolecular motif for TPP complexes. The title complexes $\text{Ni}(\text{X})(\text{NO})(\text{P}(\text{C}_6\text{H}_5)_3)_2$, with $\text{X} = \text{NCS}^-$, N_3^- , or Cl^- ; while closely related have quite different supramolecular structures.

The primary extended interactions in the isothiocyanato complex are the expected 6PE between adjacent TPP ligands which occur in parallel chains made up of alternating; $d[\text{P}\cdots\text{P}] = 7.087 \text{ \AA}$, colinearity = 176.9° and $d[\text{P}\cdots\text{P}] = 7.246 \text{ \AA}$, colinearity = 173.0° , 6PE. Adjacent chains are joined by four phenyl ring regions to form layers dominated by *ef* $\text{C}-\text{H}\cdots\pi$ interactions. Layers are joined together by nitrosyl-phenyl and phenyl-phenyl interactions.

The chloro complex contains a benzene solvate which can be viewed as lying within a cavity with one end inserted into the cleft of a bis-TPP nickel fragment

located on a pseudo two-fold axis utilizing one complex-to-benzene *ef* and one benzene-to-complex *ef* interaction to each of the TPP ligands. The central region of the cavity is occupied by six additional *ef* interactions, and the cavity is completed by the chloro and nitrosyl ligands of another molecule. Thus, the benzene molecule, able to form considerably more C–H \cdots π interactions, becomes the major link between surrounding molecules. 6PE also contribute to the supramolecular structure.

The shortest intermolecular P \cdots P distances in the azido complex are 7.411 Å and 7.825 Å with colinearities of 86.9° and 117.7°, thus not 6PE. The strongest nonbonded interaction is a 2.493 Å *intramolecular* C–H \cdots π interaction to the lone pair on the N bonded to Ni destroying the pseudo three-fold symmetry of one TPP ligand, while another strong *intramolecular* C–H \cdots π interaction to the azido ligand π cloud involves the other TPP ligand, thus disrupting the both possibilities to form 6PEs. The azido ligand is also involved in intermolecular nonbonded interactions. Thus, as the strongest hydrogen bond acceptor, the azido ligand becomes the most important determiner of the supramolecular structure.

School of Chemistry
Academic Year 2002

Student
Advisor
Coadvisor
Coadvisor

Acknowledgments

I would like to express my deepest and sincerest gratitude to my advisor, Assoc. Prof. Dr. Kenneth J. Haller for his kindness to give me a good opportunity to study in this field, his supervision, his valuable suggestions, and his scholarship support throughout my study. I would also like to express my gratitude to all the teachers of the School of Chemistry who taught and helped me during my study at SUT. I wish to express my special thanks to the head of the School of Chemistry, Asst. Prof. Dr. Malee Tangsathikulchai for giving me good opportunity to study in the School of Chemistry and for her warm hearted support, encouragement, and help. Special thanks also to Asst. Prof. Dr. Kunwadee Rangriwatananon for her warm hearted support, encouragement, and help.

Thanks to Suranaree University of Technology for a Research Grant to support my thesis research, and for a Travel Grant to support my attendance at the 27th Science and Technology of Thailand meeting in Haad Yai, Thailand. Thanks to the Asian Crystallographic Association for a Bursary Award to support my attendance at AsCA'01, the 4th meeting of the Asian Crystallographic Association in Bangalore, India, and to MacScience Co. Ltd. for a Registration Grant for the same meeting. Thanks to the International Union of Crystallography for a Bursary Award for travel to Geneva, Switzerland to attend the XIX Congress and General Assembly of the IUCr. These opportunities to travel and present my results to a broader audience have been invaluable.

I would also like to thank all of my friends for their help and encouragement throughout the time of my studies.

Finally, I would like to take this opportunity to express my deepest appreciation and sincere gratitude to my dear parents and sister for their love, devotion, understanding, consolation, and encouragement for my success in study.

Angkana Kiatpichitpong

Contents

	Page
Abstract in Thai	I
Abstract in English	III
Acknowledgments	V
Contents	VI
List of Tables	VIII
List of Figures	IX
List of Abbreviations	X
List of Nomenclature	XI
List of Units and Conversion Factors	XII
Chapters	
I Introduction	1
II Concepts and Theoretical Background	9
2.1 What is Supramolecular Chemistry?	9
2.2 Supramolecular Interactions	11
2.3 Multiple Phenyl Embraces	16
2.4 Introduction to X-Ray Diffraction	19
III Experimental	26
3.1 Instrumentation	26
3.2 Materials and Equipment	27
3.3 Techniques	30
3.4 Syntheses	38
3.5 Analysis of Crystal Structures	44
IV Results and Discussion	48
4.1 Supramolecular Structure of Ni(NCS)(NO)(PPh ₃) ₂	48
4.2 Supramolecular Structure of NiCl(NO)(PPh ₃) ₂	54
4.3 Supramolecular Structure of NiN ₃ (NO)(PPh ₃) ₂	62
V Conclusions	74
References	76

Contents (Continued)

	Page
Appendices	
Appendix A ORTEP Instruction Format and Atomic Coordinates	82
Appendix B Supplementary Tables of Contact Distances and Angles	92
Appendix C Abstracts of Presentations of Portions of This Thesis Work	99
Curriculum Vitae	102

List of Tables

Table	Page
1.1 Four-Coordinate Nickel Nitrosyl Phosphine Complexes Approximating the Linear Limiting Geometry	6
1.2 Four-Coordinate Nickel Nitrosyl Phosphine Complexes with Distorted Tetrahedral Geometry	7
3.1 Physical Characterization of $\text{NiX}_2(\text{PPh}_3)_2$ and $\text{NiX}(\text{NO})(\text{PPh}_3)_2$ where X = Br, Cl	41
4.1 Concerted Hydrogen Bond Interactions and Selected Interatomic C–H···X Distances Defining the $\text{Ni}(\text{NCS})(\text{NO})(\text{PPh}_3)_2$ Supramolecular Structure .	50
4.2 Concerted Hydrogen Bond Interactions and Selected Interatomic C–H···X Distances Defining the $\text{NiCl}(\text{NO})(\text{PPh}_3)_2$ Supramolecular Structure	58
4.3 Concerted Hydrogen Bond Interactions and Selected Interatomic C–H···X Distances Defining the $\text{NiN}_3(\text{NO})(\text{PPh}_3)_2$ Supramolecular Structure	66
A.1 Crystal Data and Nonhydrogen Coordinates for $\text{Ni}(\text{NCS})(\text{NO})(\text{PPh}_3)_2$	86
A.2 Calculated Hydrogen Atom Coordinates for $\text{Ni}(\text{NCS})(\text{NO})(\text{PPh}_3)_2$	87
A.3 Crystal Data and Nonhydrogen Coordinates for $\text{NiCl}(\text{NO})(\text{PPh}_3)_2$	88
A.4 Calculated Hydrogen Atom Coordinates for $\text{NiCl}(\text{NO})(\text{PPh}_3)_2$	89
A.5 Crystal Data and Nonhydrogen Coordinates for $\text{NiN}_3(\text{NO})(\text{PPh}_3)_2$	90
A.6 Calculated Hydrogen Atom Coordinates for $\text{NiN}_3(\text{NO})(\text{PPh}_3)_2$	91
B.1 Description of the Short Intermolecular Phosphorus-Phosphorus Contacts for $\text{Ni}(\text{NCS})(\text{NO})(\text{PPh}_3)_2$	93
B.2 Table of Symmetry Operations for $\text{Ni}(\text{NCS})(\text{NO})(\text{PPh}_3)_2$	94
B.3 Description of the Short Intermolecular Phosphorus-Phosphorus Contacts for $\text{NiCl}(\text{NO})(\text{PPh}_3)_2$	95
B.4 Table of Symmetry Operations for $\text{NiCl}(\text{NO})(\text{PPh}_3)_2$	96
B.5 Description of the Short Intermolecular Phosphorus-Phosphorus Contacts for $\text{NiN}_3(\text{NO})(\text{PPh}_3)_2$	97
B.6 Table of Symmetry Operations for $\text{NiN}_3(\text{NO})(\text{PPh}_3)_2$	98

List of Figures

Figure	Page
1.1 Limiting and Intermediate Geometries of the MNO Triatomic Fragment .	5
2.1 Representative Phenyl-Phenyl Interactions	15
2.2 Colinearity Parameter and d[P-P] in Sixfold Phenyl Embraces	17
2.3 Representative Sixfold Phenyl Embrace (6PE)	18
2.4 Variation in Atomic Scattering Factor with Scattering Angle	20
2.5 Reflection of X-Rays from Crystal Lattice Planes	21
2.6 Direct and Reciprocal Lattices	22
2.7 Variation of X-Ray and Neutron Atomic Scattering Factors with Scattering Angle for Stationary Atoms	23
3.1 Schlenk Glassware and Vacuum/Inert Atmosphere Line	29
3.2 Drying Solid Reagents and Solvents	31
3.3 Refluxing under an Inert Atmosphere	32
3.4 Filtration under an Inert Atmosphere	34
3.5 Recrystallization	36
3.6 IR Spectra of NiCl ₂ (PPh ₃) ₂ and NiBr ₂ (PPh ₃) ₂	42
3.7 IR Spectra of NiCl(NO)(PPh ₃) ₂ and NiBr(NO)(PPh ₃) ₂	42
3.8 Molecular Structure of NiCl ₂ (PPh ₃) ₂	43
4.1 6PE Linking Ni(NCS)(NO)(PPh ₃) ₂ Molecules into Chains	52
4.2 4PE Linking Chains of Ni(NCS)(NO)(PPh ₃) ₂ Molecules	53
4.3 Interlayer Interactions of Ni(NCS)(NO)(PPh ₃) ₂	55
4.4 Layer of 6PE and 4PE in Ni(NCS)(NO)(PPh ₃) ₂	56
4.5 Benzene Solvate in the Ni(PPh ₃) ₂ Cleft of the NiCl(NO)(PPh ₃) ₂ Molecule	61
4.6 Benzene Solvate in the Bowl Shaped Cavity of NiCl(NO)(PPh ₃) ₂	63
4.7 6PE Linking NiCl(NO)(PPh ₃) ₂ Molecules into Chains	64
4.8 C–H···N Interactions to the Azido Ligand of NiN ₃ (NO)(PPh ₃) ₂	69
4.9 Azido Ligand Environment in NiN ₃ (NO)(PPh ₃) ₂	71
4.10 Chain of Azido and Phenyl Interactions in NiN ₃ (NO)(PPh ₃) ₂	72

List of Abbreviations

Abbreviation

<i>cif</i>	file name extension of crystallographic information file.
CSD	Cambridge Structure Data base of organic crystal structures.
dppb	bis(1,2-bis(diphenylphosphino)benzene
dppe	bis(1,2-bis(diphenylphosphino)ethane
<i>ef</i>	edge-to-face interaction
<i>ff</i>	face-to-face interaction
H··C	Hydrogen-carbon interatomic distances
H··N	Hydrogen-nitrogen interatomic distances
<i>ins</i>	file name extension of SHELX instruction input file
Me	methyl group (CH ₃)
np	(2-diphenylphosphinoethyl)amine
O4PE	orthogonal fourfold phenyl embrace
Ph	phenyl group (C ₆ H ₅)
P4PE	parallel fourfold phenyl embrace
P··P	nonbonded Phosphorus-Phosphorus distances
SHELX	generic name for George Sheldrick's crystallographic programs
SHELXL	George Sheldrick's public domain structure refinement program
3PE	threefold phenyl embrace
4PE	fourfold phenyl embrace
6PE	sixfold phenyl embrace

List of Nomenclature

Symbols

Meaning

$d[A-B]$	interatomic bond distance between atoms A and B
$\angle[A-B-C]$	interatomic bond angle with atom B as vertex
$\angle[A-B-C-D]$	interatomic torsion angle about the B-C
$d[X-H\cdots Y]$	nonbonding contact between H and Y
hkl	designate lattice point or "reflection"
(hkl)	designate lattice planes or crystal faces
[hkl]	designate a direction in the lattice

List of Units and Conversion Factors

Energy: $\text{J} = \text{kg m}^2 \text{s}^{-2} = 10^7 \text{ ergs}$; $\text{erg} = \text{g cm}^2 \text{s}^{-1}$

$$4.184 \text{ J} = 1 \text{ cal}$$

Volume: $\text{m}^3 = 10^3 \text{ dm}^3 = 10^6 \text{ cm}^3$ (mL)

Temperature: $\text{K} = ^\circ\text{C} + 273.15$

Length: $\text{\AA} = 10^{-8} \text{ cm} = 0.1 \text{ nm} = 100 \text{ pm}$

Chapter I

Introduction

Nickel(I) and Nickel(II) species are being studied increasingly because of the possible involvement of these oxidation states in nickel containing metalloenzymes (Cotton, Wilkinson, Murillo & Bochmann, 1999, p836). At the same time there has been an increase of interest in study of nitrosyl chemistry because of biological implications (Stamler & Feelisch, 1996). NO is essential for the complex mechanism involving nerves, muscles, and blood pressure required for male sexual potency. It also relaxes the muscles of the intestine so food can be shunted along by muscular contraction and relaxation (Ainscough, & Brodie, 1995). Nickel and nitrosyl are also interesting in that complexes of both exhibit variable stereochemistry due to electronic and/or steric effects.

Nickel phosphine complexes exhibit catalytic activity in the cross-coupling of Grignard reagents with aryl and alkyl halides. Some of the most effective catalysts employed as selective hydrogenation, isomerization, and hydroboration catalysts contain triphenylphosphine complexes such as dichlorobis(triphenylphosphine) nickel(II) (Palo & Erkey, 1998).

Of particular interest in this study are the four-coordinate complexes of nickel. Some complexes, for example nickel tetracarbonyl (Huheey, Keiter & Keiter, 1993, p634) display tetrahedral geometry, while other complexes such as the nickel bis(1,2-bis(diphenylphosphino)benzene) cation in $[\text{Ni}(\text{dppb})_2](\text{PF}_6)_2$ complex (Miedaner, Haltiwanger & Dubois, 1991), prefer square-planar geometry. Formally Nickel(II) four-coordinate complexes formed with liganding atoms of the set C, H, O, N, P, S, F, Cl, Br, and I are more often square planar than tetrahedral.

Tetrahedral or pseudo tetrahedral complexes (with angles in the range of 100-120°) are high spin and usually of the types NiX_4^{2-} , NiX_3L^- , NiX_2L_2 and $\text{Ni}(\text{L-L})_2$ where X is a halogen, L_2 two neutral ligands or a neutral bidentate ligand, and L-L a bidentate ligand which is uninegatively charged (van Mier, Kanters & Sjoerd, 1987). The remaining complexes are mostly square planar low spin complexes. A few

complexes such as azidonitrosylbis(triphenylphosphine) nickel have intermediate geometry (Enemark, 1971) and presumably intermediate spin state values.

The tetrahedral high spin complexes are typically formed with halides or bulky ligands such as triphenylphosphine showing the apparent importance of both electronic and steric effects in determining the nickel stereochemistry (Huheey, Keiter & Keiter, 1993, p585). Depending on the ligands the balance can lie between square-planar and tetrahedral forms, indeed in the case of dibromobis(benzylidiphenylphosphine) nickel(II), $\text{Ni}[\text{P}(\text{CH}_2\text{C}_6\text{H}_5)\text{Ph}_2]_2\text{Br}_2$, both tetrahedral and square planar forms coexist in the same crystal lattice (Kilbourn & Powell, 1970).

Searching version 5.21 of the Cambridge Structural Database (CSD; Cambridge Structural Database, 2001) yielded 51 structure reports for the substructure fragment consisting of four-coordinate nickel bound to two phosphorus atoms, each of which is bound to three C_6 six aromatic sp^2 carbon atom rings in addition to the nickel atom. The search fragment thus allowed substituted triphenylphosphine ligands as well as the parent form. Nearly half of the reports are structures containing bidentate ligands: twelve reports of $\text{Ni}(\text{P-X})_2$ where P-X are bidentate ligands, eight reports of $\text{Ni}(\text{X-Y})(\text{PPh}_3)_2$ where X-Y are bidentate ligands, and two reports of $\text{NiX}_2(\text{P-P})$ where P-P is a bidentate ligand. Of the remaining reports sixteen are for structures of the type $\text{NiX}_2(\text{PPh}_3)_2$, *i.e.* X and Y are the same monodentate ligand (six with $\text{X} = \text{Y} = \text{Cl}$), while thirteen are for structures of the type $\text{NiXY}(\text{PPh}_3)_2$ where X and Y are different monodentate ligands. Three reports in the final group are $\text{NiX}(\text{NO})(\text{PPh}_3)_2$ structures, the subject of this work.

Two of the $\text{NiCl}_2(\text{PPh}_3)_2$ structures are square planar *trans*- $[\text{NiCl}_2(\text{PPh}_3)_2]$ molecules incorporating solvent molecules in their nearly isomorphous lattices; the first reported in 1985 containing 1,2-dichloroethane (Corain, Longato, Angeletti & Valle, 1985), and the second reported in 1993 containing methylene chloride (Sletten & Kovacs, 1993). The solvent molecules, reportedly, do not coordinate to the nickel complex, but solvate around the $\text{NiCl}_2(\text{PPh}_3)_2$ molecules resulting in stabilization of the *trans*- $[\text{NiCl}_2(\text{PPh}_3)_2]$ square planar geometry by the weaker dipole-dipole interactions. The Ni-P bonds and the Ni-Cl bonds in the two complexes are not significantly different at 2.243 and 2.154 Å in the dichloroethane structure and 2.241 and 2.164 Å in the methylene chloride structure.

The other four of the six structure reports for $\text{NiCl}_2(\text{PPh}_3)_2$ are of increasing structure quality for the same unsolvated crystal form, culminating in an extremely accurate determination from Brammer & Stevens (1989). The structure is distorted from tetrahedral geometry with Cl–Ni–Cl and P–Ni–P bond angles of 127.9° and 111.4° , respectively, which are larger than tetrahedral values, and Ni–P and Ni–Cl bond distances of 2.318 and 2.207 Å, respectively. Thus, the $\text{NiCl}_2(\text{PPh}_3)_2$ complex provides a direct measure of the difference in bonding radius between the high spin tetrahedral and low spin square planar nickel atoms; the high spin form being about 0.06 Å larger than the low spin form. The authors of the first of the determinations (Garton, Henn, Powell & Venanzi, 1963) attribute the distortion from tetrahedral geometry only to the steric effects of triphenylphosphine and the halide lone pairs, and suggest it cannot result from Jahn-Teller effect as the ground state of a nickel(II) atom is not orbitally degenerate. The difference in P–Ni–P and Cl–Ni–Cl bond angles is a result of interelectronic repulsion between the lone-pairs of the chlorine atoms which are expected to be larger than the bond-pairs of the phosphines. The effect is increased by the long Ni–P bond distance and the much shorter Ni–Cl bond distance.

Conventionally, metal-phosphine bonding has been described as a ligand to metal σ bond plus metal to ligand π back bond using the acceptor character of the empty $3d$ orbitals on the phosphorus atom. Orpen and Connelly (1985) used structural data to confirm the theoretical studies (Xiao, Trogler, Ellis & Berkovich-Yellin, 1983) suggesting that the σ^* phosphine orbitals are π -acid in character and act as the π -acceptor for the metal d electron back bond. The changes in M–P and P–C bond lengths in a series of reduction-oxidation related pairs of transition metal phosphine complexes is consistent with M–P bonding in the complexes containing an important π -component from metal $3d$ to ligand σ^* . Brammer and Stevens (1989) note the significant shortening of the P–C bonds in the $\text{NiCl}_2(\text{PPh}_3)_2$ complex, consistent with a π back-bonding model incorporating P–C σ^* orbitals in the acceptor role, and also the possibility of Jahn-Teller distortion in nickel(II) complexes (as compared to nickel (II) metal ion).

Both $\text{NiBr}_2(\text{PPh}_3)_2$ (Jarvis, Mais & Owston, 1968) and $\text{NiI}_2(\text{PPh}_3)_2$ (Humphry, Welch & Welch, 1988) exhibit distorted tetrahedral geometry. The X–Ni–X angles decrease from the dichloro to the dibromo to the diiodo complex (127.9 , 126.3 , and 118.1° respectively) while the Ni–X distances increase (2.207, 2.333, and 2.530 Å respectively). The X–Ni–X enlargement is attributed to steric repulsion between the

halide atom lone pairs. The inverse trend between the bond angles and bond distances may be due to the opposite effects of the increasing size of the halide atom lone pairs and the simultaneous increase in the Ni–X bond lengths.

The neutral nitric oxide molecule, NO, contains an odd number of electrons and is thus a paramagnetic radical. When it binds with transition metals the radical character is lost, NO either loses or gains one electron in the π^* orbital to give species that have been variously classified as complexes of NO^+ and NO^- in which NO serves as a three-electron or a one-electron donor respectively. The valence bond structures for $\text{N}\equiv\text{O}^+$ and $\text{N}=\text{O}^-$ have sp and sp^2 hybridization, respectively, at the nitrogen atom implying the possibility of both linear and strongly bent MNO geometries. From the valence bond structures of $\text{N}\equiv\text{O}^+$ and $\text{N}=\text{O}^-$ it would seem that there should be a direct correlation between the NO stretching frequency, ν_{NO} , and the M–N–O angle. However, although metal nitrosyl complexes do exhibit a wide range of NO stretching frequencies ($\sim 1500\text{--}2000\text{ cm}^{-1}$) they do not correlate well with the M–N–O angle unless several empirical corrections are assumed. It has been suggested that the variations arise because different types of metal centers exchange different amounts of electron occupancy with the nitric oxide molecular orbitals, complicated by the fact that the highest occupied molecular orbital of nitric oxide is of the π^* type, which creates additional difficulty for valence bond type electron-counting schemes (Feltham & Enemark, 1981). In any event, the M–N–O angle does not generally correlate with ν_{NO} in the complexes. Geometrical, electronic, and vibrational studies of the MNO triatomic or the related $\text{M}(\text{NO})_2$ species created by matrix isolation in solid argon at low temperature agree well with density functional calculations for these two forms (Krim, Manceron & Alikhani, 1999).

The $\{\text{MNO}\}^n$ moiety* as an “inorganic functional group” that is perturbed by the coordination of other ligands to the metal has been described previously (Enemark & Feltham, 1974). The group exhibits limiting geometries that are linear corresponding to a coordinated NO^+ group or bent corresponding to a coordinated NO^- group with ideal MNO angles of 180° and 120° respectively as shown in Figure 1.1. The distribution of valence electrons and thus the geometry of the $\{\text{MNO}\}^n$ moiety are dictated by the overall stereochemistry of the complex formed, leading to

* The $\{\text{MNO}\}^n$ notation is used herein to avoid ambiguity in assigning formal oxidation states in metal nitrosyls. The n corresponds to the total number of metal d and nitrosyl π^* electrons in the complex for nitric oxide assumed to be coordinated as $(\text{N}\equiv\text{O})^+$ (Enemark, Feltham, Riker-Nappier & Bizot, 1975).

geometries ranging from one limiting geometry to the other. This correlation between the stereochemistry and the MNO geometry led Enemark and Feltham to call this phenomenon “stereochemical control of valance”. One interesting example of stereochemical control of valance is given in a study of $\{\text{CoNO}\}^8$ complexes of the type $\text{Co}(\text{NO})(\text{das})_2\text{X}_2$ (where das is *ortho*-phenylenebis(dimethylarsine)) in which a linear $\{\text{MNO}\}^8$ moiety was converted into a strongly bent $\{\text{MNO}\}^8$ moiety by a simple reaction (Enemark, Feltham, Riker-Nappier & Bizot, 1975). Stereochemical control of valance provides a general pathway whereby the mechanical and chemical energy of a structure change about a transition metal catalyst can be translated directly into a chemical change in the substrate (Enemark & Feltham, 1972).

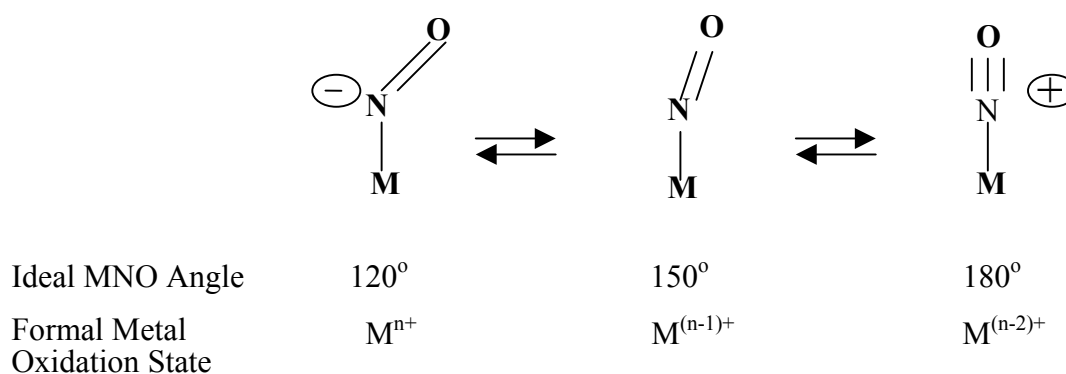


Figure 1.1. Limiting and Intermediate Geometries of the MNO Triatomic Fragment.

The same sensitivity to the stereochemistry about the metal is expected for the $\{\text{MNO}\}^{10}$ mononitrosyl nickel complexes studied herein. Two limiting possibilities have been proposed for four-coordinate complexes containing the $\{\text{NiNO}\}^{10}$ moiety; pseudo tetrahedral geometry (C_{3v} symmetry) with a linear NiNO group, and square-planar geometry with a strongly bent NiNO group (Enemark & Feltham, 1974). Intermediate distorted coordination geometries should therefore have intermediate NiNO angles.

Four complexes illustrating the higher symmetry linear limiting geometry have been studied and are given in Table 1.1 below. It is unfortunate that the quality of the first two structures is low, but while the Ni–P bonds within each complex appear to show variation, they are essentially equivalent (3.5σ level) within the accuracy of the structures, while the Ni–P bonds range over 5σ in the third complex.

Thus, the first three complexes exhibit approximate C_{3v} symmetry (both structurally and electronically) which as noted above corresponds to the limiting geometry with a linear Ni–N–O group as observed. The Ni–N–O angles in the better determined structures (entries 1 and 3 in Table 1.1) are within 5° of the expected linear limiting geometry. The local 3-fold symmetry about the Ni–N vector is not crystallographically imposed and the substituents on the phosphorus atoms do not conform to C_3 symmetry, indicating that, as previous authors have concluded (Elbaze, Dahan, Dartiguenave & Dartiguenave, 1984), the distortion of the Ni–N–O group must be from electronic effects. The fourth entry, Ni(P(OMe)₃)(NO)(1,2-C₆H₄(PMePh)₂), does not exhibit C_3 symmetry in the Ni–P bonds which differ over a range of 30° due to the third phosphorus ligand being the triphosphite P(OMe)₃ which is a stronger electron withdrawing ligand (therefore enhancing the metal to ligand π bonding). The Ni–N–O angle is linear indicating that having three phosphorus donor atoms is sufficient to create the pseudo C_3 symmetry in which the nitrosyl π^* orbitals are degenerate.

Table 1.1. Four-Coordinate Nickel Nitrosyl Phosphine Complexes Approximating the Linear Limiting Geometry (Approximate C_3 Local Symmetry).

Ni complex	X	Ni–P (Å)	Ni–N–O (°)	Reference
Ni[NO(P(OCH ₂) ₃ CCH ₃) ₃] BF ₄ ·CHCl ₃	P(OCH ₂) ₃ CCH ₃	2.191(4) 2.176(5) 2.191(4)	176.8(7)	Meiners, Rix, Clardy & Verkade, 1975.
[Ni(NO)(np) ₃]BPh ₄ (np=(Ph ₂ PCH ₂ CH ₂) ₃ N)	¹ / ₃ np	2.280(5) 2.297(5) 2.302(6)	167.7(21)	Di Vaira, Ghilardi & Sacconi, 1976.
[Ni(NO)(PMe ₃) ₃]PF ₆	PMe ₃	2.229(2) 2.239(1) 2.239(1)	175.4(5)	Elbaze, Dahan, Dartiguenave & Dartiguenave, 1984.
Ni(P(OMe) ₃)(NO) (1,2-C ₆ H ₄ (PMePh) ₂)	P(OMe) ₃	2.213(1) 2.220(1) 2.190(1)	178.0(5)	Rahman, Salem, Stephens & Wild, 1990.

One group of complexes previously studied in the context of the relationship between the Ni–N–O bond angle and the Ni coordination geometry is the low symmetry nickel complexes of the general formula NiX(NO)(PPh₃)₂ where X is a monoanion. The complexes were expected to be approximately tetrahedral on the

basis of their large dipole moments (Feltham, 1964). This was confirmed by the preliminary study (Enemark, 1971) of the $X = \text{azide}$ complex which showed its geometry to be distorted tetrahedral. The only other well characterized complex in this series also has distorted tetrahedral geometry (Haller & Enemark, 1978). Both complexes have geometries between square planar and tetrahedral and both have NiNO bond angles intermediate to the limiting cases as expected.

An interesting feature of the $\text{NiX}(\text{NO})(\text{PPh}_3)_2$ complexes that was noted but not explored in detail is the structural nonequivalence of the chemically equivalent Ni–P bond lengths. Several examples of this structural nonequivalence are now known and are included in Table 1.2. The structure determined for the nitro-nitrosyl-bis(trimethylphosphine) complex, $\text{Ni}(\text{NO}_2)(\text{NO})(\text{P}(\text{CH}_3)_3)_2$, from data collected at 135 K exhibits nonequivalent Ni–P bonds while a second structure determination from data collected at room temperature shows equivalent Ni–P distances (Kriege-Simonsen, Elbaze, Dartiguenave, Feltham & Dartiguenave, 1982).

Table 1.2. Four-Coordinate Nickel Nitrosyl Phosphine Complexes with Distorted Tetrahedral Geometry (Approximate C_s Local Symmetry).

Ni complex	X	Ni–P (Å)	Ni–N–O (°)	Reference
$\text{Ni}(\text{N}_3)(\text{NO})(\text{PPh}_3)_2$	N_3^-	2.257(2) 2.306(2)	152.7(7)	Enemark, 1971.
$\text{Ni}(\text{NCS})(\text{NO})(\text{PPh}_3)_2$	NCS^-	2.271(2) 2.328(2)	161.5(5)	Haller & Enemark, 1978.
$\text{Ni}(\text{NO}_2)(\text{NO})(\text{PMe}_3)_2$ (low temperature structure)	NO_2^-	2.228(3) 2.244(2)	166.9(6)	Kriege-Simonsen, Elbaze, Dartiguenave, Feltham & Dartiguenave, 1982.
$[\text{Ni}(\text{ONO})(\text{NO})\text{dppe}]_2$ (dppe= $\text{Ph}_2\text{PCH}_2\text{CH}_2\text{PPh}_2$)	ONO^-	2.251(3) 2.271(4)	153.4(8)	Kriege-Simonsen & Feltham, 1983.
$\text{Ni}(\text{NCS})(\text{NO})$ (1,2- $\text{C}_6\text{H}_4(\text{PMePh})_2$)	NCS^-	2.213(1) 2.234(1)	159.5(3)	Rahman, Salem, Stephens & Wild, 1990.
$[(\text{dppe})(\text{NO})\text{Ni}(\mu\text{-dppe})\text{Ni}(\text{NO})(\text{dppe})]^{2+}$; (dppe= $\text{Ph}_2\text{PCH}_2\text{CH}_2\text{PPh}_2$)	Bridging dppe	2.243(5) 2.274(5)	168.2(14)	Del Zotto, Mezzetti, Novelli, Rigo, Lanfranchi & Tiripicchio, 1990.
$\text{NiCl}(\text{NO})(\text{PPh}_3)_2$	Cl^-	2.263(6) 2.285(5)		Haller, 1978.

The first of the low symmetry four-coordinate nickel nitrosyl complexes with nonequivalent Ni–P bonds was the azido complex, Ni(N₃)(NO)(PPh₃)₂. Enemark (1971) suggested the nonequivalence could result from the nonlinear geometry of the coordinated azide which could produce different electronic environments at the two phosphorus coordination sites. A later attempt to evaluate this possibility by study of the analogous chloro complex (chloride has similar ligand field strength to azide) was inconclusive due to structural disorder. However, the related isothiocyanato complex, Ni(NCS)(NO)(PPh₃)₂, with linearly coordinated NCS⁻ ligand is structurally ordered and exhibits nonequivalent Ni–P distances, thus negating this possible electronic effect. Further, the intramolecular steric effect argument was discounted as the pattern of long and short distances is counter to that required by the steric argument. Another possibility, suggested but not explored, is that the interactions of the phenyl groups could have some effect (Haller & Enemark, 1978).

This thesis presents analysis of the structures of Ni(X)(NO)(PPh₃)₂ complexes where X is NCS⁻, Cl⁻, or N₃⁻ using coordinates from the Cambridge Structure Database (1999) to increase understanding of the structural chemistry of the low symmetry Ni(X)(NO)(PPh₃)₂ complexes. Ideas introduced by Dance and Scudder (1995) of concerted, attractive, directional weak interactions between phenyl rings which are able to engage in offset face-to-face (*off*) or edge-to-face (*ef*) concerted weak bonding interactions are applied to describe the extended supramolecular structure of the complexes.

Chapter II

Concepts and Theoretical Background

2.1 What is Supramolecular Chemistry?

Supramolecular chemistry is a young discipline. Although its concepts and roots and even many supramolecular chemical systems can be traced back to near the beginnings of modern chemistry, supramolecular chemistry as a discipline only dates back to the late 1960s or early 1970s. Perhaps the most important development leading to its emergence as a distinct branch of chemistry is the rapid increase in the power of x-ray crystallography which now allows accurate and complete determination of large and complex structures. During the last 15 years the field has expanded rapidly resulting in an enormous diversity of chemical systems which in concept, origin, or nature can be considered to be supramolecular. These systems open more traditional areas of chemistry resulting in an interdisciplinary field which has fostered collaborations among physicists, chemists of many disciplines, crystallographers, biochemists, and biologists to develop theory, prepare and synthesize materials, and provide computational models in furthering the understanding of solid state, inorganic, organic, and biochemical systems. Following are a few definitions of some key terms in supramolecular chemistry.

Jean-Marie Lehn (1995) who won the Nobel prize in 1987 for his work in the area wrote the following definition:

“Supramolecular chemistry is ‘chemistry beyond the molecule’, whose goal is to gain control over the intermolecular noncovalent bond. It is concerned with the entities of higher complexity than molecules themselves-supramolecular species and assemblies held together and organized by means of intermolecular, binding interactions. It is a highly interdisciplinary field of science and technology, bridging chemistry with biology and physics.”

Crystal Engineering: The building blocks/synthons are molecules (and ions) and the molecules interact with one another *via* the formation of noncovalent bonds to

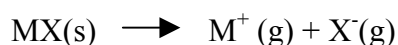
give the rational design of solid state structures exhibiting interesting electrical, magnetic, optical, and other properties. The intermolecular noncovalent interaction specificity, directionality, and predictability of intermolecular hydrogen bonds can be utilized to assemble supramolecular structures of controlled dimensionality.

Intermolecular bond: The generic term that includes ion pairing (electrostatic), hydrophobic, and hydrophilic interactions, hydrogen bonding, host-guest interactions, pi-stacking, van der Waals interactions, and coordination bonds to a metal that is to act as an attachment template.

Self-assembly: Mixing of the component compounds produces the desired aggregate through a process that comprises several steps occurring spontaneously in a single operation that concerns the recognition-directed, reversible spontaneous association of a limited number of components under the intermolecular control of relatively labile, noncovalent interactions such as coordination interactions, hydrogen bonds, and dipolar interactions. The architectural and functional features of organized supramolecular structures results from the molecular information stored in the components and from the active groups which they bear (Steed & Atwood, 2000, pp 464-467).

Crystalline material: a solid composed of atoms, ions, and/or molecules arranged with long range order in a regularly repeating three dimensional pattern.

Lattice energy, U, of an ionic solid is generally defined as the energy change associated with the process of going from crystalline solid to gas phase components:



Lattice energy of a molecular solid must have a similar meaning but may seem more complicated. The lattice energy receives contributions from attractive and repulsive electrostatic forces just as in the ionic case. There are also contributions from dipolar interactions and intermolecular repulsive forces (electrostatic), dispersion forces, zero-point energy and other vibrational components, and anything else that can change the overall energy of the components when combined into the crystalline lattice. Lattice energy provides the energy needed to stabilize energetically less favorable conformers of a molecule in a lattice giving the possibility of polymorphism or of multiple conformations in one crystal lattice.

Supramolecular synthons are "made up of spatial arrangements of potential intermolecular interactions and play the same focusing role in supramolecular synthesis that conventional synthons do in molecular synthesis" (Desiraju, 1995).

Concerted interaction: Concerned with the interactions of the entire molecular building block, including the volume of space a molecule takes up and how it meshes with neighboring molecules in a three dimensional array taking into account the relative strengths of the nonbonding contacts that are present. It is called concerted because the interaction energies between adjacent building blocks are the sum of the individual component interactions. The process of crystal engineering as viewed through the concerted interactions is a study in balance and interaction.

2.2 Supramolecular Interactions

For the purposes of this thesis the nature of supramolecular interactions concerns noncovalent bonding interactions. The term 'noncovalent' encompasses an enormous range of attractive and repulsive forces. In general, the various kinds of noncovalent interaction forces are mostly of electrostatic origin. Desiraju's (1995) classification of intermolecular forces from the crystal engineering standpoint is based in distance dependence and directionality. A fundamental difference between hydrogen bonds and van der Waals interactions lies in their different directionality characteristics. Hydrogen bonds are inherently directional, with linear or close to linear geometry favored energetically over bent geometries. In contrast van der Waals contacts are isotropic with interaction energies independent of the contact angle (Steiner & Desiraju, 1998).

The medium range forces, particularly van der Waals interactions, are isotropic in character and define molecular shape and size, and contribute favorably to the overall crystal stability as well as providing a driving force towards close packing. Generally, these forces are limited to C...H, C...C and H...H interactions. The longer-range forces, such as hydrogen bonds, on the other hand are electrostatic and anisotropic, and involve heteroatom interactions, that is interactions among N, O, S, Cl, Br, I (rarely B, F, P, Se) or between any of these elements and C or H.

Ionic forces are extremely long-range in nature and are quite specific. They direct supramolecular structures effectively, as for example those between metal cations and heteroatoms. When considering a supramolecular system it is vital to consider the interplay of these interactions and effects relating both to the host and

guest as well as to their surroundings including molecules of solvation. An adequate description must take into account the hierarchy of the interactions, being careful to consider the strong bonding forces, or the sums of the concerted weak forces that produce a strong interaction as the starting point in the analysis.

Directional Forces

Hydrogen bonding is perhaps the most important factor for molecular recognition. It is the most reliable directional interaction used in supramolecular construction, and its significance in crystal engineering can scarcely be underestimated. Hydrogen bonds are characterized by both high-strength (up to 120 kJ mol⁻¹) and distinct directionality. A very large amount of work has been carried out on the various aspects of hydrogen bonding and most workers agree to classify it into three general categories (Steed & Atwood, 2000, p392-397) according to the energy of the interaction.

1. Strong or conventional hydrogen bonds (energies 20-40 kJ mol⁻¹) in the crystalline state are generally associated with strong acids or with the hydrated proton such as the type O–H···O and N–H···O. The strong hydrogen bond is characterized by an X–H···X (X = F, O, N) angle of close to 180° and a short X···X distance, and is accompanied by a lengthening of the covalent X–H distance, such that the proton is shared almost equally between the two electronegative atoms.

2. Medium hydrogen bonds are by far the most generally occurring for hydrogen attached to electronegative atoms, especially O, and occur in most biological systems. Hydrogen bonded distances may vary over more than 0.5 Å, and X–H···X angles generally range from 140 to 178°. Hydrogen bonds have been extensively analyzed based on data found in the Cambridge Structure Database, showing that the most frequent X–H···X angle observed is about 155°. When the data are corrected for the statistical bias against an X–H approaching an acceptor to produce a hydrogen bonded angle of exactly 180° (conic correction) the most common angle for two center hydrogen bonds becomes 180°, corresponding to the line of most interaction.

About 20-25% of moderate-strength hydrogen bonds are bifurcated hydrogen bonds (three centered hydrogen bonds). These can either be symmetrical with two equal H···X distances for the two donor-acceptor interactions, or unsymmetrical. Examination of amines shows that the tendency towards bifurcation increases with the

donor-hydrogen bonding distance. Thus bifurcated bonds are more likely to occur when there is more space about the donor atom. Hydrogen bond distances tend to increase significantly when more than two centers are involved. At the same time, multicenter bonding tends to reduce the X–H...X angle, typically to 90-140°. Trifurcated four-center bonds are also known.

3. Weak hydrogen bonds (energies 2-20 kJ mol⁻¹) occur both with poor donors such as acidic C–H bonds in cases in which the carbon is attached to an electronegative group or is otherwise acidic (such as arenes, acetylenes, ethers, chloroalkanes, and similar groups) and poor acceptors such as oxygen as in the heavily studied C–H...O interaction. The angular characteristics of C–H...O interactions for different types of C–H groups show that the directionality decreases with decreasing C–H polarization. Distances and angles may cover wide ranges and the low fall-off of Coulombic electrostatic interactions with distance (r^{-2} dependence) means that even very long separations in the region of 4 Å may still be weak hydrogen bonds. In these cases good structural data combined with careful detailed analysis of the geometry of the system as a whole can be fruitful. When there are no strong interactions, weak hydrogen bonds can dominate the supramolecular structure.

Hydrogen bonds in general are composed of different types of interactions. As for an intermolecular interaction, there is a nondirectional “van der Waals” contribution, which is weakly bonding at long distance (by exchange repulsion), whereas for weakly, polarized C–H groups the electrostatic component is of similar magnitude to the van der Waals contribution. An electrostatic component (dipole-dipole, dipole-charge, *etc.*) is directional and bonding at all distances. The electrostatic component is the dominant one in a hydrogen bond (several kJ mol⁻¹). It reduces with increasing distance and with reducing dipole moment or charges involved. At their optimal geometry, van der Waals interactions contribute some tenths of a kJ mol⁻¹ to hydrogen bond energy.

Crystal structures are an important result of cooperativity; in an array of n interconnected hydrogen bonds, the total bond energy is larger than the sum of n isolated hydrogen bonds (nonadditivity). Based on structure and electrostatic analogies, such effects can be postulated to occur also with weak hydrogen bond types. There are two different mechanisms that can produce a cooperativity effect. Functional groups which may act as hydrogen bond donor and acceptor

simultaneously often form chains due to mutual polarization of the involved groups. The second mechanism relates to charge flow in suitably polarizable π -bond systems (resonance assisted hydrogen bonds). Two cooperativity hydrogen cycles involving C–H \cdots O interaction (Steiner, 1997). C–H $\cdots\pi$ contacts that are interconnected possess the essential characteristics of hydrogen bonds, including the property of cooperativity, *i.e.*, the interactions mutually increase each other's strengths, and the bond energy per contact is greater than the sum of individual isolated contacts.

Nondirectional Forces

Nondirectional forces (2-10 kJ mol⁻¹) include C \cdots C, C \cdots H and H \cdots H interactions based on competing weak electrostatic and van der Waals influences (Desiraju, 1995). C \cdots C interactions occur in aromatic systems when the rings are eclipsed or nearly eclipsed. The geometries observed for π – π stacking interactions between aromatic rings where one is relatively electron rich and one is electron poor may be due to an overall attractive van der Waals interaction proportional to the contact surface area of the two π -systems (however, this case could also be attractive due to the polarity difference between the more negative electron rich and the more positive electron poor clouds). The work presented in this thesis involves primarily the C \cdots H type of interaction occurring between phenyl or benzene rings and a small amount of the H \cdots H type of interaction occurring between phenyl or benzene rings.

Another interpretation of the π – π stacking interactions between approximately parallel aromatic molecules comes from the fact that the π – π stacks are invariably offset (leading to the designation offset face-to-face (*ff*) interaction used in this thesis) such that the hydrogen atoms on one ring are positioned at the π electron clouds of the adjacent ring (Figure 2.1). Thus, the attractive component can be viewed to be electrostatic in nature between the positively charged hydrogen atoms of one system and the negatively charged π electron cloud of the adjacent system. The offset between the two systems places the hydrogen atoms of one system in closest contact to the π electron cloud of the adjacent system while minimizing the π – π contact between the two systems. The strength of the interaction, described as a π $\cdots\pi$ interaction, depends on the ideality and the number of these interactions (Hunter & Sanders, 1990).

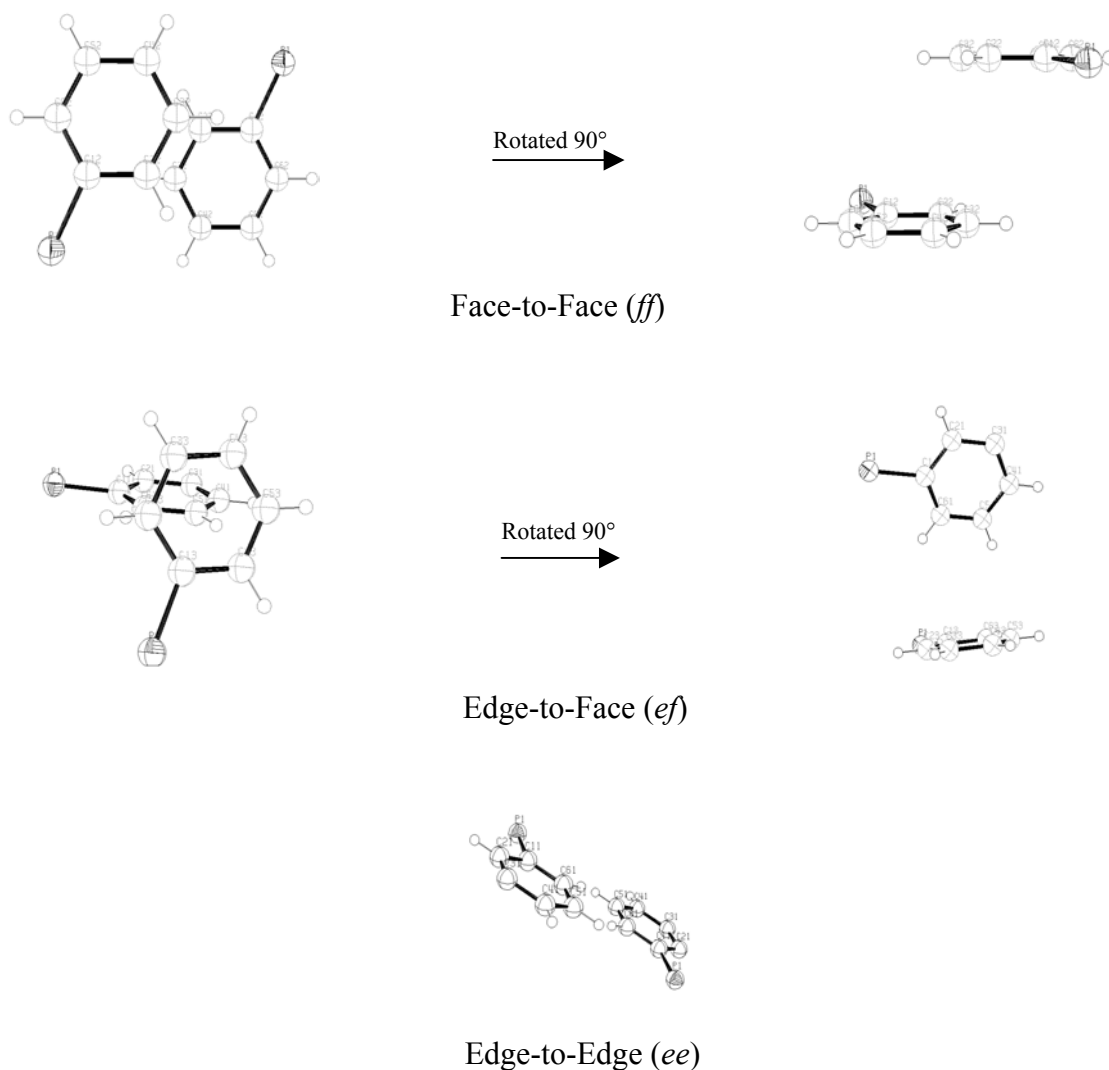


Figure 2.1. Representative Phenyl-Phenyl Interactions. For the *ef* and *ff* illustrations the left hand image is drawn projected perpendicular to the plane of one phenyl ring. A 90° rotation of the left hand image about the horizontal axis produces the right hand image.

The second mode of aromatic-aromatic interaction involves perpendicular or nearly perpendicular approach of one or two C–H units on the edge of one ring to the π electron cloud of a second ring (Nishio & Hirota, 1989). This is clearly electrostatic in nature between the positively charged hydrogen atom(s) of one system and the negatively charged π electron cloud of the adjacent system. Some authors have described this type of hydrogen bond as having the hydrogen atom buried in the π electron cloud or stuck in the π electron cloud of the adjacent aromatic system. This type of interaction is designated as an edge-to-face (*ef*) interaction and can be described as C–H $\cdots\pi$ (Figure 2.1).

The predictability of the geometry of phenyl-phenyl interactions resulting from the concerted attractive directional interactions between phenyl rings make them one type of supramolecular motif which can engage in offset face-to-face (*off*) stacking interactions in the π - π direction between adjacent aromatic rings and in the edge-to-face (*ef*) “herringbone” stacking interactions between the hydrogen atoms of the CH groups of one ring and the π system of another. The attractive geometries that extend from the edge-on relationship are well-known in the crystal structures of simple aromatic and other coplanar π systems (Steiner, 1998).

2.3 Multiple Phenyl Embraces

Crystal structures of triphenylphosphine have been analyzed in terms of the supramolecular interaction of multiple phenyl embraces which are concerted supramolecular motifs maintained by phenyl-phenyl attractive interactions. The name phenyl embrace signifies the three attributes of (1) participation of two or more phenyl groups from each partner molecule, (2) geometrical concertedness, and (3) strong attraction. This is one strategy for recognizing concerted and elaborated supramolecular motifs to increase understanding of the bonding and potential chemical reactivity.

One motif identified in the supramolecular domain is the six-fold phenyl embrace (6PE) in which three phenyl rings on one molecule are arrayed between three phenyl rings on a second molecule, such that each ring has edge-to-face (*ef*) interactions with two rings of the other molecule. Each phenyl ring projects two H atoms towards C atoms of a ring across the domain, with approximate C_3 symmetry for the pair. Thus, the six phenyl rings from two triphenylphosphine moieties exhibit a cyclic sequence of *ef* interactions. The 6PE concerted intermolecular attraction occurs frequently in crystals of compounds with terminal Ph_3P ligands, and in crystals containing the Ph_4P^+ cation (Dance & Scudder, 1996).

The 6PE is a concerted set of six intermolecular phenyl-phenyl attractive interactions between adjacent molecules. It is a higher level of intermolecular organization of the peripheral phenyl rings. The set of phenyl rings on each molecule must be correctly positioned and oriented to form the multiple phenyl embrace. In structures containing at least one Ph_3P bonded to a transition metal, M, the stereochemistry at the phosphine P is tetrahedral, and is characterized by approximate colinearity of the two P atoms and the metal atoms which complete their tetrahedral

geometry. The preponderance of P⋯P separation distances is in the range 6.4-7.4 Å and the M–P⋯P–M colinearity (half the sum of the M–P⋯P and P⋯P–M angles) ranges from 160-180° characterizing the sextuple phenyl embrace. Shorter distances correlate with greater colinearity with the tighter embraces being the more attractive. Figure 2.2 illustrates this interaction and the distance and colinearity parameters while Figure 2.3 shows a representative 6PE interaction.

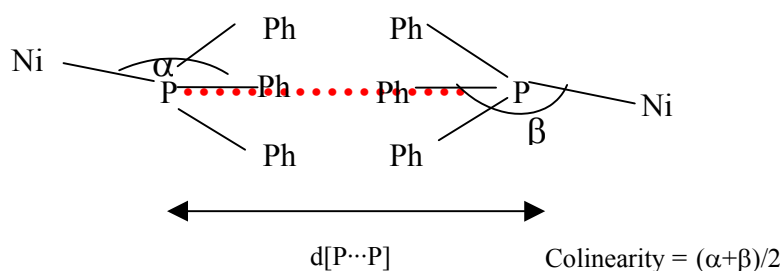


Figure 2.2. Colinearity Parameter and $d[\text{P}\cdots\text{P}]$ in Sixfold Phenyl Embraces.

The interpenetration of the two PPh_3 moieties in the 6PE is apparent from the fact that the P⋯P separations are very much less than 13.6 Å, which is twice the van der Waals radius of PPh_3 regarded as a hemisphere. The sextuple phenyl embrace usually manifests H⋯C *ef* intermolecular distances ranging from 2.8 to 3.2 Å between the interacting phenyl groups. The attractive energy of each H⋯C interaction in the *ef* conformation contributes *ca.* 2.1 kJ mol⁻¹, mostly coulombic in origin. More than 95% of compounds containing the PPh_3 fragment are centrosymmetric, and most of those contain 6PE (Dance & Scudder, 1995).

In addition to the ubiquitous 6PE several other concerted interactions (embraces) are possible among the phenyl groups. Most common after the 6PE are embraces involving four phenyl rings, two each from adjacent molecules. There are two main types of fourfold phenyl embrace (4PE). In the orthogonal fourfold phenyl embrace (O4PE) the two C–P–C planes for the four phenyl rings are approximately orthogonal and the phenyl rings are engaged in four *ef* interactions. In the parallel fourfold phenyl embrace (P4PE) the C–P–C planes are approximately parallel and the motif comprises one *ff* interaction between nearly parallel rings, one from each PPh_3 moiety, and two intermolecular *ef* interactions, one to each of the parallel rings. The energy of the *ff* interaction is greater than an *ef* interaction, but not twice as great, thus

the P4PE interaction is slightly weaker than the O4PE interaction. Dance and Scudder (1998) have also reported elaborate higher order (8-fold and 12-fold) embraces; inclusion of aromatic solvent molecules in the lattice appears to favor the more elaborate motifs.

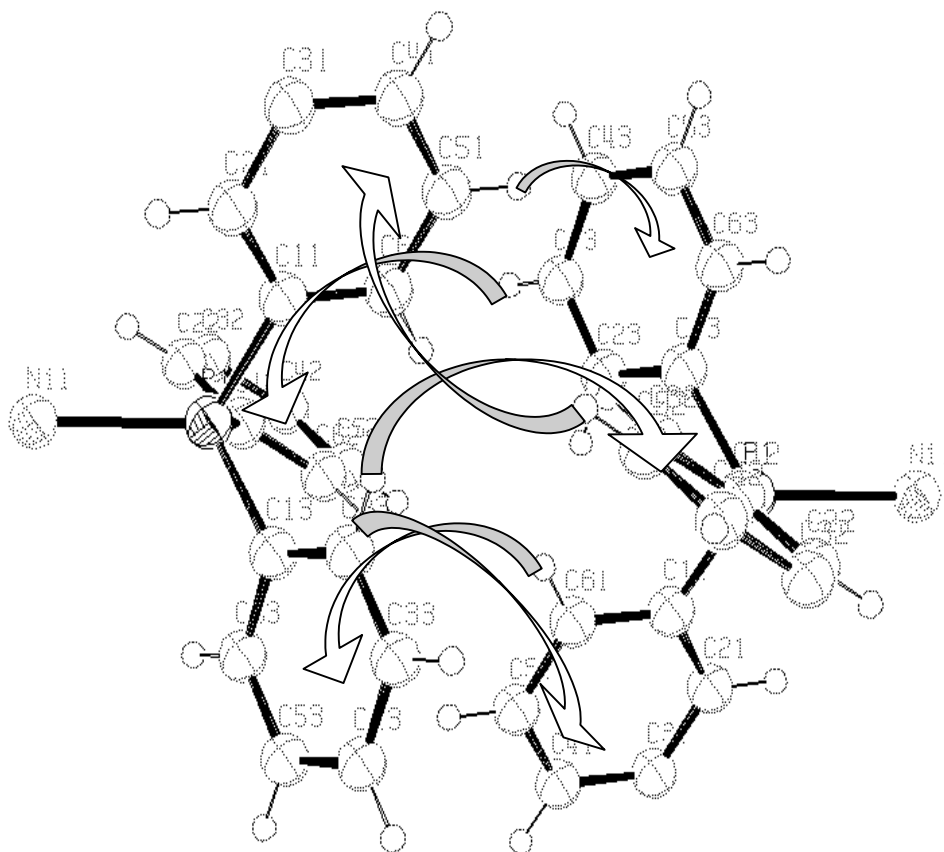


Figure 2.3. Representative Sixfold Phenyl Embrace (6PE).

2.4 Introduction to X-Ray Diffraction

X-ray crystallography is the most powerful and unambiguous method for the structure elucidation of solids available to modern scientists. X-ray diffraction has grown steadily since Max von Laue discovered in 1912 that a copper sulfate crystal could act as a three-dimensional diffraction grating upon irradiation with x-rays. Early diffraction experiments were recorded on photographic plates or film. The labor involved in determining a three-dimensional structure from these early experiments could easily lead to one's thesis being based solely on one or two structural determinations on relatively small molecules. The advent of modern high speed computers, powerful structure solution programs, automated diffractometers, focusing x-ray optics, more brilliant x-ray sources, and efficient area detectors has allowed x-ray diffraction to become widely accepted as an essential standard technique.

The basic requirement to conduct an x-ray diffraction experiment is a single crystal of suitable size that can withstand exposure to x-rays of a given energy for the duration of the x-ray experiment. Depending on the equipment hardware, the experimental conditions, and the information desired from the experiment (*e.g.* does one need to merely establish atom connectivity, to establish the absolute configuration of a resolved chiral molecule, or to determine kinetic data for a solid state reaction) an x-ray diffraction experiment may be carried out in as little as a few seconds or may take several weeks.

The Scattering of X-Rays by Electrons

The scattering of x-rays by the electrons in the crystal produces the diffraction pattern. Consider the sum of contributions to the scattered amplitude of all the electrons in all the atoms in the crystal starting from the scattering amplitude of a single electron and the variation in scattering amplitude with angle ($\sin\theta/\lambda$). The scattering amplitude of an individual neutral atom is determined by summing the contributions from all of its Z (the atomic number of the atom) electrons. The summation takes into account the path or phase differences between all the Z scattered waves and produces a scattering amplitude for the atom. The scattering amplitude is also called the "atomic scattering factor" or "atom form factor" and is given the symbol f . It is simply the ratio of the scattering amplitude of the atom divided by that of a single (classical) electron.

$$\text{Atomic scattering factor } f = \frac{\text{amplitude scattered by atom}}{\text{amplitude scattered by a single electron}}$$

At zero scattering angle ($2\theta = 0$ ($\sin\theta/\lambda = 0$), all the scattered waves are in phase and the scattering factor (f) is equal to the total number of electrons in the atom ($f = Z$). As the scattering angle ($\sin\theta/\lambda$) increases, f falls below Z because of the increasingly destructive interference effects between the Z scattered waves, the scattering of x-rays from different electrons in the atom will become more out of phase. Atomic scattering factors are plotted as a function of angle (usually expressed as $\sin\theta/\lambda$). Figure 2.4 shows such a plot for the oxygen anion O^{2-} which contains 10 electrons. When $\sin\theta/\lambda = 0$, $f = 10$ but with increasing angle f falls below 10 (Hammond., 1997, pp135-136).

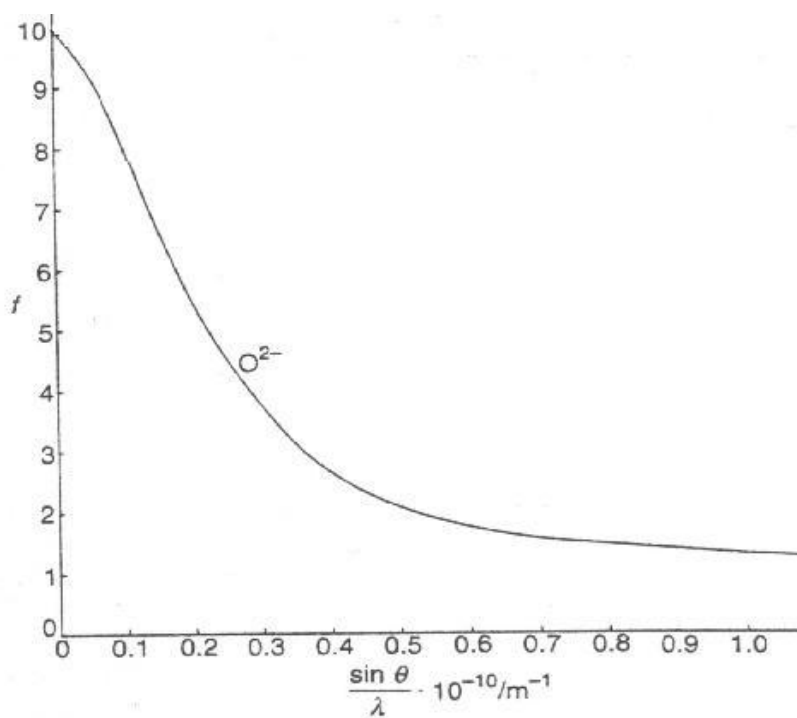


Figure 2.4. Variation in Atomic Scattering Factor with Scattering Angle.

Diffraction of X-Rays

In order to understand how the interaction of x-rays with a single crystal yields a diffraction pattern from which the three-dimensional crystal structure can be modeled, it is necessary to know basic diffraction physics. The formation of the

diffraction pattern from a crystal is normally described either in terms of the interference pattern of wavefronts scattered from a three dimensional periodic array of points, or the conceptually simpler treatment of a crystal as an analog of a series of equally spaced parallel planes of scattering material that act as mirrors and thus give an interference pattern when plane wavefronts are scattered from them. The mathematical expression used to describe how x-rays interact with a crystal to produce a diffraction pattern is given by Bragg's Law:

$$n\lambda = 2d \sin\theta$$

Where: n is an integer, λ is the wavelength of the radiation, d is the perpendicular spacing between adjacent planes in the crystal lattice, θ is the angle of "incidence" and "reflection" of the x-ray beam.

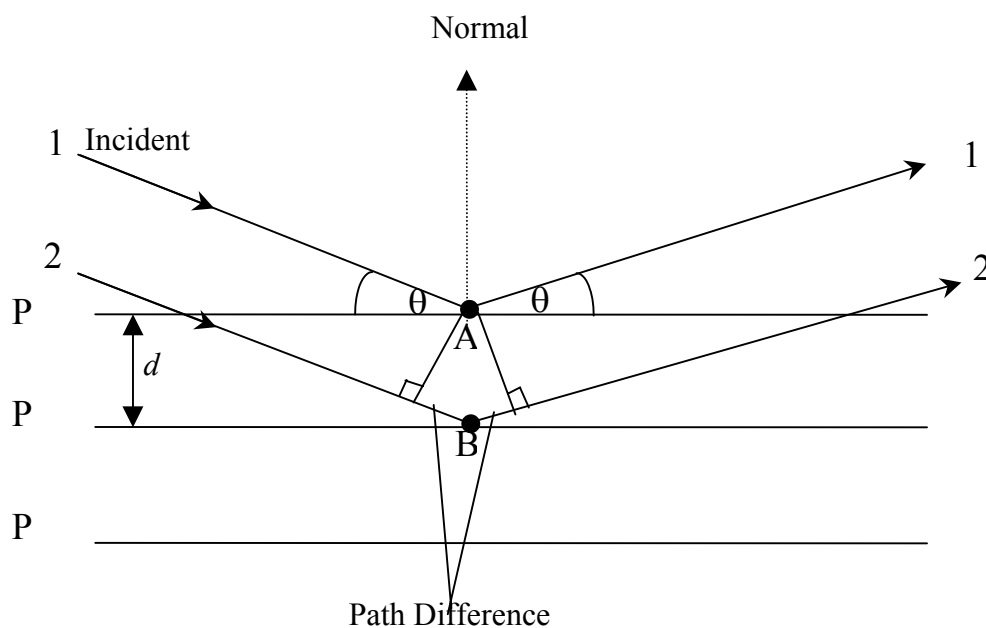
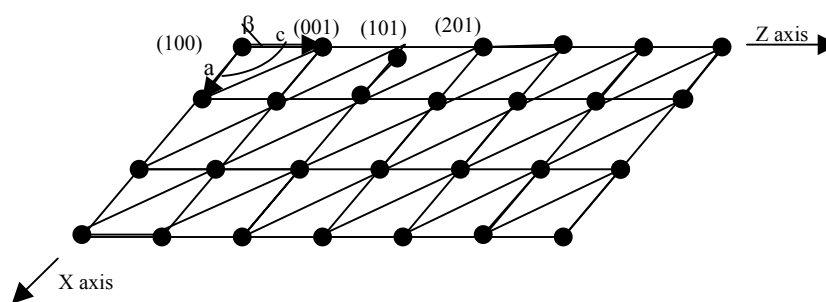


Figure 2.5. Reflection of X-Rays from Crystal Lattice Planes.

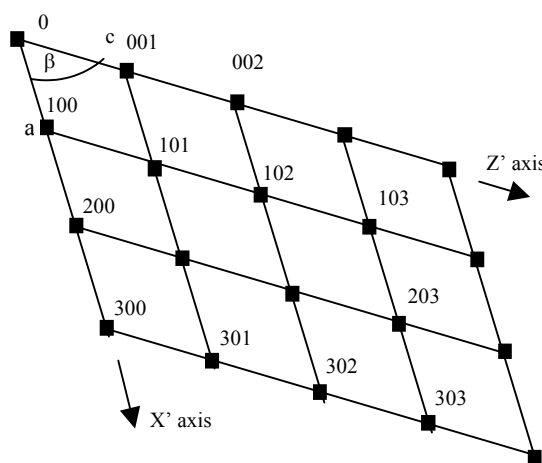
Figure 2.5 shows x-rays reflected from planes in the crystal lattice. Parallel waves 1 and 2 are incident on the parallel planes P1 and P2 passing through lattice points A and B and the wave 1 and 2 (the generated waves 1λ and 2λ) are occurred reflection making the angle θ of incidence and reflection must be equal and that the incoming and outgoing beams and the normal to the reflecting planes themselves all lie in one plane. Constructive interference (in-phase) of the wave emanating from

points A and B occurs only when the path lengths traveled are an integral multiple of the wavelength, $n\lambda$. It is seen that the path-length difference is $2d\sin\theta$. When this equals $n\lambda$ the Bragg equation is the resulting constructive interference produces a diffraction maximum or “reflection”.

Furthermore considers diffraction of x-rays from lattice planes in a unit cell, these planes must be designated in a consistent manner. This is done by assigning Miller indices to the lattice planes. Miller indices are represented by (hkl) values, which these are the indices hkl ; the spacing between successive planes is determined by the lattice geometry. Miller indices are also used to designate lattice points hkl that correspond to the (hkl) family of planes. Each “reflection” of an x-ray from a crystal is assigned a unique hkl value. Miller indices representing lattice planes and lattice points are shown in Figure 2.6 (a) and (b), respectively (Drago, 1992, pp689-691).



(a) Direct Lattice



(b) Reciprocal Lattice

Figure 2.6. Direct and Reciprocal Lattices.

X-Ray Versus Neutron Diffraction

X-ray and neutron diffraction can be used as complimentary techniques because of both similarities and differences between them. There is a fundamental physical difference the x-ray and neutrons are scattered by matter. Whereas x-ray diffraction is scattered by electron shells, however neutrons are scattered by atomic nuclei. A result of this is that the scattering factors for neutrons are not proportional to Z as are those for x-ray, nor do they diminish greatly with scattering angle. On the other hand, (Figure 2.7) neutron scattering by a stationary atom does not fall off at higher angle like that of x-ray; lower intensities at higher angles are due entirely to atomic vibrations. It is significant scattering takes place only when a neutron passes close to a nucleus, and on average the total intensity of diffraction of neutron by a crystal is low compared with that of x-rays. The relative weak scattering means that larger crystals are preferred for neutron diffraction.

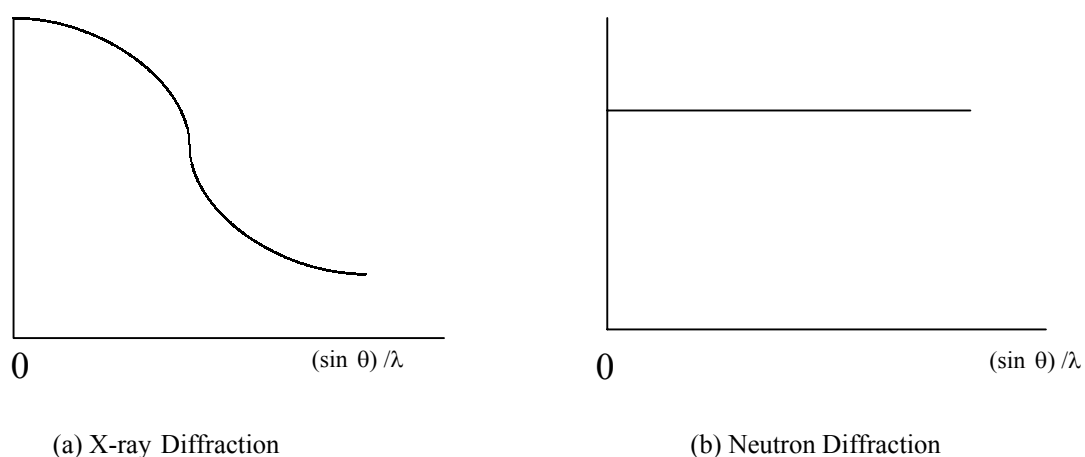


Figure 2.7. Variation of X-Ray and Neutron Atomic Scattering Factors with Scattering Angle for Stationary Atoms.

In traditional x-ray crystallography the electron density of each atom is assumed to be distributed symmetrically about the nucleus. This interpretation is more or less valid, but in reality there are deviations from spherical symmetry, caused by chemical bonding and other valence effects. The deviation from this idealized model is particularly great for hydrogen atoms which do not have core electrons, and are therefore consistently located too close to their bonded atoms by the x-ray diffraction technique.

There are more advanced types of experiment, in which both x-ray and neutrons are used to study the same structure. Since neutrons locate nuclei, from which core electron density can be calculated, and x-rays reveal the total electron density distribution, the combination provides a means of mapping valence electrons and bonding effects.

For neutron diffraction studies of hydrogen containing compounds, it is therefore advantageous to use perdeuterated samples wherever possible. Deuterium (^2H) has a larger coherent scattering amplitude and gives a much lower incoherent background than hydrogen (^1H).

The Location of Hydrogen Atoms

For studies in which precise and accurate hydrogen atom location is important, neutron diffraction is the method of choice. With single crystals, neutron diffraction studies provide a wealth of structural information for which neutron diffraction is far superior to x-ray diffraction. Especially for deuterated compounds, the neutron result is more precise, because H/D atoms scatter relatively strongly. Neutron diffraction is particularly useful in locating light atoms in crystal especially hydrogen atom positions with high accuracy because the degree of scattering by nuclei does not vary significantly with atomic number. Hydrogen atom positions are somewhat unreliable, and distinguishing between hydrogen and deuterium is nearly impossible when determined by x-ray diffraction. In neutron diffraction, because hydrogen has a negative scattering factor, whereas deuterium has a positive scattering factor, they are easily distinguished from one another.

Neutron diffraction results also have the advantage that atomic positions determined correspond to nuclear positions rather than to centroids of electron density peaks, and that the derived thermal vibrational parameters correspond more closely to the actual atomic vibrations. In x-ray analysis, deviations of the density peaks from sphericity that are caused by bonding tend to get absorbed in the thermal vibration parameters. As a result, vibrational parameters estimated from x-ray data tend to be somewhat too large.

It is generally understood that different techniques for measuring a given interatomic distance will not necessarily yield identical values. Thus, while techniques such as neutron diffraction, electron diffraction, and molecular spectroscopy give essentially equivalent results for an internuclear distance, bond distances involving

hydrogen as measured by x-ray diffraction techniques are systematically shortened. This discrepancy arises because the bond lengths as determined by the x-ray diffraction technique is a measure of the distance between the centroids of electron density of the two atoms concerned. The centroid of electron density around a covalently bonded hydrogen atom is not coincident with its nuclear position but is displaced significantly in the direction of the atom bonded to the hydrogen atom.

The limitation for other computational procedures hydrogen atom positions such as in addition hydrogen atoms tend to have larger librational amplitudes than other atoms. For most purposes it is preferable to calculate the hydrogen positions according to well-established geometrical criteria and then to adopt a refinement procedure which ensures that a sensible geometry is retained. The hydrogen distance values at low temperatures are increased by 0.01 or 0.02 Å from room temperature.

Carbon-Hydrogen Distances

In fact, H-atom coordinates are often missing from the CSD. Since hydrogen atoms play an important role in crystal packing, their positions are recalculated using standard geometrical criteria (Burgi & Dunitz, 1994, p510-511). For this study the C–H distance is set at 1.083 Å and the two H–C–C angles are assumed to be equal.

Chapter III

Experimental

3.1. Instrumentation

Instrumentation utilized for the studies reported in this thesis were located at Suranaree University of Technology unless otherwise noted in the following.

Spectral Measurement

Infrared spectra were measured on a Perkin-Elmer Model Spectrum GX (30-7000 cm^{-1}) infrared spectrophotometer. Spectra were obtained from KBr pellets.

Single Crystal X-ray Diffraction

Data were collected on the Nonius KappaCCD area detector diffractometer at the Research School of Chemistry, The Australian National University. The ANU KappaCCD system is equipped with an Oxford Cryosystems 600 variable temperature device capable of producing temperatures at the crystal from near liquid nitrogen temperature to 373 K. The operating temperature of the Cryosystems 600 was 200 K. The ANU system is connected to the internet so moderate sized files could be transferred to SUT electronically. However, due to limitations imposed on attachment size by the Center for Computing Services at SUT full frame data files could not be transferred by internet and were written to CD ROM for transfer.

The diffractometer was equipped with a highly-oriented pyrolytic graphite crystal incident beam monochromator and a molybdenum $K\alpha$ ($\lambda = 0.71073 \text{ \AA}$) x-radiation source operated at tube power levels of 50 kV and 20 mA. The KappaCCD has *ifg* focusing optics incident beam collimators which increase the x-ray intensity at the sample by approximately 50-80% for molybdenum $K\alpha$ radiation. Due to the specialized nature of area detector diffractometers and to detector specific corrections, the raw frame data must be reduced to structure factors by the software that is delivered with each individual diffractometer. This requirement produces the disadvantage that the data reduction cannot be optimized based on knowledge gained

during the structure solution and refinement stages. Additional details of the data collection and reduction are given in the relevant section of Chapter IV.

3.2. Materials and Equipment

Chemicals

1. Ethyl alcohol absolute (C_2H_6O); Carlo Erba reagent, (v/v) 99.8%, Mr 46.070, Code No. 414607 CAS No. 64-17-5.
2. Glacial acetic acid (CH_3COOH); Baker Analyzed reagent, 99.9%, Mr 60.05.
3. *n*-Hexane ($CH_3(CH_2)_4CH_3$); Carlo Erba reagent RPE, 99% (GLC), Mr 86.173, Code No. 446903 CAS No. 110-54-3.
4. Methanol (CH_3OH); Carlo Erba reagent RPE, 99%, Mr 32.042 Code No. 414816, CAS No. 67-56-1.
5. 2-Propanol ($CH_3CH(OH)CH_3$); Merck grade, Mr 60.10 g/mol, 1.09634 2500 k21971834.
6. Tetrahydrofuran (THF, (C_4H_8O)); Mallinckrodt chrom AR HPLC, Mr 72.11, Lot. 2858 KTVY-P.
7. Sodium bromide (NaBr); Fluka chemika, 99.0% (AT), Mr 102.90, 71330.
8. Sodium nitrite ($NaNO_2$), Mr 69.00.
9. Triphenylphosphine (PPh_3); Fluka, ~99% (HPLC), Mr 262.30 (603-35-0), Lot & Filling code:396768/1 42199.
10. Nickel nitrate hexahydrate ($Ni(NO_3)_2 \cdot 6H_2O$); Laboratory UNILAB reagent, AJAX Chemicals, 97.0% min, Mr 290.81, UN No. 2725.
11. Nickel chloride hexahydrate ($NiCl_2 \cdot 6H_2O$); Mr 237.71.
12. Distilled water.
13. Silicone grease.
14. Molecular Sieve No. 4A; Union Carbide Company.
15. Molecular Sieve No. 5A.
16. Nitrogen; H.P. grade 99.95%; TIG company.

All solvents and solid reagents were dried as described in section 3.3.

Equipment

Since nitrosyl bistrisphenylphosphine nickel complexes are sensitive to oxygen and water while in solution, operations were carried out using standard Schlenk apparatus connected to a double-manifold vacuum/nitrogen line. A nitrogen atmosphere was maintained over all solutions (Shriver & Drezdson, 1986).

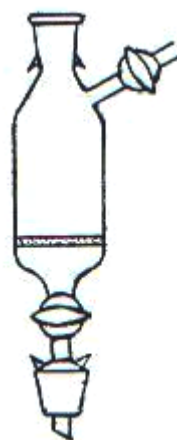
The Schlenk glassware are apparatus for maintaining an inert atmosphere during drying of reagents or solvents, preparation, filtration, crystallization, and sample transfer. Essential features of the apparatus are appropriate sidearms fitted with stopcocks and ground joints to connect various parts of the apparatus. Through these sidearms the equipment is evacuated to eliminate air and an inert gas is introduced. Basic pieces of apparatus include the Schlenk tube, the fritte, the solids container, and the dropping funnel as illustrated in Figure 3.1.

The double-manifold vacuum/inert atmosphere line (Figure 3.1) allows several pieces of apparatus to be independently used at the same time. The two manifolds are joined by a series of two-way stopcocks, which provide a ready means of switching between inert gas and vacuum. Attached to the manifold are a source of purified nitrogen or argon and a source of vacuum. Purified nitrogen was used for the experiments reported herein. The source of purified nitrogen has an oil bubbler which serves as an approximate flow indicator.

The source of vacuum is a mechanical vacuum pump protected by a dry ice-cooled or liquid nitrogen-cooled solvent trap through which all vapors from the Schlenk line pass before reaching the vacuum pump. The choice of dry ice or liquid nitrogen to cool the trap depends on the volatility of the solvents being used. Use of dry ice is only possible when all the solvents are high boiling liquids. This trap must be of large volume and easily removable since it accumulates a considerable amount of condensable. For reaction which are completed in a relatively short time or for moderately air sensitive materials Tygon tubing is acceptable for connecting the various components to material. If components of the reaction have greater air sensitivity or the length of time is long, butyl rubber tubing must be used to solve the problem of gas diffusion which occurs with Tygon tubing.



Dropping Funnel



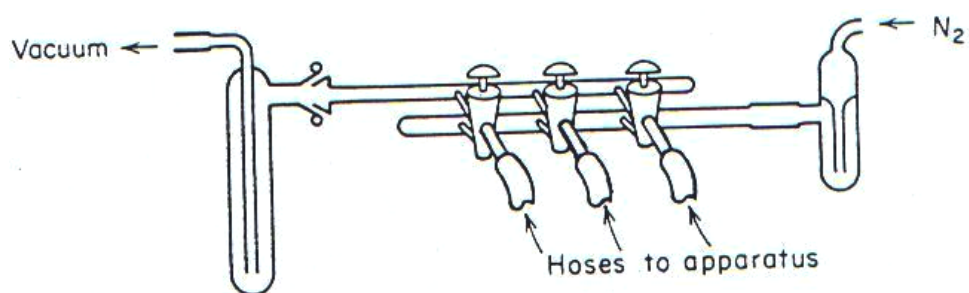
Fritte or Fritted Funnel



Schlenk Tube



Solids Container



Double-Manifold Vacuum/Inert

Figure 3.1. Schlenk Glassware and Vacuum/Inert Atmosphere Line.

3.3 Techniques

Schlenk Techniques

Leak Protection: It is important that leakage into the system is minimized during this process by ensuring that stopcocks or joints are not striated by silicone grease in conjunction with the Schlenk glassware. When lubricating ground-glass joints:

1. Lubricate only the upper part of the inner joint.
2. Avoid greasing any part of the joint which may come in contact with vapor or liquid and cause contamination. Silicone grease is especially soluble in chlorinated solvents.

Solvent Trap Maintenance: Close stopcocks of manifold and remove the tubing that connects between manifold and solvent trap from manifold before turning off the mechanical vacuum pump, so that solvent does not suck back to manifold. The trap may be cleaned with acetone. A liquid nitrogen trap must never be connected to a manifold where the vacuum source has been turned off. Failure to remove a liquid nitrogen trap from a manifold after shutting off the vacuum will result in the condensation of liquid air in the trap. If warmed up, this liquid air will evaporate and may pressurize the apparatus, presenting an extreme explosion hazard.

Maintaining an Inert Atmosphere: Description of valve manipulation to always keep N₂ over reagents and reactions. In these experiments a high vacuum is not necessary because the purge cycle is repeated several times. The frequency with which these purging cycle are performed that the manifold by an initial stopcock is opened to vacuum for pumping to eliminate air in equipment (such as a reaction Schlenk tube before reaction) then turn on stopcock to nitrogen line for filling with inert gas. In many operations it is necessary to open the apparatus briefly. In these cases turn on the stopcock to the nitrogen line so an inert atmosphere flush is maintained out of the opening to minimize the entrance of air. The entrance of air may also be reduced by using a long-necked flask with a small cross section for the neck.

Drying Solid Reagents: Solid reagents were dried under vacuum over Molecular Sieve No. 5A by placing Molecular Sieve in one solids container connected to the vacuum manifold (Figure 3.2a) and the solid reagent in the other solids container, both connected together with ground joint. When the solid reagents

are dried under vacuum the moisture in the solid reagents are absorbed in the Molecular Sieve until the solid reagents are dried to a fine powder such as NaNO_2 or to plates such as PPh_3 , which pour freely when the solids container is gently shaken.

Drying Solvent Reagents: All of the solvents were dried conveniently by use of 1/6-in. pellets of No. 5A Molecular Sieve placed in the solvent (except methanol for which No. 4A Molecular Sieve was used). Each solvent was degassed by purging nitrogen through it just prior to use (Figure 3.2b).

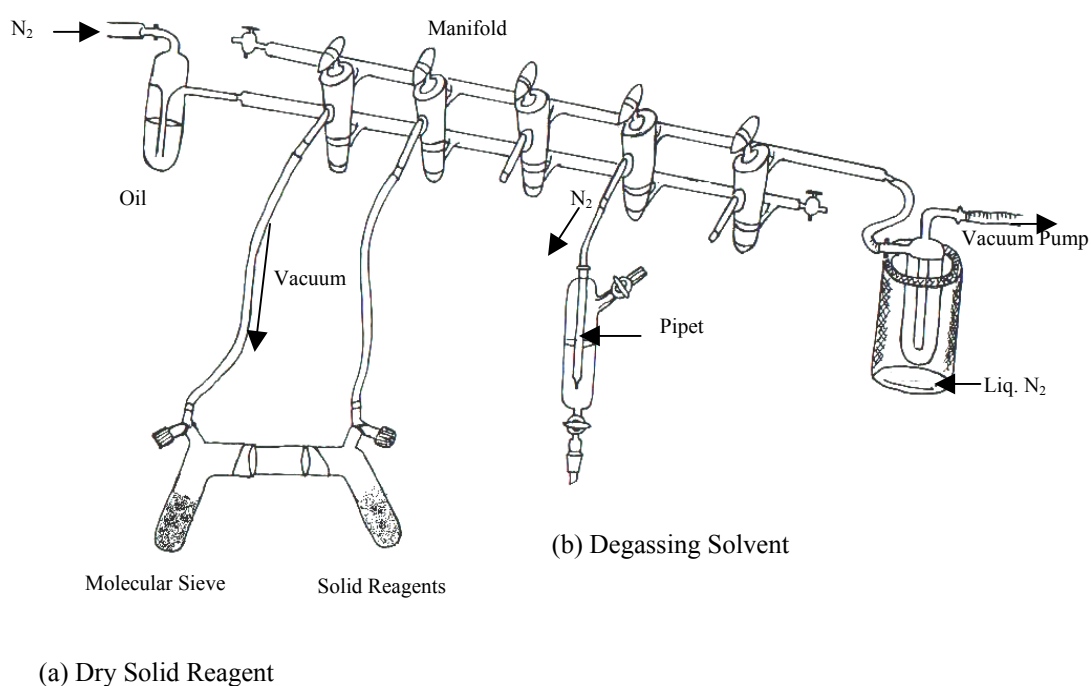


Figure 3.2. Drying Solid Reagents and Solvents.

Refluxing under an Inert Atmosphere: (Figure 3.3): (Errington, 1997). The reflux procedure allows one to heat a reaction mixture for an extended period of time without loss of solvent. The condenser, which is fixed in a vertical position directly above the heated flask, condenses all vapors to liquid. Because none of the vapors escape, the volume of liquid remains constant. Reflux procedures are carried out as follows:

1. The Schlenk tube is charged with reactants and solvent as described for each experiment. The level of solvent is less than half full. A few boiling stones are

added to prevent bumping. A brisk nitrogen flush from the direction of stopcock on the Schlenk tube.

2. Attach a stopcock to condenser and turn on the stopcock for flush the condenser several times with nitrogen and while attach to the Schlenk tube.

3. Attach the condenser to the Schlenk tube and ensure that there are no leaks. (Check the bubbler on the nitrogen line. If it leaks there will be no bubbles on the oil bubbler.)

4. Turn on the cooling water. The water inlet to the condenser is the lower one. The water outlet to the condenser is the upper one.

5. Heat the Schlenk tube gradually until the solvent reflux for starting the desired period of time. While refluxing close the condenser and Schlenk stopcock. In reactions where a gas is evolved, it can be swept out of the apparatus by attaching a bubbler to the top of the condenser and maintaining a slow stream of nitrogen through the system.

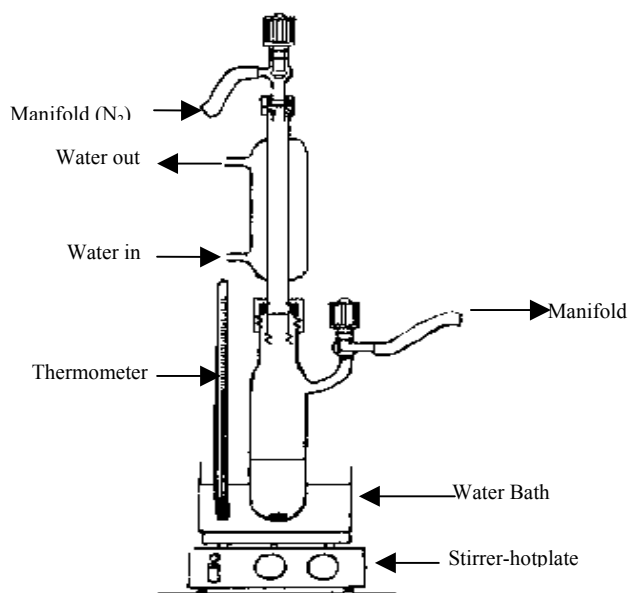


Figure 3.3. Refluxing under an Inert Atmosphere.

Filtration under an Inert Atmosphere: These are using a fine porosity glass sintered fritte. All glassware must be cleaned and dried before use.

1. Assemble the fritte and receiver Schlenk tube (Figure 3.4a) attach the receiver Schlenk tube to the manifold and flush the apparatus with nitrogen and then repeat the purging process a couple of times.

2. Turn up the nitrogen flow to both receiver Schlenk tube and reaction Schlenk tube and connect the reaction Schlenk tube to the inverted fritte so that all the taps are aligned on the same side (Figure 3.4b). Make sure there are no leaks and that the two Schlenk tubes are securely connected to the fritte.

3. Hold the apparatus in two hands and, while swirling the reaction flask to suspend the solid in the liquid, carefully tilt the apparatus with the taps pointing upwards so that the suspension pours into the fritte without entering the side tube.

4. Gradually bring the apparatus to the vertical position and allow the solid to settle out under gravity (Fig 3.4c). If the solid is finely divided, it is important to keep both (receiver and reaction Schlenk tube) taps open to nitrogen at this stage, as a pressure differential may force some of the fine solid through the sinter.

5. Once a pad of solid has formed on the sinter, the filtration rate can be increased by a slight reduction in the pressure below the sinter by opening the Schlenk tube receiver stopcock to vacuum adjust a few. This procedure prevent too great a pressure reduction which may cause finely divided solid to enter receiver or block the sinter.

6. Disconnect the receiver under a nitrogen stream and stopper the receiver Schlenk tube (Fig 3.4d). Clean the filter immediately after use and dry it in a hot oven.

Filtration under an Air Atmosphere: Buchner funnel wet the filter paper with solvent, apply vacuum to be sure the filter paper lies flat so crystals cannot escape around the edge and under the filter paper, then pour the solution on the filter paper. The precipitate on the filter may be washed with small volumes of cold solvent and dried by suction of aspirator pump. Always remove the tubing from your Buchner flask before you turn off the water tap, so that water does not suck back.

Crystallization under an Air Atmosphere: Scratching the inside of flask with a stirring rod at the air-liquid interface can often induce crystallization. One theory holds that part of the freshly scratched glass surface has angles and planes corresponding to the crystal structure, and crystals start growing on these spots.

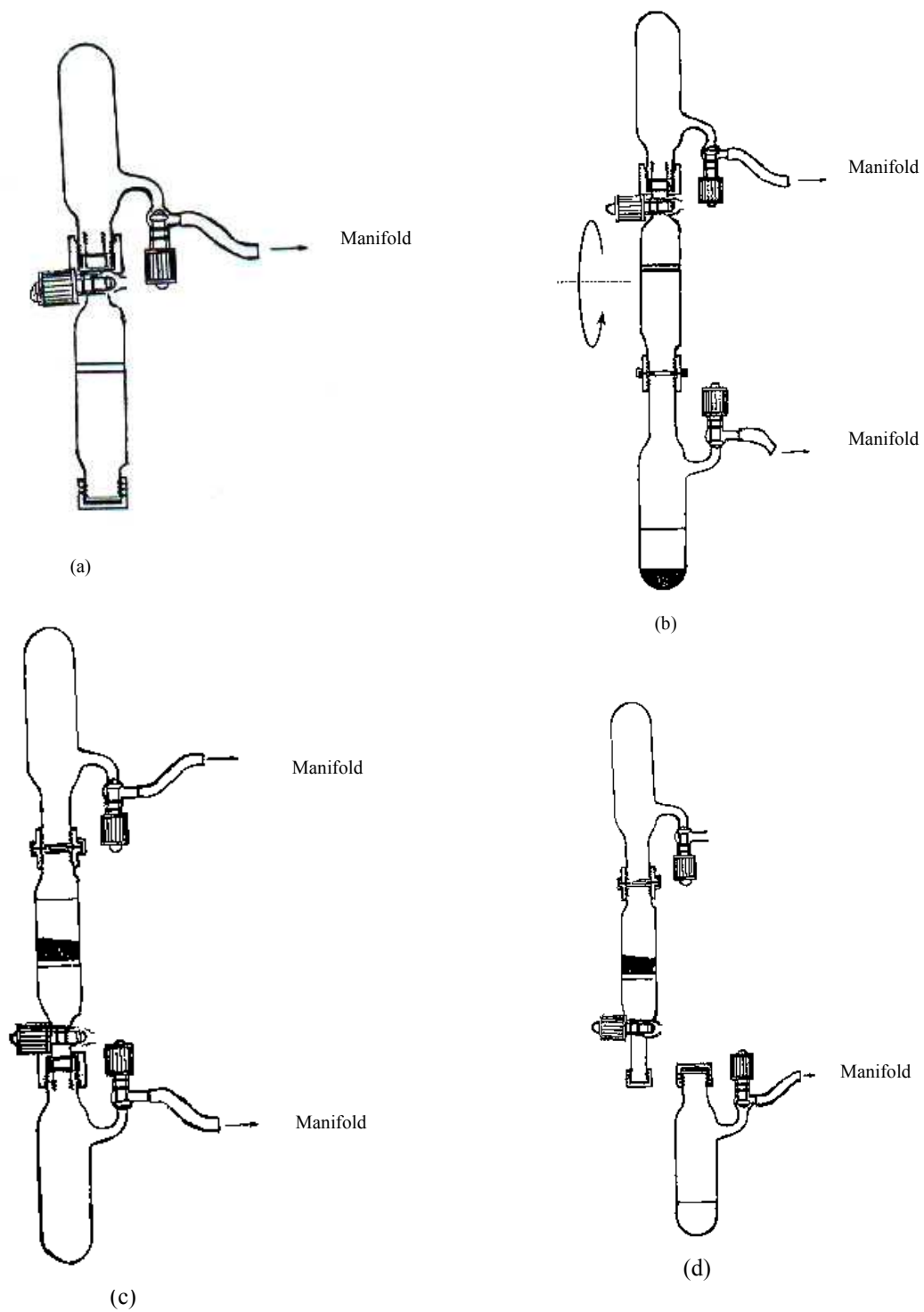


Figure 3.4 Filtration under an Inert Atmosphere.

Recrystallization: The optimum size for a crystal for a single crystal x-ray structure determination is one which has dimensions of approximately 0.2 – 0.4 mm in at least two of the three dimensions. Often, crystals obtained from reactions are finer precipitates so must be recrystallized to obtain a suitable size. Furthermore, precipitation is a relatively fast process and occurs in minutes or hours. In this case impurities in the solution are often trapped as the precipitate forms, resulting in impure crystals. The impurity is effected to size and single crystal. The crystallization process is very slow and requires relatively long periods of time (day to weeks) to ensure that no impurities will be trapped in the crystal lattice as the crystal grows. Thus a solid is often simultaneously purified as suitable for single crystals are formed by recrystallization.

Recrystallization by dissolving the compound in a hot solvent until saturated solution, filtering the solution to separate solid impurities from the solution and then allowing the desired crystals to form in the filtrate while the impurities remain in solution by following factor and techniques.

Several factors which affect the size of the crystals during crystal growth are:

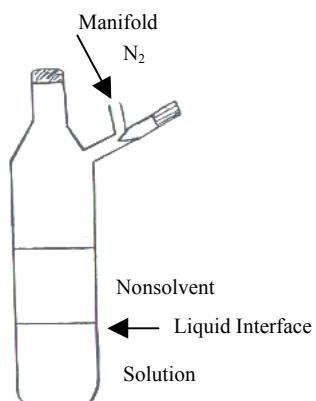
1. Solvent. Choose a solvent in which compound is moderately soluble. If the solute is too soluble, this will often result in small crystal size. Avoid solvents in which the compound forms supersaturated solutions. Supersaturated solutions tend to give crystals which are too small size.

2. Nucleation. Many nucleation site results in a smaller average crystal size, and is not desirable. Conversely, the fewer site at which crystals begin to grow will result in fewer crystals each of larger size. In many recrystallizations ambient dust in the laboratory provide sites of nucleation. It is important to minimize dust or other extraneous particulate matter in the crystal growing vessel.

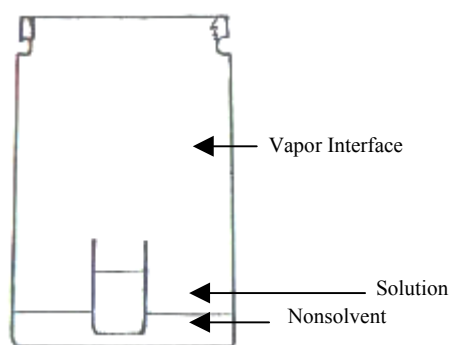
3. Mechanics. Mechanical disturbance of the crystal growing vessel results in size of crystals.

4. Time. This is related to mechanics.

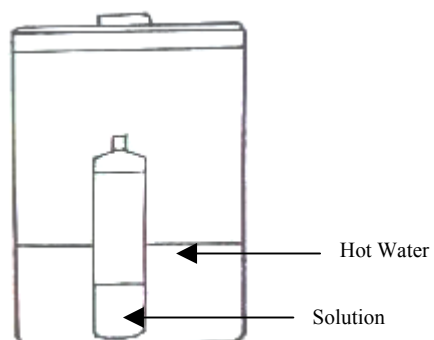
Solvent Diffusion (Layer Technique): (Figure 3.5a) This method is good for milligram amounts of materials which are moderately sensitive to ambient conditions (air, moisture) by using Schlenk glassware and maintaining a nitrogen atmosphere throughout the experiment. If the density of the solution is greater than that of the



(3.5a) Solvent Diffusion (Layer Technique)



(3.5b) Vapor Diffusion



(3.5c) Slow Cooling

Figure 3.5. Recrystallization.

nonsolvent place the solution in the Schlenk tube and slowly add the nonsolvent down the wall of the tube so it forms a layer on top of the solution. Stopper, purge to establish a nitrogen atmosphere, then close the stopcock to maintain the nitrogen atmosphere over the solution. Set the apparatus in a quiet place at about 23°C for 2-3 days. If the density of the nonsolvent is greater than that of the solution place the nonsolvent in the tube first and dribble the solution on the top of it.

Vapor Diffusion: (Fig 3.5b) A filtrate is placed in a small tube which is placed inside the larger container. A second solvent (nonsolvent) is placed in the outer container. The nonsolvent is chosen such that when mixed with the solution, the solute will become less soluble. The outer container is sealed and placed in a quiet place. Slow diffusion of nonsolvent into the solution and of solvent out of the solution will cause crystals to form. If the nonsolvent is more volatile than the solvent the solution level will increase, preventing microcrystalline crusts from forming on the sides of the small tube.

Slow Cooling: (Figure 3.5c) This is good for solute-solvent systems which are less than moderately soluble and the solvent's boiling point is less than 100°C. A saturated solution of the compound is heated to or just below its boiling point. Transfer the solution to a clean tube and stopper. Transfer the test tube to a dewar flask containing water heated to a temperature just below the solvent boiling point. The water level must exceed the solvent level in the test tube, but can be adjusted to change the thermal mass of the system and thus the rate of cooling. Cover the dewar flask to retain heat and allow the vessel to stand until cool.

Preparation of IR Samples by the alkali halide disc method. This method involves mixing 2-3 mg of solid sample with 100-200 mg dry alkali halide powder (potassium bromide (KBr) is completely transparent in the mid-infrared region), the mixture is ground with an agate mortar and pestle, and subjected to a pressure of about 10 ton in⁻² (1.575×10^5 kg cm⁻²) in an evacuated die. This sinters the mixture and produces a clear transparent disc. Certain factors need to be considered when preparing KBr discs. The following problems may arise:

1. The ratio of the sample to KBr is wrong.
2. The disc is too thick or too thin. Thin discs are fragile and difficult to handle, while thick discs transmit too little radiation. A disc of about 1 cm diameter

made from about 200 mg of material usually results in a good thickness of about 1 mm.

3. The crystal size of the sample is too large. Excessive scattering of radiation results, particularly at high wavenumbers. The crystal size must be reduced, normally by grinding the solid using a mortar and pestle.

4. The KBr is not perfectly dry. This results in the appearance of bands due to water. The KBr is kept desiccated and warm prior to use and discs are made just prior to use to minimize this problem.

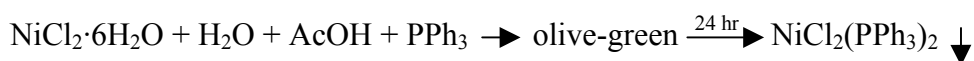
3.4 Synthesis

Preparation of $\text{NiX(NO)}(\text{PPh}_3)_2$ compounds were carried out as two steps.

Preparation of Bistriphenylphosphinedihalonickel complexes

Bistriphenylphosphinedichloronickel ($\text{NiCl}_2(\text{PPh}_3)_2$) (Venanzi, 1958).

A solution of nickel chloride hexahydrate 2.3794 g, 0.01 mole in 2 mL water in a 150 mL erlenmeyer flask was dissolved with glacial acetic acid 50 mL. To this solution is added a solution of triphenylphosphine 5.2474 g, 0.02 mole dissolved in 25 mL glacial acetic acid in a 50 mL erlenmeyer flask with gentle warming to insure solution. The olive-green microcrystalline precipitate, when kept in contact with its mother-liquor (glacial acetic) for 24 hr, gave dark blue crystals which were filtered off using a Buchner funnel. Yield of dark blue $\text{NiCl}_2(\text{PPh}_3)_2$ 5.252 g, 0.0080 mole (80.29%). Melting point and IR peaks are tabulated at the end of the experimental section. Additional characterizations were not attempted.



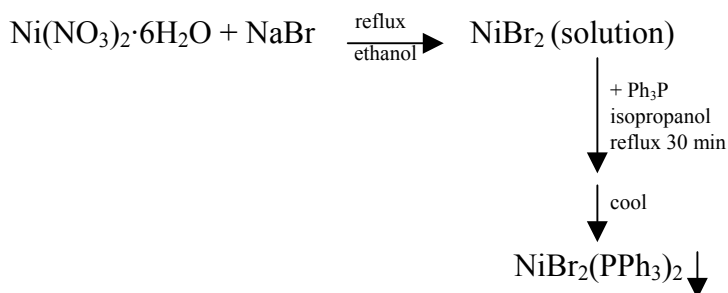
Preparation of Bistriphenylphosphinedibromonickel Complexes ($\text{NiBr}_2(\text{PPh}_3)_2$) (Parkin, 1994).

Charge a 250 mL round bottomed flask with nickel nitrate 1.5294 g, 0.00526 mole, ethanol 25 mL and five glass beads stir or swirl, heating gently, to dissolve. Add finely ground sodium bromide 1.1172 g, 0.01086 mole. Fit the flask with a reflux condenser and reflux on a water bath for 20 minutes to produce the green bromide solution. During the time the reflux is continuing, prepare a solution of 2.8102 g, 0.0107 mole of triphenylphosphine in 30 mL of propan-2-ol dried over No. 5A

Molecular Sieve in a dry 250 mL round bottomed flask. Add five glass beads, fit the flask with a reflux condenser, and bring to reflux on a steam bath.

Cool the green bromide solution in an ice bath. Scratch the inside of the flask with a glass rod to precipitate the sodium nitrate and any unreacted sodium bromide. Filter the nickel bromide solution through a Buchner funnel into a filter flask. Transfer the green bromide solution transferred to a conical flask with three glass beads and heated gently on a hotplate.

Add the hot nickel bromide solution to the refluxing triphenylphosphine solution by carefully pouring it down the reflux condenser. Allow the reflux to continue for 30 minutes. Cool the reaction mixture to room temperature and place in a quiet place for 2 days to obtain a green product. Filter with a Buchner funnel and wash the green precipitate on the filter with cold ethanol. Yield of green $\text{NiBr}_2(\text{PPh}_3)_2$ 2.5957 g, 0.00349 mole (67.73%). Melting point and IR peaks are tabulated at the end of the experimental section. Additional characterizations were not attempted.



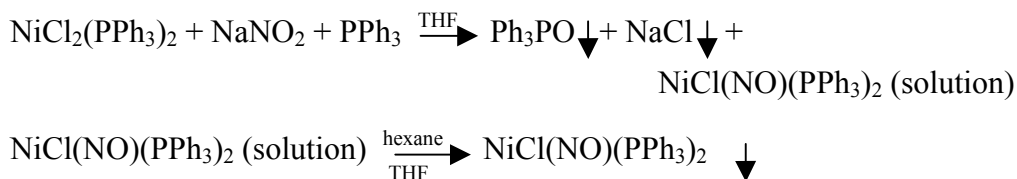
Preparation of Bistriphenylphosphinehalonitrosylnickel Complexes (Feltham, 1963).

Preparation of Bistriphenylphosphinechloronitrosylnickel complexes by reaction of $\text{NiCl}_2(\text{PPh}_3)_2$ with NaNO_2 to form $\text{NiCl}(\text{NO})(\text{PPh}_3)_2$.

A mixture of 4.4477 g, 0.00680 mole of $\text{NiCl}_2(\text{PPh}_3)_2$ as prepared above and 1.7747 g, 0.00676 mole of PPh_3 were dissolved in 50 mL of THF. Freshly ground NaNO_2 , 7.9945 g, 0.11586 mole, dried under vacuum over Molecular Sieve No. 5A, was added along with five glass beads to a standard Schlenk apparatus connected to a double manifold vacuum/nitrogen line. The solution was refluxed under a nitrogen atmosphere for 35 min on a steam bath, cooled, filtered, and concentrated to 35 mL. Addition of 25 mL of n-hexane gave a blue oil which was separated and treated with 50 mL of cold methanol to induce crystallization. The dark blue $\text{NiCl}(\text{NO})(\text{PPh}_3)_2$

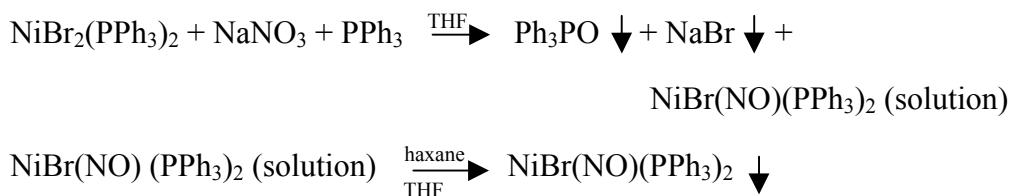
crystals were separated and dried yielding 1.4373 g, 0.00221 mole (32.59%). Melting point and IR peaks are tabulated at the end of the experimental section.

The product crystals were recrystallized from THF/hexane by liquid diffusion. A single crystal examined by a single crystal x-ray diffraction experiment gave the results reported on page 43. Additional characterizations were not attempted.



Preparation of Bistriphenylphosphinebromonitrosylnickel complexes by reaction of NiBr₂(PPh₃)₂ with NaNO₂ to form NiBr(NO)(PPh₃)₂.

A mixture of 7.5258 g, 0.0101 mole of NiBr₂(PPh₃)₂ as prepared above and 2.6551 g, 0.0101 mole of PPh₃ were dissolved in 75 mL of THF. Freshly ground NaNO₂ 11.9912 g, 0.1738 mole, dried under vacuum over Molecular Sieve No. 5A, was added along with seven glass beads to a standard Schlenk apparatus connected to a double manifold vacuum/nitrogen line. The solution was refluxed under a nitrogen atmosphere for 35 min on a steam bath, cooled, filtered, and concentrated to 50 mL. Addition of 40 mL of n-hexane gave a blue oil which was separated and treated with 50 mL of cold methanol to induce crystallization. The dark blue NiBr(NO)(PPh₃)₂ crystals were separated and dried yielding 2.671 g, 0.0033 mole (32.40%). Melting point and IR peaks are tabulated at the end of the experimental section. The sample was recrystallized from THF/hexane by liquid diffusion. Additional characterizations were not attempted.



Characterization

Study of Infrared Spectra

The NiX₂(PPh₃)₂ and NiX(NO)(PPh₃)₂ complexes where X = Br, Cl were characterized by infrared spectra. The infrared spectra of these compounds are shown in Figure 3.6 and 3.7 and the infrared frequencies in Table 3.1. The NiBr(NO)(PPh₃)₂

gives stretching frequencies at 1733, 419 and 374 cm^{-1} . The $\text{NiCl}(\text{NO})(\text{PPh}_3)_2$ gives stretching frequencies which are different $\text{NiBr}(\text{NO})(\text{PPh}_3)_2$ at 1713, 1263, 1156, 846, 801, 722, 576 and 419 cm^{-1} . It has been formerly reported by Nakamoto (1997, p185) that nickel-halide stretching of $\text{NiX}_2(\text{PPh}_3)_2$ where $\text{X} = \text{Br}^-$, Cl^- is about 341-215 cm^{-1} . The result of previous workers showed that Ni-P bands are near 450-410 cm^{-1} (Nakamoto, 1997, p197), hence, the bands found at 419 cm^{-1} in the two complexes are assigned to be the nickel-phosphorus stretching bands.

Table 3.1 Physical Characterization of $\text{NiX}_2(\text{PPh}_3)_2$ and $\text{NiX}(\text{NO})(\text{PPh}_3)_2$ where $\text{X} = \text{Br}^-$, Cl^- .

Complexes	% Yield	Color	Melting Point (C°)	Infrared Frequencies (cm^{-1})		
				ν_{NO}	ν_{NiN}	ν_{NiP}
$\text{NiCl}_2(\text{PPh}_3)_2$	80.29	olive green	247-250			418 ^w
$\text{NiBr}_2(\text{PPh}_3)_2$	67.78	green	222-225			418 ^w
$\text{NiCl}(\text{NO})(\text{PPh}_3)_2$	32.59	dark blue	209-210	1715 ^s	573	419 ^m
$\text{NiBr}(\text{NO})(\text{PPh}_3)_2$	62.14	green blue	200-203	1733 ^s	573	419 ^w

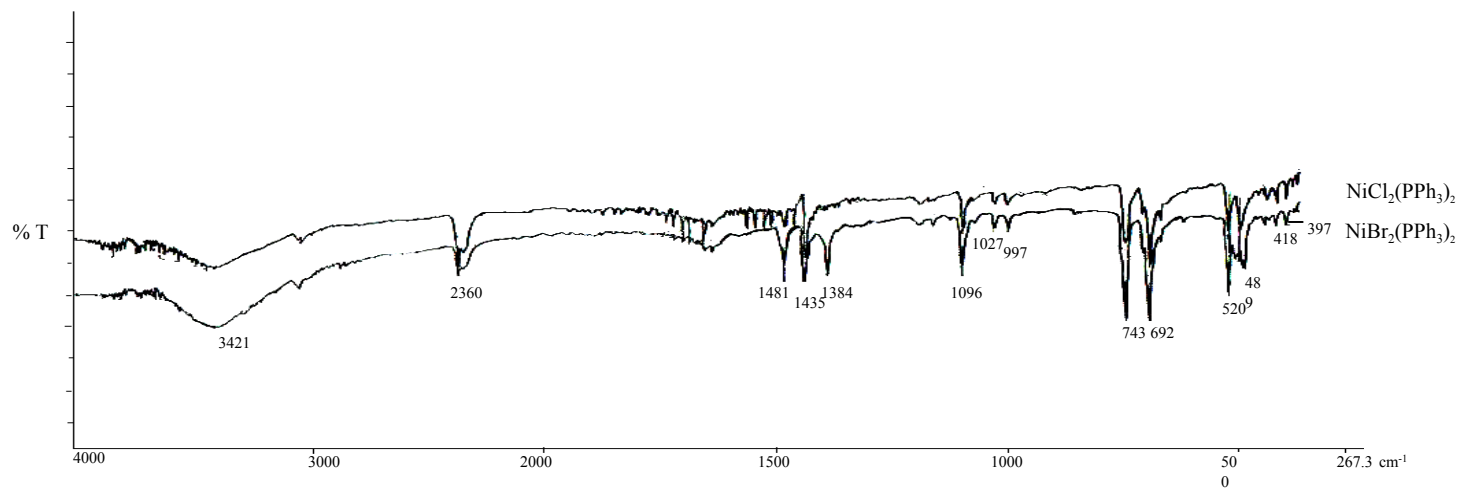


Figure 3.6. IR Spectra of $\text{NiCl}_2(\text{PPh}_3)_2$ and $\text{NiBr}_2(\text{PPh}_3)_2$.

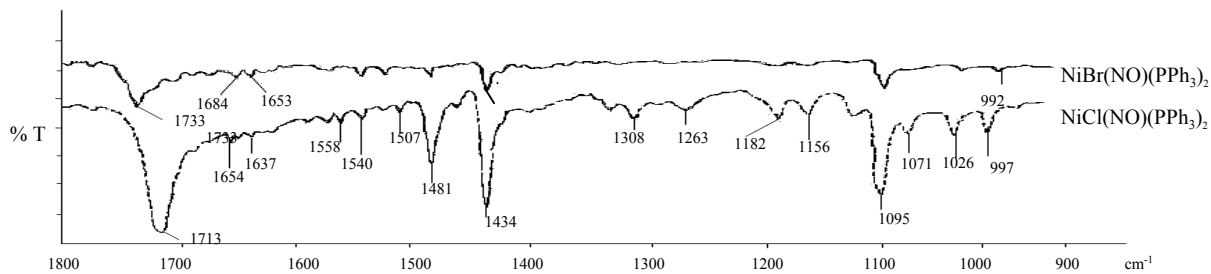
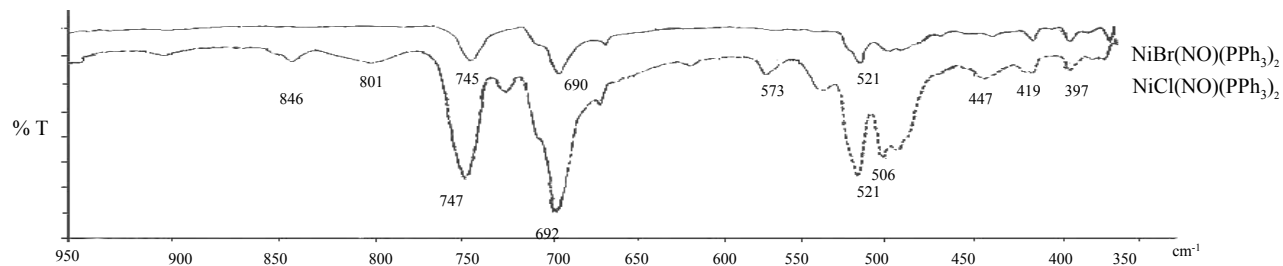


Figure 3.7. IR Spectra of $\text{NiCl}(\text{NO})(\text{PPh}_3)_2$ and $\text{NiBr}(\text{NO})(\text{PPh}_3)_2$.

Data Collection and Structure Work from Single Crystal X-ray Diffraction.

Crystal data: $C_{36}H_{30}NiCl_2P_2$, $M_r = 654.159$ Daltons, olive green square plate, $0.16 \times 0.25 \times 0.29$ mm, $T = 200$ K; monoclinic, $P2/c$ (No.13) $a = 11.6298(3)$ Å $b = 8.1224(2)$ Å $c = 17.2972(4)$ Å, $\beta = 107.094(1)^\circ$, $V = 1561.74(7)$ Å³, $Z = 2$, $d_{\text{calc}} = 1.391$ Mg/m³, $\lambda_{\text{MoK}\alpha} = 0.71073$ Å, $\mu = 9.2$ cm⁻¹, 24,324 data collected, 3890 unique data, multiscan absorption correction, 3,316 unique observed data ($F_o > 4\delta(F_o)$), $F(000) = 676$, $R_{\text{merge}}(\text{sym}) = 0.042$, $R_1(\text{obs}) = 0.0370$, $wR_2(\text{all}) = 0.0971$, max $c/e = 0.002$, max correlation coefficient = 0.563, $\rho_{\text{max}} = 0.52$ e/Å³, $\rho_{\text{min}} = -0.51$ e/Å³, $\rho_{\text{error}} = 0.07$ e/Å³.

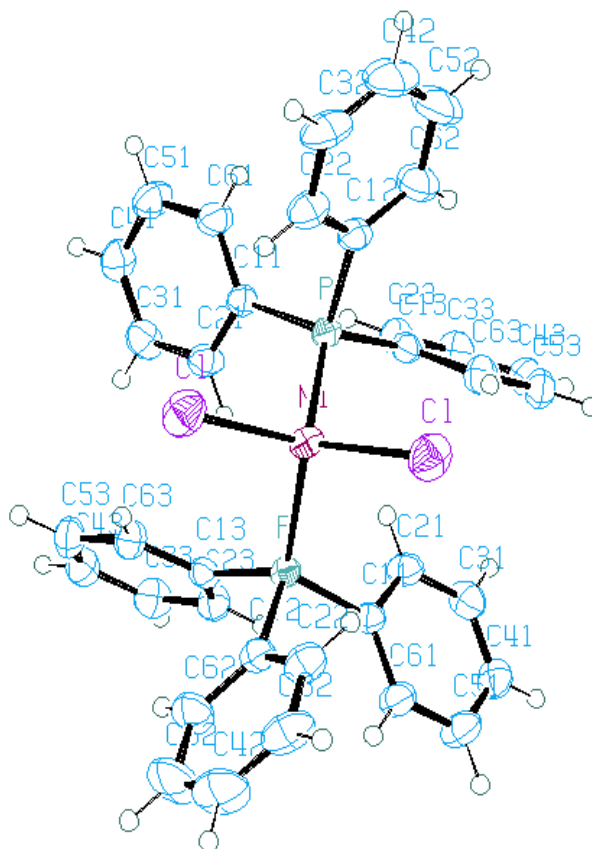


Figure 3.8. Molecular Structure $NiCl_2(PPh_3)_2$.

3.5 Analysis of Crystal Structure

Methodology

Data were obtained from the December, 1999 release of the Cambridge Structural Data base (CSD) in the form of crystallographic information files or *cif* files (Hall, Allen & Brown, 1991). Reference code AZNPNI is from *Four-Coordinate Metal Nitrosyls. I. The Structure of Azidonitrosylbis(triphenylphosphine)nickel, NiN₃(NO)(PPh₃)₂* from Enemark, (1971). CLTPNI01 and TPNTCN are from *Four-Coordinate Metal Nitrosyls. 2. Structure of NiX(NO)(PPh₃)₂ Complexes* from Haller & Enemark (1978). Data retrieved from the CSD are in the form of cell parameters, space group symmetry operations, crystal data, and crystal coordinates of the atoms in the structure. The retrieved data are listed in Appendix A.

The *cif* were edited to create SHELX *ins* type files for the nonhydrogen atoms. Interatomic bond distances and angles were calculated with SHELXL (Sheldrick, 1993) and compared with the published distances and angles to verify that the crystallographic parameters were all correct. In the case of TPNTCN the distances and angles for carbon-hydrogen did not agree. Comparison of the coordinates from the CSD with the published coordinates indicated that 0.8776 the *y* coordinate is incorrect in the CSD; it was changed to 0.8876 the value from Haller & Enemark. Idealized hydrogen atom positions were included in the CSD for AZNPNI and TPNTCN but not for CLTPNN01. Further, the C–H distances in the CSD were calculated assuming ideal x-ray geometry; $d[\text{C–H}] = 0.95 \text{ \AA}$. Idealized positions for the hydrogen atoms for all three structures were calculated with SHELXL (HFIX 43) assuming planar geometry about each phenyl carbon atom with the two C–C–H angles equal and $d[\text{C–H}] = 1.083 \text{ \AA}$, the distance determined from neutron diffraction studies (Burgi & Dunitz, 1994).

The supramolecular structure interactions were identified by a combination of distance and angle calculations along with examination of graphical images of molecules and fragments of molecules. Inter- and intra-molecular contact distances were calculated with the ORTEP-III program (Burnett & Johnson, 1996). The analysis was begun by calculating the Ni–P \cdots P'–Ni' colinearity angles and the P \cdots P separations in the range 5.5–8.0 \AA identified by Dance and Scudder (1995) for concerted phenyl embraces. The criteria for inclusion of all interaction of Ni(X)(NO)(PPh₃)₂ were examined between P \cdots P separation consider the near P \cdots P distances

around P1 and P2 from one molecule (position 55501 in the language of Atom Designator Codes used by ORTEP as explained in Appendix A) to P1 and P2 of another molecule with symbol NNTTTSS (as described in Appendix A). For the purposes of this thesis the maximum P···P distance considered was 12 Å. Since the colinearity angle, M–P···P'–M', is required the calculations were initiated by a 102 instruction to ORTEP which gives both interatomic distances and interatomic angles about each origin atom (see Appendix A for a description of the 102 instruction).

The crystal data are interpreted from the ORTEP instruction and the results of the calculation are given in the output file of the program. The calculated results are the coordinates of the phosphorus and nickel atoms for each P···P interaction within the distance criteria specified, the P···P distances, the M–P···P' and P···P'–M' angles, and the atom designator codes for all atoms involved in each P···P interaction. The coordinates of the midpoint of each P···P interaction and the colinearity angle for each interaction were calculated from the ORTEP results and are tabulated in Appendix B. The coordinates of the P···P midpoints were included in the ORTEP input file to aid in drawings and in consideration of additional interactions between the phenyl rings on interacting pairs of PPh₃ ligands related to each other through some type of phenyl embrace. The definition of M–P···P'–M', the colinearity parameter, is half the sum of M–P···P'(α) and P···P'–M'(β) angle $((\alpha+\beta)/2)$ (Figure 2.2 illustrates the colinearity parameter).

Six-fold phenyl embraces (6PE) are characterized by intermolecular $d[\text{P}\cdots\text{P}] < 8 \text{ \AA}$ and $\angle[\text{M}-\text{P}\cdots\text{P}'-\text{M}']$ colinearity in the range 160-180 ° (Dance & Scudder, 1995) and fourfold phenyl embrace (4PE) that P···P distance be $\leq 9 \text{ \AA}$.

Additional potential intermolecular contacts were identified by calculating contact distances to the idealized hydrogen atom positions (edge-to-face contacts), to the phenyl carbon atoms (face-to-edge contacts), and to the hydrogen bond acceptors for other nonbonded contacts. Ring C···H contact distances less than 3.4 Å were examined graphically to determine if they were face-to-face contacts. Remaining ring C···H contact distances less than 3.2 Å were examined to determine if they were edge-to-face contacts or van der Waals edge-to-edge contacts.

Interactions between adjacent phenyl rings are indicated as edge-to-face, van der Waals edge-to-edge or face-to-face interactions based on the calculated distances and the relative positions of the two rings. The relative positions of the rings involved

in a given separation were analyzed graphically, generally by drawing the contents of a sphere in direct space with an appropriate radius about the P...P midpoint, or centered on the hydrogen atom of the interaction. The sphere was drawn projected on one of the interacting phenyl rings and then drawn perpendicular to the same interacting phenyl ring. Sometimes it was useful to draw the same two views of the other ring as well. For consider direction of each phenyl ring interaction which is type π stacking if phenyl rings are perpendicular to each other is *ef* interaction, or if phenyl rings are parallel to each other as *off* π stacking. Finally, counting how many interactions of the phenyl rings are concerted with each other gives the order of the phenyl-phenyl embrace.

When calculating contact distances between carbon atoms of the phenyl rings of one molecule (55501) to hydrogen atoms of the phenyl rings of another molecule (NNTTSS) or from hydrogen atoms of phenyl rings of one molecule to the carbon atoms of the phenyl rings of another molecule, a maximum cut off distance of 3.4 Å was used. As only distances were required, a 101 instruction was input into ORTEP.

The two phenyl rings in each *ef* contact are inclined to each other and one or two H atoms of one ring are directed towards C atoms of the other. The two phenyl rings in each edge-to-edge van der Waals contact have H atoms of one ring directed towards H atoms of the second ring. C...H contact distances in the appropriate range for edge-to-edge interactions, 2.8 to 3.2 Å (Dance & Scudder, 1995) were examined carefully to distinguish between *ef* and edge-to-edge character.

Offset face-to-face (*off*) contacts require two rings that are approximately parallel and positioned such that H atoms of one are closest to C atoms of the other. Contact regions up to 3.4 Å (the normal π ... π contact distance) were examined graphically to verify that the rings were in the appropriate relationship.

If the three phenyl rings of a PPh₃ group of one molecule interacts to the three phenyl rings of a PPh₃ group on an adjacent molecule resulting in three edge-to-face and three face-to-edge interactions the multiple phenyl embrace is a six-fold phenyl embrace, a 6PE. In the most common motif the six phenyl groups of two adjacent triphenylphosphine ligands can arrange such that there are six concerted *ef* interactions alternating from ligand A to ligand B, B to A, A to B, *etc.* The concerted six fold phenyl embrace (6PE) thus formed will often be the strongest intermolecular interaction in a molecular crystal. Sextuple phenyl embraces result when the phenyl

rings of two triphenylphosphine ligands are arranged in interlocking C_3 propeller configurations, usually related by an inversion center. An individual *ff* or *ef* interaction is only a few kJ mol^{-1} , but when concerted, the cooperative result can easily reach $50\text{-}60 \text{ kJ mol}^{-1}$.

For fourfold phenyl embrace (4PE) involving two phenyl groups on each partner, with two geometrical subclasses depending on whether the $C_{\text{ipso}}PC_{\text{ipso}}$ planes on each molecule are approximately parallel (the POPE) or approximately orthogonal (the OQPE).

Edge-to-edge contacts are much weaker with the two phenyl rings interacting by hydrogen-hydrogen contacts to each other.

The second part the supramolecular structure interaction in concerted NO and X (monoanion) to phenyl ring. calculated by 102 instructions input into the ORTEP program. The consider phenyl rings to NO and X contacts from van der Waals of C–H \cdots O (2.7 Å), C–H \cdots N (2.75 Å), C–H \cdots Cl (2.95 Å), C–H \cdots S (3.0 Å) interactions and angles for direction of interactions. The van der Waals radii used were as follows: C = 1.75, H = 1.20, Cl = 1.75, N = 1.55, O = 1.50, S = 1.80 Å (Taylor & Kennard, 1982).

Chapter IV

Results and Discussion

Four-coordinate nickel nitrosyl bis(triphenylphosphine) complexes were studied. The nitrosyl binds to nickel by forming a ligand to metal σ -bond which is reinforced by back donation of e^- density from the π -type d orbital of nickel to the partially occupied π^* orbital of the nitrosyl. The nickel nitrosyl bonding thus strongly depends on the relative energies of the metal d orbitals and the nitrosyl π^* orbitals and on their relative populations. The nitrosyl stretching bands in the infrared spectrum are strong and sharp for the $\text{NiBr}(\text{NO})(\text{PPh}_3)_2$ and $\text{NiCl}(\text{NO})(\text{PPh}_3)_2$ complexes with stretching frequencies at 1733 and 1713 cm^{-1} respectively, in agreement with the values previously reported by Feltham (1964). The nitrosyl stretching frequencies decrease on substitution of Br with Cl indicating weakening of the N–O bond which must result from an increase in the population of the nitrosyl π^* orbitals. This is presumably because the smaller covalent radius allows a stronger σ -bond interaction of the higher field, more electronegative chloro ligand than the bromo ligand, thus increasing the effective electron density of the Ni d orbitals.

4.1 Supramolecular Structure of $\text{Ni}(\text{NCS})(\text{NO})(\text{PPh}_3)_2$

The structure of the isothiocyanato complex has been reported by Haller & Enemark (1978). The complex crystallizes in the triclinic space group P-1 with two molecules per unit cell. The pseudo tetrahedral molecule has enlarged P–Ni–P and N–Ni–N angles (111.98(6) and 116.82(22) $^\circ$ respectively) and a dihedral angle between the N–Ni–N and P–Ni–P planes of 81.73 $^\circ$. The distinctly nonlinear nitrosyl group has an Ni–N–O angle of 161.5(5) $^\circ$. One unusual feature of the structure is the nonequivalence of the two chemically equivalent Ni–P distances, Ni–P(1) = 2.271(2) and Ni–P(2) = 2.328(2) Å, which are 28 σ different. The NCS $^-$ ligand is linearly coordinated to the Ni atom thus not breaking the symmetry of the nickel d orbitals relative to the two phosphine ligands. The previous report suggested the difference could be caused by intermolecular packing interactions of the phenyl groups of the phosphine ligands, but did not attempt to explore this possibility.

The coordinates for the nonhydrogen atoms and the calculated coordinates for the hydrogen atoms of Ni(NCS)(NO)(PPh₃)₂ are given in Tables A.1 and A.2 in Appendix A. The intermolecular P⋯P contacts for which there are C–H⋯π interactions are tabulated in Table 4.1, along with the midpoints of the P⋯P vector, the symmetry relationship between the two phosphines, the P⋯P distance and the M–P⋯P–M colinearity parameters, the individual C–H⋯π interaction distances, and the appropriate identifiers defined by Dance and Scudder to aid discussion about the interactions. The individual angles that contribute to the colinearity parameter are given in Table B.1 in Appendix B.

The supramolecular structure of Ni(NCS)(NO)(PPh₃)₂ consists of parallel one dimensional zigzag chains propagating in the [-1 1 0] direction. Each of the crystallographically independent phosphines interacts with a neighboring molecule through a 6PE motif across an inversion center; at (1/2, 1, 1/2) for the P1Ph₃⋯P1Ph₃ and at (1, 1/2, 1/2) for the P2Ph₃⋯P2Ph₃ interaction. Each chain (Figure 4.1) is thus made up of alternating P1Ph₃⋯P1Ph₃ and P2Ph₃⋯P2Ph₃ 6PE interactions. The P⋯P interaction distance is 7.246 Å with an M–P⋯P–M colinearity angle of 173.04° for P(1)⋯P(1) and 7.087 Å with an M–P⋯P–M colinearity angle of 176.94° for P(2)⋯P(2). Thus, the P1⋯P1 intermolecular distance is longer than the P2⋯P2 intermolecular distance and the M–P1⋯P1–M angle less than the M–P2⋯P2–M angle, which following Dance and Scudder indicates that the P2⋯P2 interaction is the stronger 6PE. However, for the P1⋯P1 interaction the distances from the three phenyl edges on one molecule to the three phenyl faces on the molecule across the inversion center are 3.196, 2.789, and 2.986 Å while in the P2⋯P2 interaction these distances are 3.440, 2.966, and 2.986 Å.

Adjacent chains are connected together in the [0 0 1] direction by P4PE four phenyl ring motifs (one offset *ff* interaction and two *ef* interactions) across inversion centers to form a two dimensional network dominated by edge-to-face C–H⋯π interactions (Figure 4.2). The translation related P4PE interactions from the P1 phosphine are both to P1 phosphines of the adjacent chains ($d[\text{P1}\cdots\text{P1}] = 7.997 \text{ \AA}$, colinearity = 104.69°). The two identical *ef* interaction distances are 2.760 Å. The other pair of P4PE interactions are from the P2 phosphine to P2 phosphines of the adjacent chains ($d[\text{P2}\cdots\text{P2}] = 8.805 \text{ \AA}$, colinearity = 106.03°). The nearest *ef* distances at 2.910 Å are 0.15 Å longer than those of the P4PE interaction between the P1

Table 4.1. Concerted Hydrogen Bond Interactions and Selected Interatomic C–H...X Distances Defining the Ni(NCS)(NO)(PPh₃)₂ Supramolecular Structure.

Phenyl-Phenyl Contacts							
D[Pn...Pn ^{S*}] (Å)	Midpoint Pn...Pn ^{S*}	Colinearity (°)	Contact Distances C–H...C (<i>ef</i>)				
P1...P1 ^K 7.246 (67602)	(1/2, 1, 1/2)	173.04	C–H _(P1R3) ...C ^K π _(P1R2) C–H _(P1R1) ...C ^K π _(P1R3) C–H _(P1R2) ...C ^K π _(P1R1)	3.196 2.789 2.986	C ^K –H ^K _(P1R2) ...Cπ _(P1R1) C ^K –H ^K _(P1R3) ...Cπ _(P1R2) C ^K –H ^K _(P1R1) ...Cπ _(P1R3)	2.986 3.196 2.789	6PE
P2...P2 ^L 7.087 (76602)	(1, 1/2, 1/2)	176.94	C–H _(P2R6) ...C ^L π _(P2R5) C–H _(P2R4) ...C ^L π _(P2R6) C–H _(P2R5) ...C ^L π _(P2R4)	3.440 2.966 2.986	C ^L –H ^L _(P2R5) ...Cπ _(P2R4) C ^L –H ^L _(P2R6) ...Cπ _(P2R5) C ^L –H ^L _(P2R4) ...Cπ _(P2R6)	2.986 3.440 2.966	6PE
P1...P1 ^J 7.997 (67702)	(1/2, 1, 1/2)	104.69	C–H _(P1R2) ...C ^J π _(P1R1)	2.760	C ^J –H ^J _(P1R2) ...Cπ _(P1R1)	2.760	P4PE
P2...P2 ^H 8.805 (76702)	(1, 1/2, 1)	106.03	C–H _(P2R6) ...C ^H π _(P2R5) C–H _(P2R5) ...C ^H π _(P2R6)	2.910 2.938	C ^H –H ^H _(P2R5) ...Cπ _(P2R6) C ^H –H ^H _(P2R6) ...Cπ _(P2R5)	2.938 2.910	P4PE
P1...P2 ^L P2...P1 ^L 11.025 (66602)	(0.3079, 0.1069, 0.2953) (0.3988, 0.5986, 0.5053)	115.63	C–H _(P2R6) ...C ^L π _(P1R1) C–H _(P1R1) ...C ^L π _(P2R6) C–H _(P1R6) ...C ^L π _(P2R6)	2.794 3.135 3.197	C ^L –H ^L _(P1R1) ...Cπ _(P2R6) C ^L –H ^L _(P2R6) ...Cπ _(P1R1)	3.135 2.794	O4PE
P1...P2 ^G P2...P1 ^G 8.096 (77602)	(1, 1, 1/2) (1, 1, 1/2)	89.92	C–H _(P1R3) ...C ^G π _(P2R4) C–H _(P2R4) ...C ^G π _(P1R2)	2.976 3.278	C ^G –H ^G _(P2R4) ...Cπ _(P1R2) C ^G –H ^G _(P1R3) ...Cπ _(P2R4)	3.278 2.976	D3PE
P1...P1 ^B P2...P2 ^B 9.947 (55601)	(0.6921, 0.8931, 1.2047) (0.8945, 0.6958, 1.1941)	90.00	C–H _(P2R5) ...C ^B π _(P2R4) C–H _(P1R2) ...C ^B π _(P1R3)	3.109 3.192	C ^B –H ^B _(P1R3) ...Cπ _(P1R2)	3.334	D2PE
P2...P2 ^C 9.947 (55401)	(0.8945, 0.6958, 0.1941)	90.00	C–H _(P2R4) ...C ^C π _(P2R5)	2.996	C ^C –H ^C _(P2R5) ...Cπ _(P2R4)	3.109	<i>ee</i>
P1...P2 ^F P2...P1 ^F 9.424 (77702)	(0.8988, 1.0986, 1.0053) (1.1012, 0.9013, 0.9947)	58.54	C–H _(P2R5) ...C ^F π _(P1R2)	3.198	C ^F –H ^F _(P2R5) ...Cπ _(P1R2)	3.198	D2PE
P2...P1 ^D 9.909 (65501)	(1.2933, 0.7944, 0.6994)	116.12	C–H _(P2R4) ...C ^D π _(P1R1)	3.260	C ^D –H ^D _(P1R1) ...Cπ _(P2R5) C ^D –H ^D _(P1R1) ...Cπ _(P2R4)	2.936 3.231	3PE

P1...P2 ^E 9.909 (45501)	(0.2933, 0.7944, 0.6994)	116.12	C-H _(P1R1) ...C ^E π _(P2R5) 2.936 C-H _(P1R1) ...C ^E π _(P2R4) 3.231	3PE
NO-Phenyl and Cl-Phenyl Contact				
C-H...X	C-H...NO		C-H...NCS	
Intramolecular Contact Distances	C-H _(P2R5) ...N2	2.902	C-H _(P1R1) ...N1	2.535
	C-H _(P1R2) ...N2	3.023	C-H _(P2R6) ...N1	2.829
	C-H _(P1R3) ...N2	3.032	C-H _(P1R2) ...N1	2.919
	C-H _(P1R3) ...O1	2.948	C-H _(P2R6) ...C1	2.827
Intermoleclar Contact Distances			C-H _(P1R1) ...C1	2.839
	C ^G -H ^G _(P2R5) ...N2	2.961	C ^B -H ^B _(P1R3) ...N1	3.166
	C ^G -H ^G _(P2R4) ...O1	2.638	C ^B -H ^B _(P1R3) ...C1	2.883
	C ^G -H ^G _(P1R3) ...O1	2.911	C ^B -H ^B _(P1R3) ...S1	3.200
	C ^G -H ^G _(P1R3) ...O1	3.184	C ^M -H ^M _(P2R6) ...S1	3.185
			C ^H -H ^H _(P2R5) ...S1	3.130

*P_n represents P1 or P2 as appropriate

Superscripts are used to denote the symmetry operation (given in Appendix B) for the transformation of the atom coordinates (given in Appendix A) for the described interaction. If no transformation is required (symmetry operation A) no superscript is given.

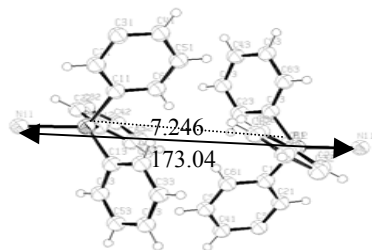


Figure 4.1b. The 6PE Interaction between P1...P1 of Ni(NCS)(NO)(PPh₃)₂.

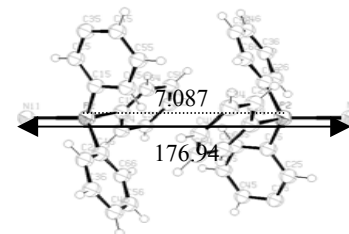


Figure 4.1c. The 6PE Interaction between P2...P2 of Ni(NCS)(NO)(PPh₃)₂.

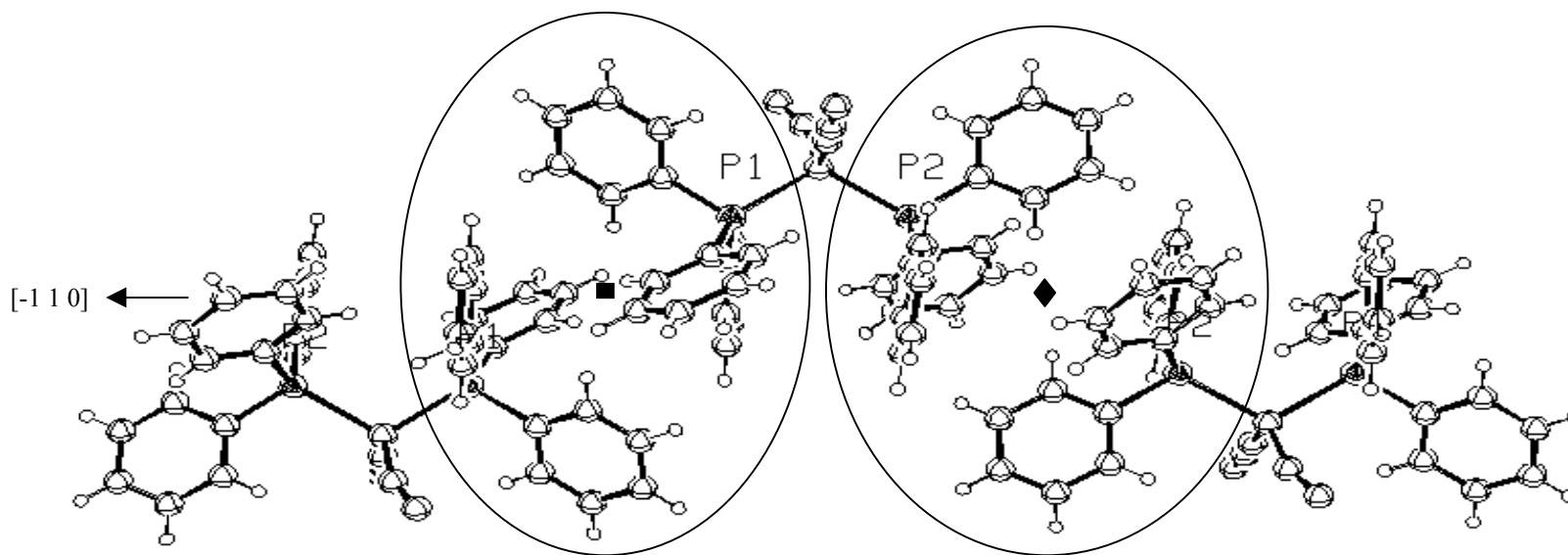


Figure 4.1a. 6PE Linking Ni(NCS)(NO)(PPh₃)₂ Molecules into Chains.

■ is the inversion center at $1/2 \ 1 \ 1/2$

◆ is the inversion center at $1 \ 1/2 \ 1/2$

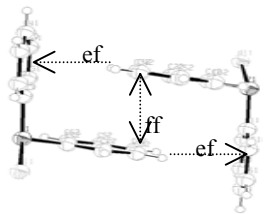


Figure 4.2b. The P4PE Interaction between P1...P1 of Ni(NCS)(NO)(PPh₃)₂ Illustrating the Parallel Nature of the Face-to-Face Interaction.

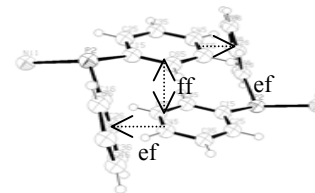


Figure 4.2c. The P4PE Interaction between P2...P2 of Ni(NCS)(NO)(PPh₃)₂ Illustrating the Parallel Nature of the Face-to-Face Interaction.

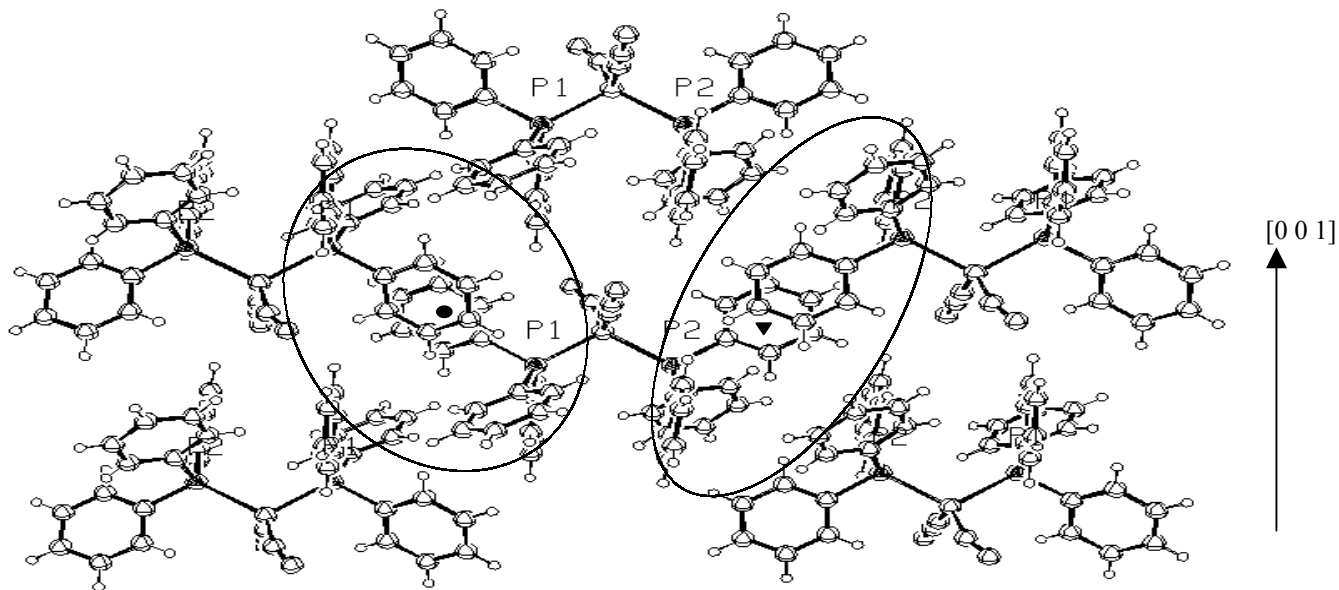


Figure 4.2a. 4PE Linking Chains of Ni(NCS)(NO)(PPh₃)₂ Molecules.

- is the inversion center at (1/2 1 1)
- ▼ is the inversion center at (1 1/2 1)

phosphines but are complemented by a second set of interactions at 2.938 Å. The offset *ff* distances are similar for the two types of P4PE interactions.

The two dimensional layers are interconnected in two ways. The stronger interconnection occurs about the inversion center at (1, 1, 1/2) where there is a pair of P1...P2 3PE interactions ($d[\text{P1}\cdots\text{P2}] = 8.096 \text{ \AA}$, colinearity = 89.92°). Each 3PE contains two *ef* interactions. First, the edge of phenyl ring (P1R3) interacting to the face of phenyl ring (P2R4) and the edge of phenyl ring (P2R4) interacting to the face of phenyl ring (P1R2) for an M1P1Ph₂...PhP2M2, and second the inversion related interaction from PhP2M2 of layer one to M1P1Ph₂ of the adjacent layer. The stronger interconnection is completed by an inversion related pair of C–H...O interactions between phenyl group P2R4 and the oxygen atom of the NO group at 2.638 Å. There are also weaker intramolecular C–H...N and C–H...O contacts to the nitrosyl ligand, but these are less significant than the other interactions listed above. The weaker interconnection is by way of a short intramolecular C–H...N contact between the NCS ligand and phenyl group P1R1 at 2.535 Å. The combination per molecule between two layers is thus a cooperative eight interaction set linking the layers into a three dimensional supramolecular array as shown in Figure 4.3. The location of these eight interaction links is indicated by the ovals in Figure 4.4.

When compare between the two 6PE interactions, the P1...P1 distance (7.246 Å) is longer than the P2...P2 distance (7.087 Å) but the interactions of the phenyl groups on P1...P1 are stronger than the interactions of the phenyl groups on P2...P2. Comparing the P4PE interactions, the P1...P1 distance (7.997 Å) is shorter than the P2...P2 distance (8.805 Å). P1 is also involved in a strong intramolecular interaction to the nitrogen of NCS (2.535 Å) while P2 has a strong intermolecular interaction to the oxygen of NO (2.638 Å).

4.2 Supramolecular Structure of NiCl(NO)(PPh₃)₂

The structure of the NiCl(NO)(PPh₃)₂ complex has also been reported by Haller & Enemark (1978). The crystals of the complex contain four formula units of NiCl(NO)(PPh₃)₂ and four formula units of benzene per monoclinic unit cell with systematic absences consistent with space groups Cc (No. 9) and C2/c (No. 15). Thus, there would be one molecule per asymmetric unit for space group Cc or one-half molecule per asymmetric unit for space group C2/c.

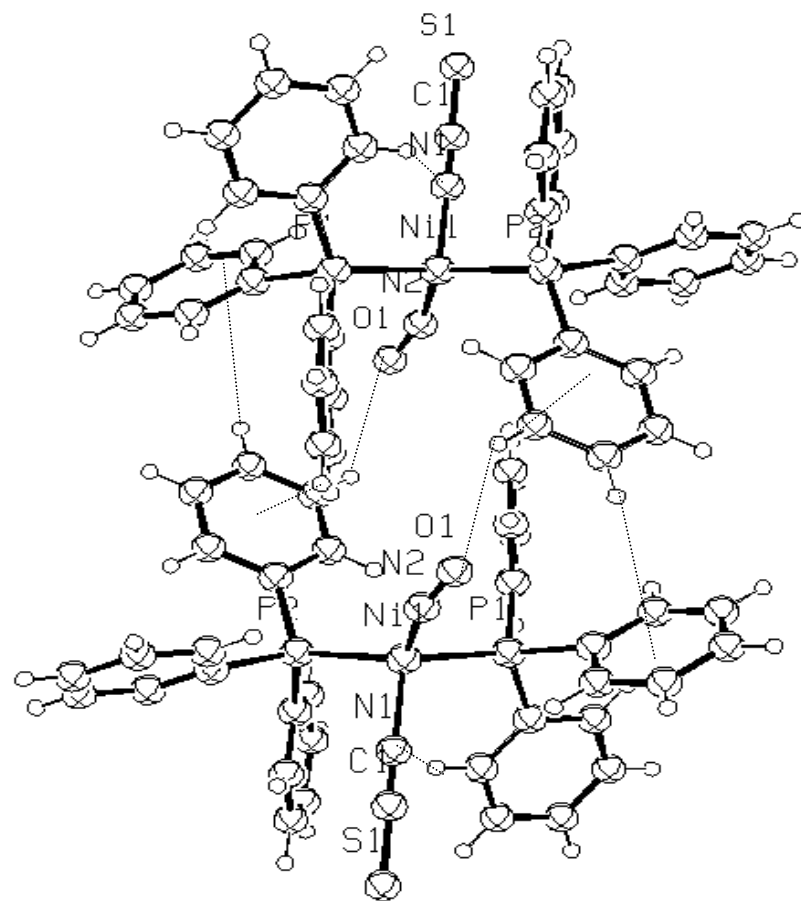


Figure 4.3. Interlayer Interactions of Ni(NCS)(NO)(PPh₃)₂.

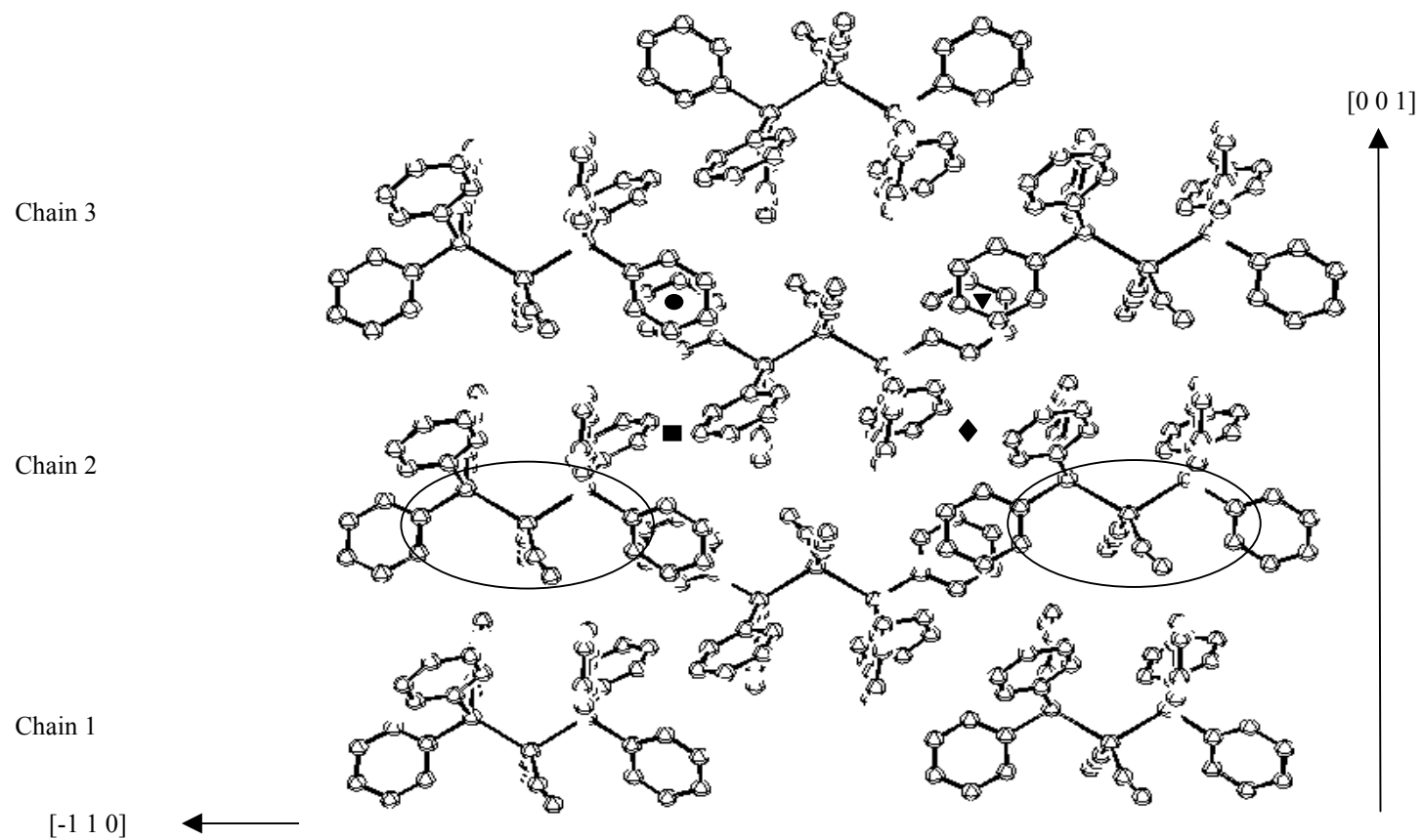


Figure 4.4. Layer of 6PE and 4PE Ni(NCS)(NO)(PPh₃)₂.

Structure refinement was complicated by disorder of the chloro and nitrosyl ligands and several models were explored (Haller, 1978) for each of the possible space groups but no satisfactory model of the disorder could be obtained with the refinement technology of the time. The problem arises because the size of the coordinated chloro and nitrosyl ligands are such that the midpoint of the N–O vector and the Cl atom position can be nearly superposed by the approximate twofold axis defined by the Ni(PPh₃)₂ portion of the molecule. It was not possible to accurately determine the geometry of the NO group or the position of the chloro ligand, but the geometry of the Ni(PPh₃)₂ portion of the molecule, the benzene of solvation, and the basic packing should be correct. The pseudo tetrahedral complex has a P–Ni–P angle of 121.0° in all of the models refined.

The Ni–P distances are required to be equal in space group C2/c and were found to be 2.263(6) and 2.287(5) Å (4σ different) in space group Cc. As none of the models refined were statistically superior it must be assumed that the Ni–P distances are equivalent in this complex.

The coordinates for the nonhydrogen atoms and the calculated coordinates for the hydrogen atoms of NiCl(NO)(PPh₃)₂·C₆H₆ are given in Tables A.3 and A.4 in Appendix A. The intermolecular P···P contacts for which there are C–H···π interactions are tabulated in Table 4.2, along with the midpoints of the P···P vector, the symmetry relationship between the two phosphines, the P···P distance and the M–P···P–M colinearity parameters, the individual C–H···π interaction distances, and the appropriate identifiers defined by Dance and Scudder to aid discussion about the interactions. The individual angles that contribute to the colinearity parameter are given in Table B.3 in Appendix B.

The benzene solvate of crystallization lies on the pseudo two-fold axis through the nickel atom of the complex. The benzene solvate can be viewed as lying within a cavity made up of ten phenyl rings from seven neighboring molecules and the chloro and nitrosyl groups of an eighth molecule forming an extensively concerted group of interactions with its environment. One end of the benzene is inserted into the cleft of the bis(triphenylphosphine) nickel fragment located on the pseudo two-fold axis utilizing one complex-to-benzene *ef* and one benzene-to-complex *ef* interaction to each of the triphenylphosphine ligands. These four interactions to one molecule make up the base of the bowl-shaped cavity. Figure 4.5 provides a view from the benzene

Table 4.2. Concerted Hydrogen Bond Interactions and Selected Interatomic C–H...X Distances Defining the NiCl(NO)(P(C₆H₅)₃)₂ Supramolecular Structure.

Benzene–Phenyl Contacts							
		Contact Distances C–H _(B) ...C ^S		Contact Distances C ^S –H ^S ...C _(B)			
NiP ^S R ^S – Benzene	C–H _(B) ... C ^B π _(P1R1)	2.791	C ^B –H ^B _(P2R5) ...Cπ _(B)	3.063			
	C–H _(B) ... C ^B π _(P2R4)	3.065	C ^B –H ^B _(P1R2) ...Cπ _(B)	3.199			
	C–H _(B) ... C ^B π _(P1R2)	3.167					
	C–H _(B) ... Cπ _(P2R5)	3.333					
	C–H _(B) ... C ^F π _(P1R1)	2.995					
	C–H _(B) ... C ^H π _(P2R4)	3.055					
				C ^E –H ^E _(P2R5) ...Cπ _(B)	2.723		
			C ^D –H ^D _(P1R2) ...Cπ _(B)	2.833			
			C ^J –H ^J _(P1R23) ...Cπ _(B)	3.138			
			C ^L –H ^L _(P2R6) ...Cπ _(B)	3.281			
NiPR–Benzene ^S	C–H _(P2R5) ... C ^C π _(B)	3.063	C ^C –H ^C _(B) ...Cπ _(P1R1)	2.791			
	C–H _(P1R2) ... C ^C π _(B)	3.199	C ^C –H ^C _(B) ...Cπ _(P2R4)	3.065			
			C ^C –H ^C _(B) ...Cπ _(P1R2)	3.167			
			C ^C –H ^C _(B) ...Cπ _(P2R5)	3.333			
	C–H _(P1R2) ... C ^E π _(B)	2.833					
	C–H _(P2R5) ... C ^D π _(B)	2.723					
	C–H _(P1R3) ... C ^L π _(B)	3.138					
	C–H _(P2R6) ... C ^J π _(B)	3.281					
			C ^L –H ^L _(B) ...Cπ _(P1R1)	2.995			
			C ^G –H ^G _(B) ...Cπ _(P2R4)	3.055			
Phenyl -Phenyl Contacts							
D[Pn...Pn ^S] (Å)	Midpoint Pn...Pn ^S	Colinearity (°)	Contact Distances C–H...C				
P1...P2 ^M 7.163 (44404)	(-0.2494, -0.2504, 0.0010)	174.15	C–H _(P1R3) ...C ^M π _(P2R5)	3.219	C ^M –H ^{M?} _(P2R5) ...Cπ _(P1R1)	3.333	6PE
			C–H _(P1R1) ...C ^M π _(P2R6)	2.803	C ^M –H ^M _(P2R6) ...Cπ _(P1R2)	2.872	
			C–H _(P1R2) ...C ^M π _(P2R4)	2.965	C ^M –H ^M _(P2R4) ...Cπ _(P1R3)	2.990	

P2...P1 ^K 7.163 (54504)	(0.2506, -0.2496, 0.5010)	174.15	C-H _(P2R4) ...C ^K π _(P1R3) C-H _(P2R5) ...C ^K π _(P1R1) C-H _(P2R6) ...C ^K π _(P1R2)	2.990 3.333 2.872	C ^K -H ^K _(P1R3) ...C π _(P2R5) C ^K -H ^K _(P1R1) ...C π _(P2R6) C ^K -H ^K _(P1R2) ...C π _(P2R4)	3.219 2.803 2.965	6PE
P1...P2 ^E 7.900 P1...P1 ^E 9.223 (55402)	(0.0006, -0.0004, 0.0010) (0.0962, 0.0000, - 0.0908)	82.54 77.24	C-H _(P1R3) ...C ^E π _(P2R5)	3.282	C ^E -H ^E _(P1R1) ...C π _(P1R3)	3.293	3PE
P2...P2 ^H 9.479 (45503)	(-0.2494, 0.1126, 0.2510)	99.30	C-H _(P1R3) ...C ^H π _(P1R2)	3.236	C ^H -H ^H _(P1R2) ...C π _(P1R3) C ^H -H ^H _(P2R4) ...C π _(P1R3)	3.045 2.968	PE
P2...P1 ^G 9.479 P1...P1 ^G 10.90 (54503)	(0.2506, - 0.3878, 0.2510) (0.1538, - 0.3883, 0.1592)	99.30 90.00	C-H _(P2R4) ...C ^G π _(P1R3) C-H _(P1R2) ...C ^G π _(P1R3)	2.968 3.045	C ^G -H ^G _(P1R3) ...C π _(P1R2)	3.236	PE
P2...P2 ^F 10.900 P2...P1 ^F 9.463 (55503)	(0.2500, 0.1126, 0.3429) (0.2506, 0.1122, 0.2510)	90.00 99.78	C-H _(P2R6) ...C ^F π _(P2R5)	3.296	C ^F -H ^F _(P2R5) ...C π _(P2R6) C ^F -H ^F _(P1R1) ...C π _(P2R6)	3.081 2.974	PE
P1...P2 ^I 9.0463 P2...P2 ^I 10.900 (44503)	(-0.2494, - 0.3878, 0.2510) (-0.1526, - 0.3874, 0.3429)	99.78 90.00	C-H _(P1R1) ...C ^I π _(P2R6) C-H _(P2R5) ...C ^I π _(P2R6)	2.974 3.081	C ^I -H ^I _(P2R6) ...C π _(P2R5)	3.296	PE
P2...P1 ^D 7.900 (55502)	(0.0006, 0.0004, 0.5010)	82.54			C ^D -H ^D _(P1R3) ...C π _(P2R5)	3.277	ef

NO-Phenyl and Cl-Phenyl contact				
C-H...X	C-H...NO		C-H...Cl	
Intramolecular Contact Distances	C-H _(P1R3) ...N1	2.476	C-H _(P1R1) ...Cl	2.589
	C-H _(P2R4) ...N1	2.637	C-H _(P2R6) ...Cl	2.646
	C-H _(B) ...N1	3.091	C-H _(B) ...Cl	3.037
	C-H _(P2R4) ...O1	2.274		
	C-H _(P1R3) ...O1	2.672		
Intermoleclar Contact Distances	C ^F -H ^F _(P1R1) ...N1	2.823	C ^H -H ^H _(P4R4) ...Cl	2.965
	C ^F -H ^F _(P1R1) ...O1	2.797		
	C ^F -H ^F _(P1R1) ...O1	3.161		
	C ^E -H ^E _(P2R5) ...N1	2.824		
	C ^E -H ^E _(P2R5) ...O1	2.619		
	C ^E -H ^E _(P2R5) ...O1	3.007		

*P_n represents P1 or P2 as appropriate

Superscripts are used to denote the symmetry operation (given in Appendix B) for the transformation of the atom coordinates (given in Appendix A) for the described interaction. If no transformation is required (symmetry operation A) no superscript is given.

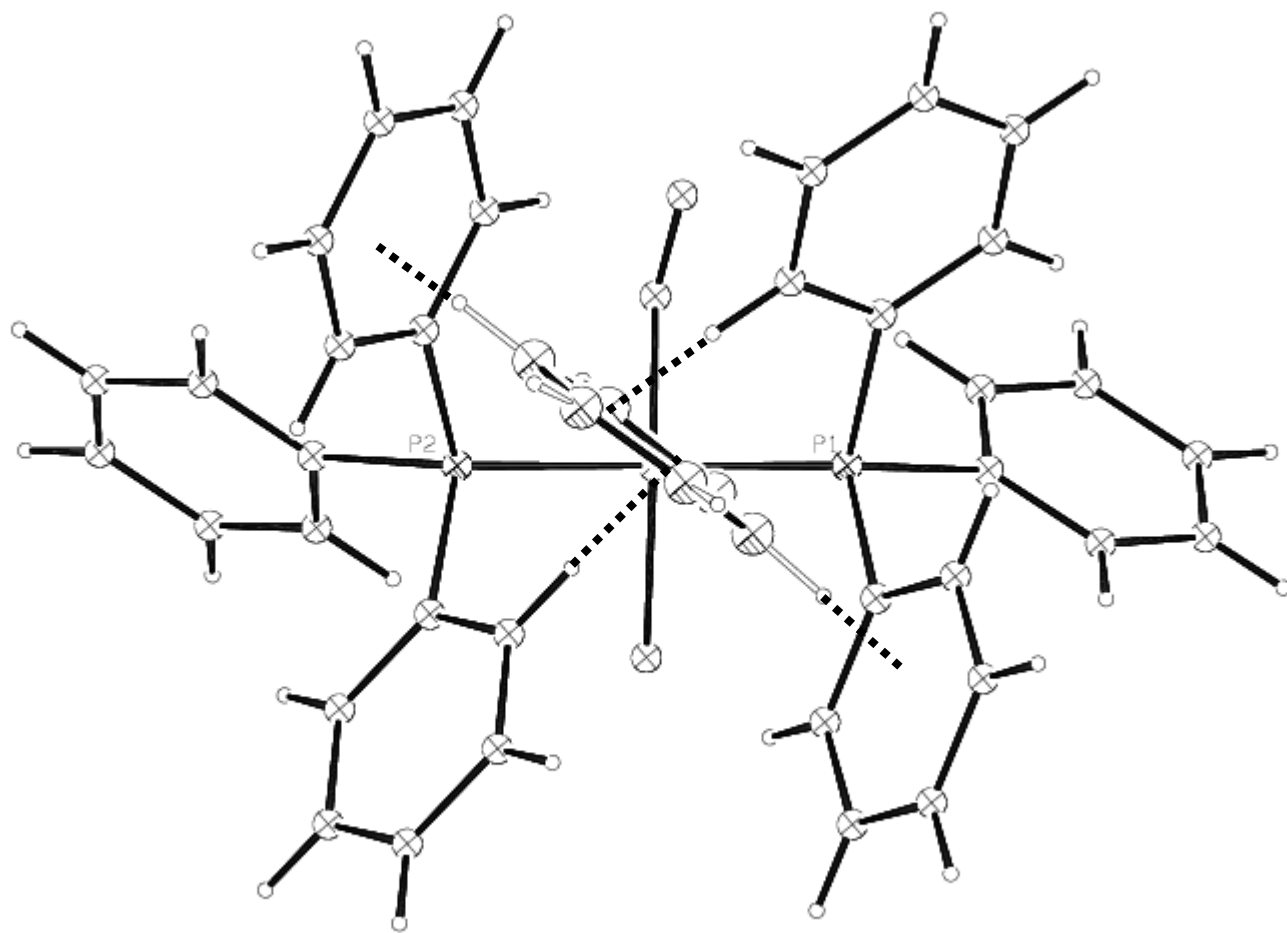


Figure 4.5. Benzene Solvate in the $\text{Ni}(\text{PPh}_3)_2$ Cleft of the $\text{NiCl}(\text{NO})(\text{PPh}_3)_2$ Molecule.

solvate down the pseudo two-fold axis showing the arrangement of the surrounding phenyl groups.

The central region is dominated by six phenyl rings from three pairs of two-fold related complex molecules located about the cavity as shown in Figure 4.6. One pair of the phenyl rings forms strong complex-to-benzene *ef* interactions of 2.723 Å from P2R5 and 2.833 Å from P1R2; a second pair forms weaker benzene-to-complex *ef* interactions of 2.995 and 3.055 Å; the third pair are farther away forming very weak *ee* interactions. An eighth molecule of complex closes the cavity above the benzene molecule with its pseudo two-fold related chloro and nitrosyl ligands. Due to the refinement problems related to the disorder problems noted above, reliable chloro and nitrosyl ligand interaction distances cannot be calculated and are not included in this discussion.

The large number of concerted interactions makes it probable that this feature plays a dominant role in determining the supramolecular structure. Dance & Scudder (1998) report another benzene of solvation in a similar highly concerted phenyl ring interaction environment with a contribution to the packing energy of $-14.1 \text{ kcal mol}^{-1}$.

The structure also contains the expected 6PE creating one dimensional chains in the [1 0 1] direction. The 6PE are located across the pseudo inversion centers near $(-1/4, -1/4, 0)$ and $(1/4, -1/4, 0)$ in space group Cc. The two phosphines are equivalent with $d[\text{P}\cdots\text{P}] = 7.163 \text{ Å}$ and colinearity = 174.15° . The parallel zigzag chains (zigzag up and down perpendicular to the plane of the page) are illustrated in Figure 4.7.

The only other short phosphine-phosphine interaction is a 3PE with $d[\text{P}\cdots\text{P}] = 7.900 \text{ Å}$ and colinearity = 82.54° . The next shortest phosphine-phosphine interaction is at 9.223 Å . The paucity of short phenyl-phenyl interactions reinforces the supposition above that the highly concerted interactions about the benzene solvate dominate the supramolecular structure.

4.3 Supramolecular Structure of $\text{Ni}(\text{N}_3)(\text{NO})(\text{PPh}_3)_2$

The structure of the $\text{Ni}(\text{N}_3)(\text{NO})(\text{PPh}_3)_2$ complex has been reported by Enemark (1971). The compound crystallizes in the monoclinic space group $\text{P}2_1/\text{c}$ with four molecules per unit cell. The structure consists of discrete $\text{Ni}(\text{N}_3)(\text{NO})(\text{PPh}_3)_2$ molecules with pseudo tetrahedral coordination geometry about the Ni atom. The P–Ni–P angle is $120.52(8)^\circ$, the N_3 –Ni–NO angle is $128.8(3)^\circ$, and the dihedral angle

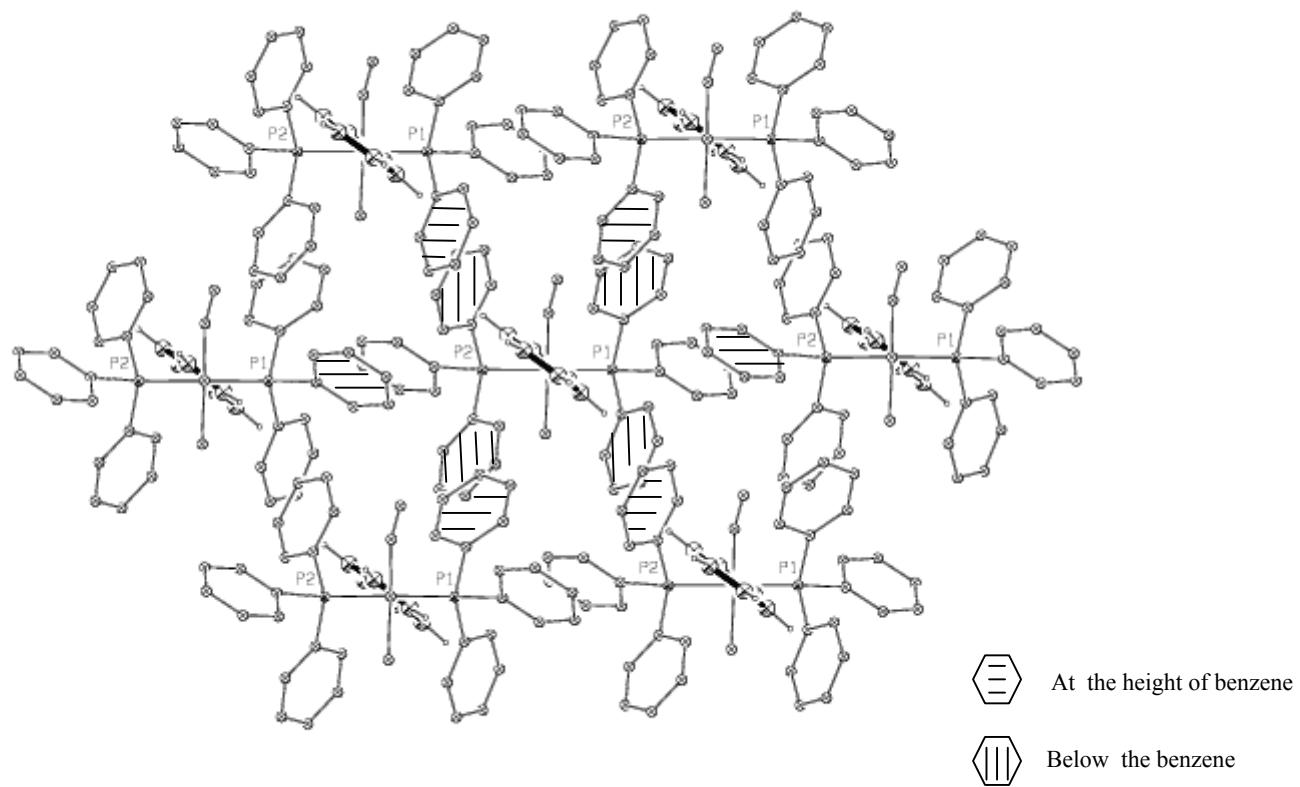


Figure 4.6. Benzene Solvate in the Bowl Shaped Cavity of $\text{NiCl}(\text{NO})(\text{PPh}_3)_2$

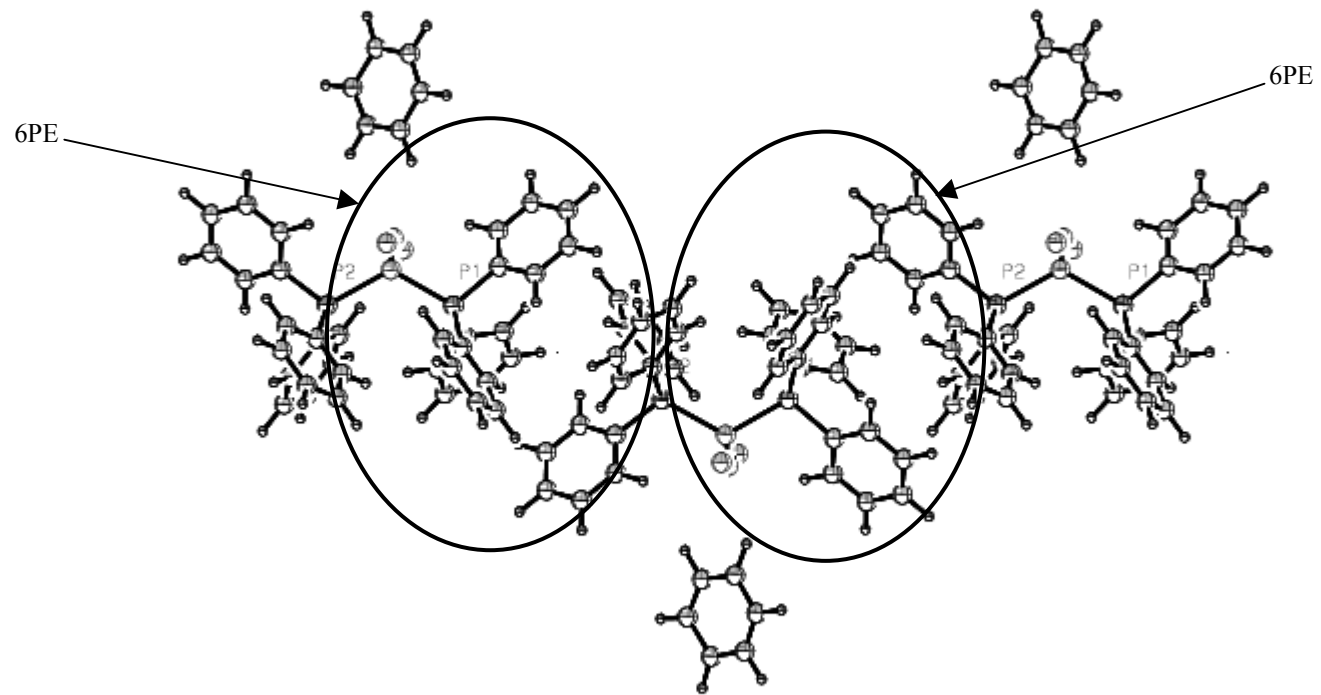


Figure 4.7. 6PE Linking NiCl(NO)(PPh₃)₂ Molecules into Chains.

between the P–Ni–P and N₃–Ni–NO planes is 85.1(2)°. The coordination of the NO group is distinctly nonlinear with an Ni–N–O angle of 152.7(7)°. The distances of Ni–N₃ = 2.018(8) Å, Ni–NO = 1.686(7) Å, and N–O = 1.164(8) Å are normal. The complex displays nonequivalent Ni–P distances of Ni–P(1) = 2.257(2) Å and Ni–P(2) = 2.306(2) Å (23σ difference), similar to the isothiocyanato complex. The azide ligand is nonlinearly coordinated to the Ni atom and thus is asymmetrically related to the two phosphine ligands. Examination of the intramolecular nonbonded interactions involving the azide ligand confirms that the nonequivalence of the Ni–P bonds does not result from this asymmetry.

The coordinates for the nonhydrogen atoms and the calculated coordinates for the hydrogen atoms of Ni(N₃)(NO)(PPh₃)₂ are given in Tables A.5 and A.6 in Appendix A. The intermolecular P···P contacts for which there are C–H···π interactions are tabulated in Table 4.3, along with the midpoints of the P···P vector, the symmetry relationship between the two phosphines, the P···P distance and the M–P···P–M colinearity parameters, the individual C–H···π interaction distances, and the appropriate identifiers defined by Dance and Scudder to aid discussion about the interactions. The individual angles that contribute to the colinearity parameter are given in Table B.5 in Appendix B.

The shortest intermolecular nonbonded P···P distances in Ni(N₃)(NO)(PPh₃)₂ are 7.411 Å and 7.825 Å with colinearities of 86.9° and 117.7°, thus not sextuple phenyl embraces. The strongest nonbonded interaction in the structure, shown in the Figure 4.8 schematic diagram of the azide environment, is a 2.395 Å C–H···N *intramolecular* hydrogen bond interaction from P2R5 to the ligand sp² lone pair orbital on N(1), the nitrogen bonded to the nickel atom ($\angle[\text{Ni}-\text{N}(1)\cdots\text{H}65] = 94.69^\circ$ and $\angle[\text{N}(2)-\text{N}(1)\cdots\text{H}(65)] = 132.01^\circ$) destroying the pseudo 3-fold symmetry of one triphenylphosphine ligand (P2), thus making formation of a sextuple phenyl embrace to P2 impossible. Another strong C–H···N *intramolecular* interaction of 2.647 Å from ring P1R1 to the N(2)–N(3) π cloud region of the azide ligand ($\angle[\text{N}(1)-\text{N}(2)\cdots\text{H}(21)] = 97.55^\circ$, $\angle[\text{N}(2)-\text{N}(3)\cdots\text{H}(21)] = 68.92^\circ$, and $\angle[\text{N}(3)-\text{N}(2)\cdots\text{H}(21)] = 84.17^\circ$) involving the other triphenylphosphine ligand (P1), thereby disrupting the second possibility to form a sextuple phenyl embrace.

The azide ligand is also involved in five *intermolecular* nonbonded interactions. If one assumes that N(1) is sp² ($\angle[\text{Ni}-\text{N}(1)-\text{N}(2)] = 128.1^\circ$, sum of

Table 4.3. Concerted Hydrogen Bond Interactions and Selected Interatomic C–H...X Distances Defining the Ni(N₃)(NO)(P(C₆H₅)₃)₂ Supramolecular Structure.

N ₃ -Phenyl Contact			
Intramolecular Contact of C-H...N Distances		Intermolecular Contacts of C-H...N Distances	
C-H _(P2R5) ...N1	2.395	C ^G -H ^G _(P1R1) ...N1	2.773
C-H _(P1R1) ...N1	2.941	C ^G -H ^G _(P1R1) ...N1	2.987
C-H _(P1R1) ...N2	2.647	C ^G -H ^G _(P1R1) ...N2	2.607
C-H _(P1R2) ...N2	2.945	C ^G -H ^G _(P2R6) ...N3	2.631
C-H _(P1R1) ...N3	2.823	C ^G -H ^G _(P1R1) ...N3	2.824
		C ^M -H ^M _(P1R2) ...N1	2.750
		C ^M -H ^M _(P1R2) ...N2	2.600
		C ^M -H ^M _(P1R2) ...N3	2.952
		C ^H -H ^H _(P2R5) ...N2	3.012
		C ^H -H ^H _(P2R5) ...N3	2.757
		C ^H -H ^H _(P2R5) ...N3	3.042
		C ^D -H ^D _(P2R6) ...N3	2.491
NO-Phenyl Contact			
Intramolecular Contact of C-H...N Distances		Intermolecular Contact of C-H...N Distances	
C-H _(P2R4) ...N4	2.716		
C-H _(P1R2) ...N4	2.755		
Intramolecular Contact of C-H...O Distances		Intermolecular Contacts of C-H...O Distances	
C-H _(P2R4) ...O	2.687	C ^M -H ^M _(P1R3) ...O	2.849
		C ^M -H ^M _(P1R3) ...O	2.946
		C ^J -H ^J _(P2R5) ...O	2.889
		C ^J -H ^J _(P2R5) ...O	3.259
		C ^F -H ^F _(P2R4) ...O	3.237

Phenyl-Phenyl Contacts							
d[Pn...Pn ^S] (Å)	Midpoint Pn...Pn ^S	Colinearity (°)	Phenyl-Phenyl Contact Distances C-H...C				
P1...P2 ^I 8.811 P2...P1 ^I	(0.0177, 0.4134, 0.5864)	114.90	C-H _(P2R4) ...C ^I π _(P1R3)	3.229	C ^I -H ^I _(P1R3) ...Cπ _(P2R6)	2.844	D4PE
			C-H _(P2R4) ...C ^I π _(P1R1)	3.080	C ^I -H ^I _(P1R1) ...Cπ _(P2R4)	2.966	
P1...P1 ^I 8.978 (46603)	(-1/2, 1/2, 1/2)	100.62	C-H _(P1R3) ...C ^I π _(P1R1)	2.851	C ^I -H ^I _(P1R3) ...Cπ _(P1R1)	2.851	
			C-H _(P1R3) ...C ^I π _(P2R6)	2.844	C ^I -H ^I _(P2R4) ...Cπ _(P1R3)	3.229	
			C-H _(P1R1) ...C ^I π _(P2R4)	2.966	C ^I -H ^I _(P2R4) ...Cπ _(P1R1)	3.080	
P1...P2 ^F 8.728 (44502)	(-0.4911, 0.2077, 0.3364)	128.83	C-H _(P1R3) ...C ^F π _(P2R4)	3.161	C ^F -H ^F _(P2R4) ...Cπ _(P1R3)	3.379	4PE
			C-H _(P1R3) ...C ^F π _(P2R5)	2.900			
P2...P1 ^E 8.728 (45502)	(-0.5088, 0.7077, 0.1635)	128.83	C-H _(P2R5) ...C ^E π _(P1R3)	3.205	C ^E -H ^E _(P1R3) ...Cπ _(P2R4)	3.161	4PE
			C-H _(P2R4) ...C ^E π _(P1R2)	2.802	C ^E -H ^E _(P1R3) ...Cπ _(P2R5)	2.900	
			C-H _(P2R4) ...C ^E π _(P1R3)	3.379			
P1...P2 ^G	(0.0177, 0.4134, 0.5864)	98.37	C-H _(P1R1) ...C ^G π _(P2R6)	2.821	C ^G -H ^G _(P2R6) ...Cπ _(P1R2)	3.150	D3PE
P2...P1 ^G 8.764 (56603)	(-0.0177, 0.5866, 0.4135)		C-H _(P2R6) ...C ^G π _(P1R2)	3.150	C ^G -H ^G _(P1R1) ...Cπ _(P2R6)	2.821	
P2...P2 ^L (56504)			C-H _(P2R6) ...C ^L π _(P2R5)	3.318	C ^L -H ^L _(P2R5) ...Cπ _(P2R6)	3.277	<i>ee</i>
P1...P1 ^K 7.825 (55504)	(-0.2675, 0.2500, 0.6251)	117.72			C ^K -H ^K _(P1R2) ...Cπ _(P1R1)	2.944	
P2...P1 ^J 8.962	(-0.5088, 0.5866, - 0.1729)	79.02	C-H _(P2R4) ...C ^J π _(P2R5)	2.977	C ^J -H ^J _(P2R4) ...Cπ _(P2R5)	2.977	
P2...P2 ^J 7.411 (46503)	(-1/2, 1/2, 0)	86.93	C-H _(P2R5) ...C ^J π _(P1R3)	3.340			
P2...P1 ^C 10.961 (55401)			C-H _(P2R5) ...C ^C π _(P1R1)	3.344	C ^C -H ^C _(P1R1) ...Cπ _(P2R5)	3.008	

P1...P2 ^B 10.961 (55601)			C-H _(P1R1) ...C ^B π _(P2R5)	3.088	C ^B -H _(P2R5) ...C π _(P1R1)	3.344	
----------------------------------------	--	--	-----------------------------------------------------------------	-------	------------------------------------------------------------------	-------	--

*P_n represents P1 or P2 as appropriate

Superscripts are used to denote the symmetry operation (give in Appendix B) for the transformation of the atom coordinates (given in Appendix A) for the described interaction. If no transformation is required (symmetry operation A) no superscript is given.

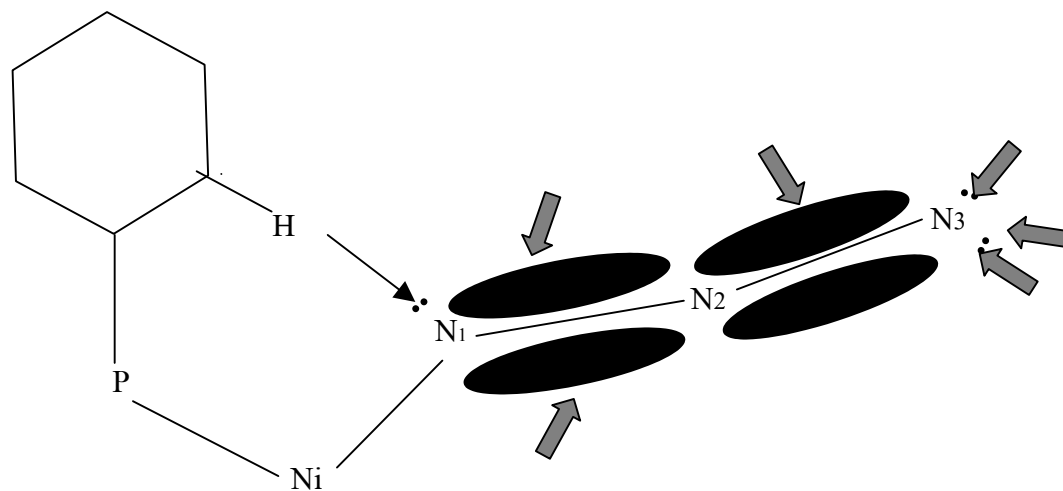


Figure 4.8. C—H...N Interactions to the Azido Ligand of $\text{NiN}_3(\text{NO})(\text{PPh}_3)_2$.

angles about N(1) = 355.1°) the π bond density between N(1) and N(2) will be in the plane perpendicular to the Ni–N(1)–N(2) plane. This model would be the same as the result observed from structure correlation for carbonyl groups in organic compounds (Bilton, Allen, Shields & Howard, 2000) where 85% of the observations have hydrogen bonding interactions to opposite sides of the carbonyl group.

Two of the five intermolecular nonbonded interactions to the azide ligand are C–H $\cdots\pi$ interactions from phenyl rings to this π cloud region. One interaction from ring P1R2 on a glide related molecule at 2.600 Å, (\angle [N(1)–N(2) \cdots H(52)] = 88.19°, \angle [N(2)–N(1) \cdots H(52)] = 70.94°, and torsional \angle [Ni–N(1)–N(2) \cdots H(52)] = 77.6°) is located in the expected position. The second from ring P1R1 on an inversion related molecule at 2.607 Å, (\angle [N(1)–N(2) \cdots H(41)] = 89.26°, \angle [N(2)–N(1) \cdots H(41)] = 70.05°, and torsional \angle [Ni–N(1)–N(2) \cdots H(41)] = –167.2°) however is not located opposite the first, \angle [H(52)–N(2)–H(41)] = 115.07°, bringing the comparison into question. Three C–H \cdots N interactions to the lone pairs on N(3) complete the interaction environment around the azide ligand. Two of three are the C_(P2R6)–H \cdots N(3) distance is 2.491 Å (\angle [N(2)–N(3) \cdots H(36)] = 133.69°) and the C_(P2R6)–H \cdots N(3) distance is 2.631 Å (\angle [N(2)–N(3) \cdots H(56)] = 122.64°) approaching in strength to the intermolecular interaction at the N(1) lone pair.

The third intermolecular C–H \cdots N(3) interaction from a different inversion related molecule, C_(P2R5)–H \cdots N(3) is to the lone pair on N(3) between the interaction of the C_(P2R6)–H \cdots N(3) and the C_(P2R6)–H \cdots N(3) at 2.757 Å (\angle [N(2)–N(3) \cdots H(45)] = 125.03°, Ni–N(2)–N(3)–H(45) torsion angle is 158.3). The hydrogen bond environment of the azide ligand is illustrated in Figure 4.9. Interestingly, and probably coincidentally, the lone pair on N(3) shows a tendency to form a bifurcated hydrogen bond at the lone pair on N(3) when the azide ligand N(2)–N(3) π electron cloud is engaged in an intramolecular interaction. Consistent with the observation of Bilton, Allen, Shields & Howard (2000), the donor hydrogen atoms that are involved in intramolecular hydrogen bonds do not form intermolecular hydrogen bonds.

As the azide ligand is the strongest hydrogen bond acceptor in the complex, although no clear extended two or three dimensional pattern is discernable, the interactions involving it are probably the most important determiners of the supramolecular structure of the complex. One chain with strong interactions (azide) alternating with weak interactions (C–H $\cdots\pi$) is illustrated in Figure 4.10.

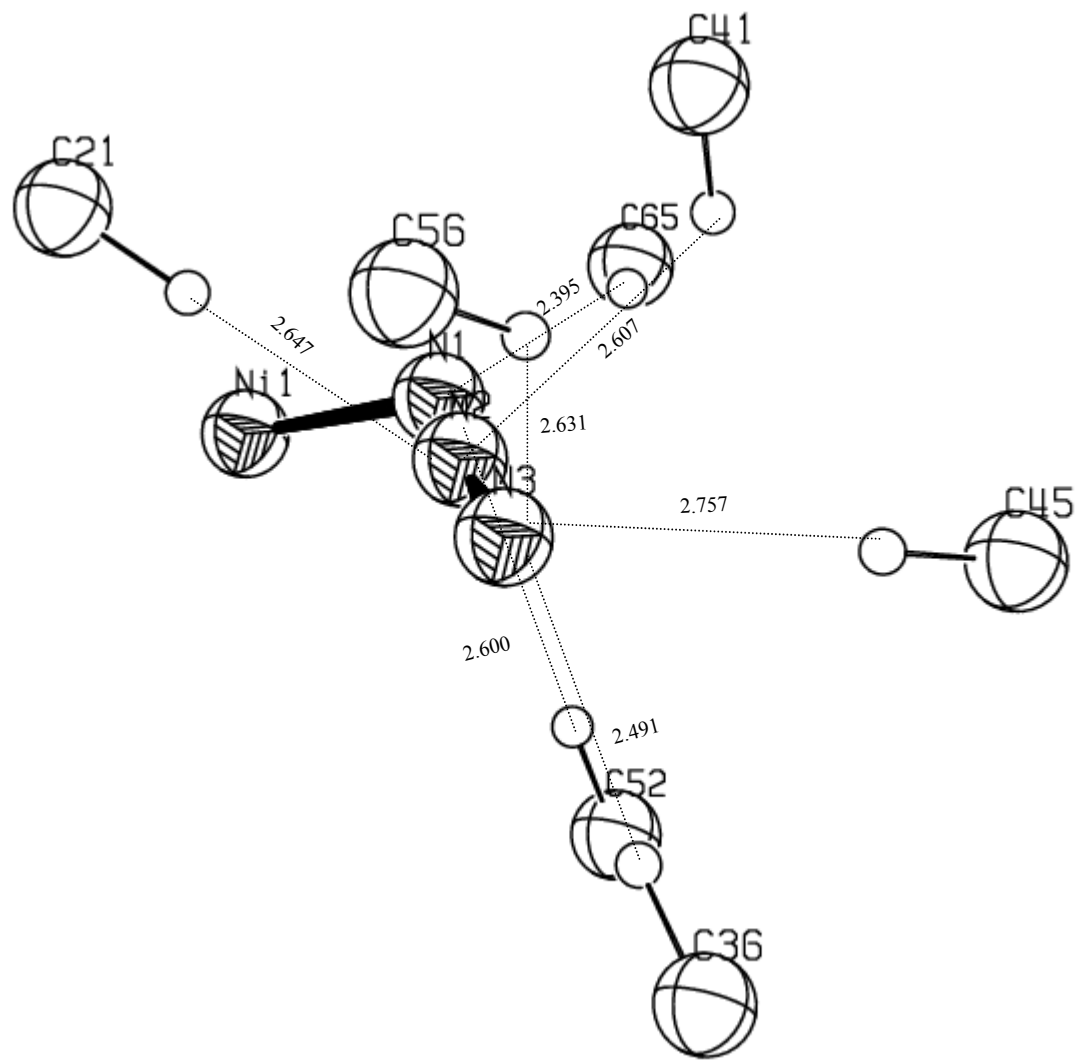


Figure 4.9. Azido Ligand Environment in $\text{NiN}_3(\text{NO})(\text{PPh}_3)_2$

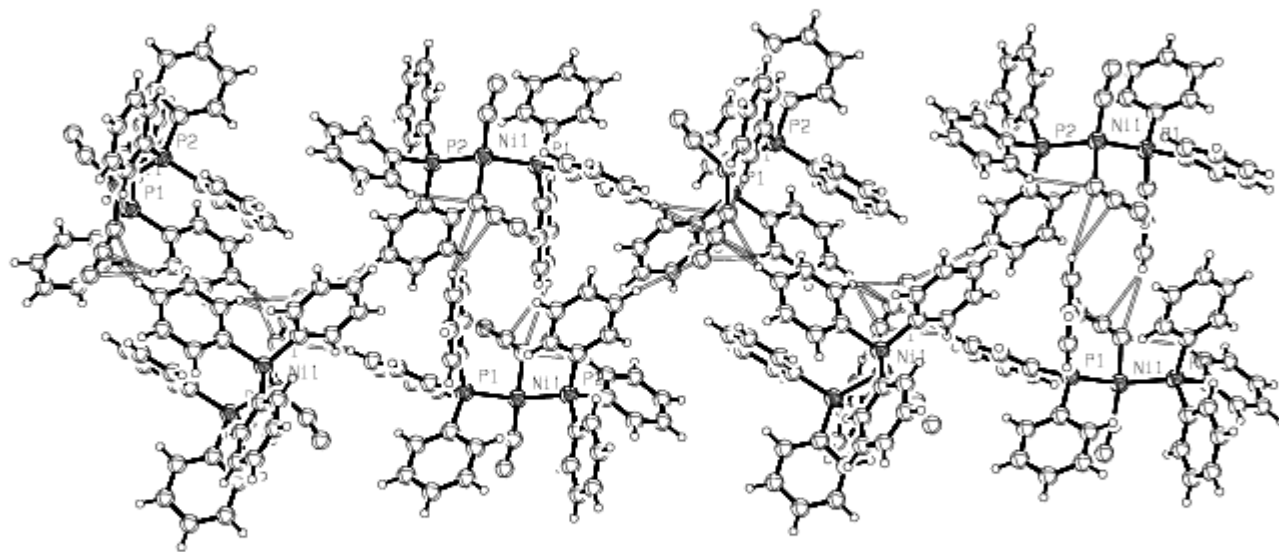


Figure 4.10. Chain of Azido and Phenyl Interactions in $\text{NiN}_3(\text{NO})(\text{PPh}_3)_2$.

The nitrosyl ligand should also be a better hydrogen bond acceptor than a phenyl ring. The strongest interaction to the nitrosyl is a moderately strong intramolecular $C_{(P2R4)}-H \cdots \pi_{NO}$ bond at 2.687 Å ($\angle[N(4)-O(1) \cdots H(24)] = 78.90^\circ$, $\angle[O(1)-N(4) \cdots H(24)] = 76.16^\circ$). Two C–H \cdots O intermolecular interactions involving oxygen atom lone pairs, a $C_{(P1R3)}-H \cdots O$ interaction at 2.849 Å, ($\angle[N(4)-O(1)-H(53)] = 153.11^\circ$; $\angle[Ni-N(4)-O(1)-H(53)] = -166.3^\circ$) and a $C_{(P2R5)}-H \cdots O$ interaction at 2.889 Å ($\angle[N(4)-O(1)-H(25)] = 140.73^\circ$; $\angle[Ni-N(4)-O(1)-H(25)] = 108.6^\circ$) are weaker than the corresponding interactions for the azide ligand.

Phenyl-phenyl interactions are still abundant and still important in determining finer details of the crystal structure. The multiple phenyl embraces between Ph_3P in direction of inversion with $P(1) \cdots P(2)$, $P(2) \cdots P(1)$ separation of 8.764 Å and $Ni-P \cdots P-Ni$ angle colinearity parameter is 98.37° . Two phenyl ring from P1R2 and P1R1 have edge-face interactions to one phenyl from P2R6 and another, phenyl ring from P2R6 has edge-to-face interactions to two phenyl rings from P1R2 and P1R1, distances are 2.821 Å and 3.150 Å. Each set has triplet interactions resulting from a concerted two 2PE interaction, one $C_{(P1R41)}-H \cdots \pi$ intermolecular interaction to the $N(1)-N(2)$ π electron cloud of the azide ligand, and one $C_{(P2R6)}-H \cdots N(3)$ to the azide ligand with a distance of 2.631 Å. Combined with the inversion center, these interactions produce a six component cooperative effect to form local dimers.

Contacts to the next molecule along the [1 0 0] direction with $P1 \cdots P2$ and $P2 \cdots P1$ separated at 8.881 Å and $Ni-P \cdots P-Ni$ angle colinearity parameter of 114.90° show eight weak phenyl-phenyl interactions between the two molecules across the inversion center, and two intramolecular $C_{(P1R1)}-H \cdots N(2)$ interactions at 2.647 Å to the azide ligand $N(2)-N(3)$ π electron cloud and two intramolecular $C_{(P2R4)}-H \cdots \pi_{NO}$ interactions at 2.687 Å to the nitrosyl ligand π electron cloud.

Chapter V

Conclusions

Nickel nitrosyl bis(triphenylphosphine) complexes are consisted of intermolecular forces of aromatic compounds are three phenyl ring on phosphorus atom, notably the ubiquitous edge-to-face (herringbone) and face-to-face (stacking) patterns. Thus their structure features are best described in terms of supramolecular descriptors, that is patterns of interactions rather than in terms of molecular descriptors, that are ligands. While molecular structure to supramolecular structure correspondence are relation between ligand groups and patterns of interactions and so questions relating to the prediction of supramolecular structure from molecular structure: (i) are difficult to answer; (ii) may have multiple answers.

Examine the supramolecular structure interactions of the low symmetry pseudo tetrahedral $\text{NiX}(\text{NO})(\text{PPh}_3)_2$ complexes using the recently formulated concerted interaction model based on phenyl-phenyl contacts. The title complexes with $\text{X} = \text{NCS}^-$, N_3^- , and Cl^- while closely related have quite different form in a hierarchical supramolecular structures of the weak $\text{C-H}\cdots\pi$ and $\text{C-H}\cdots\text{X}$ interactions.

The primary extended interactions in the isothiocyanato complex are the expected 6PE between adjacent TPP ligands which occur in parallel chains made up of alternating, $d[\text{P-P}] = 7.087 \text{ \AA}$, colinearity = 176.9° and $d[\text{P-P}] = 7.246 \text{ \AA}$, colinearity = 173.0° , 6PE. Adjacent chains are joined by four phenyl ring regions to form layers dominated by *ef* $\text{C-H}\cdots\pi$ interactions. Layers are joined together by nitrosyl-phenyl and phenyl-phenyl interactions.

The chloro complex contains a benzene solvate which can be viewed as lying within a cavity with one end inserted into the cleft of a bis-TPP nickel fragment located on a pseudo two-fold axis utilizing one complex-to-benzene *ef* and one benzene-to-complex *ef* interaction to each of the TPP ligands. The central region of the cavity is occupied by six additional *ef* interactions, and the cavity is completed by the chloro and nitrosyl ligands of another molecule. Thus, the benzene molecule, able

to form considerably more C–H \cdots π interactions, becomes the major link between surrounding molecules.

The shortest intermolecular P–P distances in the azido complex are 7.411 Å and 7.825 Å with colinearities of 86.9° and 117.7°, thus not 6PE. The strongest nonbonded interaction is a 2.493 Å *intramolecular* C–H \cdots N interaction to the lone pair on the N bonded to Ni destroying the pseudo three-fold symmetry of one TPP ligand, while another strong *intramolecular* C–H \cdots N interaction to the azido ligand π cloud involves the other TPP ligand, thus disrupting the both possibilities to form 6PEs. The azido ligand is also involved in intermolecular nonbonded interactions. Thus, as the strongest hydrogen bond acceptor, the azido ligand becomes the most important determiner of the supramolecular structure.

This study does not eliminate the possibility that the nonequivalence of the Ni–P bonds is due to supramolecular effects. NMR studies could be used to explore if the nonequivalence persists in solution indicating it is an electronic effect of the NiX(NO)(PPh₃)₂ system.

References

References

- Ainscough, E. W. & Brodie, A. M. (1995). Nitric Oxide-Some Old and New Perspectives. *J. Chem. Ed.* 72, 686-692.
- Becalska, A., Batchelor, J. R., Einstein, W. B. F., Hill, H. R. & Palmer, J. B. (1992). Solid-State Photochemistry and Structure of trans-(Et₃P)₂Ni(N₃)₂: Photodeposition of Nickel. *Inorg. Chem.* 31, 3118-3123.
- Bilton, C., Allen, F. H., Shields, G. P. & Howard, J. A. K. (2000). Intermolecular Hydrogen Bonds: Common Motifs, Probabilities of Formation and Implications for Supramolecular Organization. *Acta Cryst.* B56, 849-856.
- Brammer, L. & Stevens, E. D. (1989). Structure of Dichlorobis(triphenylphosphine) nickel(II). *Acta Cryst.* C45, 400-403.
- Burgi, H.-B. & Dunitz, J. D. (1994). *Structure Correlation*, Vol. 2, VCH Publishers, New York.
- Burnett, M. N. & Johnson C. K. (1996). ORTEP-III: Oak Ridge Thermal Ellipsoid Plot Program for Crystal Structure Illustrations, Report ORNL-6895, Oak Ridge National Laboratory, Oak Ridge.
- Cambridge Structural Database. (1999). Cambridge Crystallographic Data Centre, 12 Union Road, Cambridge, England.
- Cambridge Structural Database. (2001). Version 5.21, Cambridge Crystallographic Data Centre, 12 Union Road, Cambridge, England.
- Corain, B., Longato B., Angeletti R. & Valle G. (1985). Trans-[dichlorobis(triphenylphosphine)nickel(II)]·(C₂H₄Cl₂)₂: a Clathrate of the Allogon of Venanzi's Tetrahedral Complexes. *Inorg. Chim. Acta*, 10415-10418.
- Cotton, F. A., Wilkinson, G., Murillo, C. A. & Bochmann, M. (1999). *Advanced Inorganic Chemistry*, 6th ed., John Wiley & Sons, New York, 835-854.
- Dance, I., & Scudder, M. (1995). The Sextuple Phenyl Embrace, a Ubiquitous Concerted Supramolecular Motif. *J. Chem. Soc., Chem. Commun.* 1039-1040.
- Dance, I. & Scudder, M. (1996). Concerted Supramolecular Motifs: Linear Columns and Zigzag Chains of Multiple Phenyl Embraces Involving Ph₄P⁺ Cations in Crystals. *J. Chem. Soc., Dalton Trans.* 3755-3769.
- Dance, I. & Scudder, M. (1998). Crystal Supramolecularity: Elaborate Six-, Eight- and Twelve-Fold Concerted Phenyl Embraces in Compounds [M(PPh₃)₃]^z and [M(PPh₃)₄]^z. *New J. Chem.* 481-492.
- Del Zotto, A., Mezzetti, A., Novelli, V., Rigo, P., Lanfranchi, M. & Tiripicchio, A. (1990). Nickel Nitrosyl Complexes with Diphosphines. The Crystal and Molecular Structure of [(dppe)(NO)Ni(μ-dppe)Ni(NO)(dppe)][BF₄]; (dppe = Ph₂PCH₂CH₂PPh₂). *J. Chem. Soc. Dalton Trans.* 3, 1035-1042.

- Desiraju, G. R. (1995). Supramolecular Synthons in Crystal Engineering-A New Organic Synthesis. *Angew. Chem. Int. Ed, Engl.* 34, 2311-2327.
- Di Vaira, M., Ghilardi, C. A. & Sacconi, L. (1976). Synthesis and Structural Characterization of Some Nitrosyl Complexes of Iron, Cobalt, and Nickel with Poly(tertiary phosphines and arsines). *Inorg. Chem.* 15, 1555-1561.
- Drago, R. S. (1992). *Physical Methods for Chemists*, 2nd Edition, Saunders College Publishing, pp689-691.
- Elbaze, G., Dahan, F., Dartiguenave, M. & Dartiguenave, Y. (1984). Nickel-Nitrosyl Complexes: Structure of Nitrosyltris(trimethylphosphine) Nickel Hexafluorophosphate, $\{\text{Ni}(\text{NO})(\text{PM}_3)_3\}\text{PF}_6$. *Inorg. Chim. Acta*, 87, 91-97.
- Enemark, J. H. (1971). Four-Coordinate Metal Nitrosyls 1. the Structure of Azido-nitrosylbis(triphenylphosphine)nickel, $\text{Ni}(\text{N}_3)(\text{NO})(\text{P}(\text{C}_6\text{H}_5)_3)_2$. *Inorg. Chem.* 10, 1952-1956.
- Enemark, J. H. & Feltham, R. D. (1972). Stereochemical Control of Valence and Its Application to the Reduction of Coordinated NO and N_2 . *Proc. Nat. Acad. Sci. USA*, 69, 3534-3536.
- Enemark, J. H. & Feltham, R. D. (1974). Principles of Structure, Bonding, and Reactivity for Metal Nitrosyl Complexes. *Coord. Chem. Rev.*, 13, 339-406.
- Enemark, J. H., Feltham, R. D., Riker-Nappier, J. & Bizot, K. F. (1975). Stereochemical Control of Valence IV. Comparison of the Structures and Chemical Reactivities of Five- and Six-Coordinate Complexes of the $\{\text{CoNO}\}^8$ Group. *Inorg. Chem.* 14, 624-632.
- Errington, R. J. (1997). *Advanced Practical Inorganic and Metalorganic Chemistry*. 1sted. London.
- Feltham, R. D. (1964). Metal Nitrosyls. I, II, III Triphenylphosphine Nitrosyl Nickel Complexes. *Inorg. Chem.* 3, 116-122.
- Feltham, R. D. & Enemark, J. H. (1981). Structure of Metal Nitrosyls, in *Topics in Stereochemistry*. Vol. 12, Geoffrey, G. L., Ed., 155ff.
- Garton, G., Henn, D. E., Powell H. M. & Venanzi, L. M. (1963). Tetrahedral Nickel(II) Complexes and the Factors Determining Their Formation. Part V. The Tetrahedral Co-ordination of Nickel in Dichlorobistriphenylphosphinenickel. *J. Chem. Soc. Chem. Comm.* 3625-3629.
- Hall, S. R., Allen, F. H. & Brown, I. D. (1991). The Crystallographic Information File (CIF): a New Standard Archive File for Crystallography. *Acta Cryst.* A47, 655-685.
- Haller, K. J. (1978). *Structural Studies of the Binding of Small Molecules to Transition Metals*. PhD Dissertation, The University of Arizona, Tucson.
- Haller, K. J. & Enemark, J. H. (1978). Four-Coordinate Metal Nitrosyls 2. Structure of $\text{NiX}(\text{NO})(\text{P}(\text{C}_6\text{H}_5)_3)_2$ Complexes. *Inorg. Chem.* 17, 3552-3558.
- Hammond, C. (1997). *The Basics of Crystallography and Diffraction*, International Union of Crystallography; Oxford University Press Inc.:New York.

- Huheey, J. E., Keiter, E. A. & Keiter, R. L. (1993). *Inorganic Chemistry: Principles of Structure and Reactivity*. 6th ed. Harper Collins College, New York, 585, 634.
- Humphry, R. W., Welch, A. I. & Welch, D. A. (1988). Diiodobis(triphenylphosphine)nickel(II). *Acta Cryst.* C44, 1717-1719.
- Hunter, C. A. & Sanders, J. K. M. (1990). The Nature of π - π Interaction. *J. Am. Chem. Soc.* 112, 5525-5534.
- Jarvis, J. A. J., Mais, R. H. B. & Owston, P. G. (1968). The Stereochemistry of Complexes of Nickel(II). Part II. The Crystal and Molecular Structure of Dibromobis(triphenylphosphine) Nickel(II). *J. Chem. Soc. (A)*, 1473-1486.
- Kilbourn, B. T. & Powell, H. M. (1970). Allogons: Isomerism in the Crystal and Molecular Structure of the Green Form of Dibromobis(benzylidiphenylphosphine)nickel(II); $\text{Ni}[\text{P}(\text{CH}_2\text{Ph})\text{Ph}_2]_2\text{Br}_2[\text{square}] \cdot \text{Ni}[\text{P}(\text{CH}_2\text{Ph})\text{Ph}_2]_2\text{Br}_2[\text{tetrahedral}]$. *J. Chem. Soc. (A)*, 1688-1693.
- Kriege-Simonsen, J., Elbaze, G., Dartiguenave, M., Feltham, R. D., & Dartiguenave, Y. (1982). Oxygen Atom Transfer Reactions. 2. Reaction of Carbonmonoxide with $\text{Ni}(\text{NO}_2)_2(\text{PMe}_3)_2$ Structure of Nitrosylbis(trimethylphosphine)nickel, $\text{Ni}(\text{NO}_2)(\text{NO})(\text{PMe}_3)_2$ *Inorg. Chem.* 21, 230-236.
- Kriege-Simonsen, J. & Feltham, R. D. (1983). Oxygen Atom Transfer Reactions. 3. The Crystal Structures of $\text{Ni}(\text{NO}_2)_2\text{dppe}$ and $[\text{Ni}(\text{ONO})(\text{NO})\text{dppe}]_2$. *Inorg. Chim. Acta*, 17, 185-194.
- Krim, L., Manceron, L. & Alikhani, M. E. (1999). Vibrational Spectra and Structures of Nickel Mononitrosyl Complexes. An IR Matrix Isolation and DFT Study. *J. Phys. Chem. A*. 103, 15, 2592-2598.
- Lehn, J.-M. (1995). *Supramolecular Chemistry: Concepts and Perspectives*. VCH.
- Meiners, J. H., Rix, C. J., Clardy, J. C. & Verkade, J. G. (1975). Preparation, Properties, and Crystal Structure of a Cationic Nickel Nitrosyl Bicyclic Phosphite Complex. *Inorg. Chem.* 14(4), 705-710.
- Miedaner, A., Haltiwanger, C. R., & Dubois, L. D. (1991). Relationship between the Bite Size of Diphosphine Ligands and Tetrahedral Distortions of "Square-Planar" Nickel(II) Complexes: Stabilization of Nickel(I) and Palladium(I) Using Diphosphine Ligands with Large Bites. *Inorg. Chem.* 30, 417-427.
- Nakamoto, K. (1997). *Infrared and Raman Spectra of Inorganic and Co-ordination Compounds*. 5th Edition, John Wiley.
- Nishio, M. & Hirota, M. (1989). CH/ π Interaction: Implications in Organic Chemistry. *Tetrahedron*, 45, 23, 7201-7245.
- Orpen, G. A. & Connelly, N. G. (1985). Structure Evidence for the Participation of P-X σ^* Orbitals in Metal-PX₃ Bonding. *J. Chem. Soc., Chem. Commu.* 1310-1311.
- Palo, D. R. & Erkey, C. (1998). Solubility of Dichlorobis(triphenylphosphine)nickel(II) in Supercritical Carbon Dioxide. *J. Chem. Eng. Data*, 43, 47-48.

- Parkin, I. P. (1994). Nickel Dihalide Phosphine Complexes. *Inorganic Experiments*. J. Dereck Woollins (ed.) VCH, New York, 102.
- Rahman, A. F. M. M., Salem, G., Stephens, F. S. & Wild, S. B. (1990). Stability and Stereochemistry of Tetrahedral Nickel Nitrosyl Complexes: Crystal and Molecular Structure of (R*,S*)-anti-[NiNCS(NO){1,2-C₆H₄(PMePh)₂}] and (R*,S*)-anti-[NiNO{P(OMe)₃}{1,2-C₆H₄(PMePh)₂}]PF₆. *Inorg. Chem.* 29, 5225-5230.
- Scudder, M. & Dance, I. (1999). Crystal Supramolecularity: an Unusual Occurrence of Benzene Trapped in Edge-to-Edge Conformation. *Cryst. Eng. Comm.* [On Line] The Royal Society of Chemistry, 8.
- Sheldrick, G. M. (1993). *SHELX Program for the Refinement of Crystal Structure*. University of Goettingen, Germany.
- Shriver, D. F. & Drezdson, M. A. (1986). *The Manipulation of Air-Sensitive Compounds*. 2nd ed. John Wiley & Sons.
- Sletten, J. & Kovacs, J. A. (1993). Structure of trans-[dichlorobis(triphenylphosphine) Nickel(II)]·2CH₂Cl₂. *J. Crystallogr. Spectrosc. Res.*, 23, 239-241.
- Stamler, J. S. & Feelisch, M. (1996). "Biochemistry of Nitric Oxide and Redox – Related Species, in *Methods in Nitric Oxide Research*. Feelisch & Stamler, Eds, John Wiley & Sons, 19-28.
- Steed, J. W. & Atwood, J. L. (2000). *Supramolecular Chemistry*. John Wiley & Sons, England, pp392-397, 464-467.
- Steiner, T., (1997). Unrolling the Hydrogen Bond Properties of C-H...O Interactions. *Chem. Commun.* 727-734.
- Steiner, T. (1998). Molecular Columns Assembled by Specific Interactions Operating in Concert with Six-fold Phenyl Embraces. *ACA Transactions.* 33, 165-173.
- Steiner, T. & Desiraju, G. R. (1998). Distinction between the Weak Hydrogen Bond and the van der Waals Interaction. *J. Chem. Soc., Chem. Commun.* 891-892.
- Taylor, R. & Kennard, O. (1982). Crystallographic Evidence for the Existence of C-H...O, C-H...N, and C-H...Cl Hydrogen Bonds. *J. Am. Chem. Soc.* 104, 5063-5070.
- van Mier, G. P.M., Kanters, J. A. & Sjoerd H. (1987). A Tetrahedrally Surrounded Nickel(II) Complex: The Structure of Dichloro[2-(diphenylphosphino)-N,N-dimethylbenzylamine-N,P]nickel(II). *Acta Cryst.* C43, 2327-2330.
- Venanzi, M. L. (1958). Tetrahedral Nickel(II) Complexes and the Factors Determining Their Formation Part I. Bistriphenylphosphine Nickel(II) Compounds. *J. Chem. Soc.* 719-724.
- Xiao, S-X., Trogler, W. C., Ellis, D. E. & Berkovich-Yellin, Z. (1983). Theoretical Study of the Frontier Orbitals of Metal-Phosphine Complexes. *J. Am. Chem. Soc.* 105, 7033-7040.

Appendices

Appendix A

ORTEP Instruction Format and Atomic Coordinates

The crystal structure illustrations are drawn using the Oak Ridge Thermal Ellipsoid Plot program ORTEP-III (Burnett & Johnson, 1996). The ORTEP-III is illustrated all atoms are represented as spheres with sphere radii. The formation input data to ORTEP-III are showed in Appendix1. The data are used for calculations is accurate that verify by optimized structure against the one expected from correlation to molecular parameters, i.e. distance, angle, and the atomic coordination sphere and the distribution among symmetry operators.

Originally, the input to ORTEP-III since the input must generally be very precisely formatted as required by the FORTRAN code. Data input consists of five types of information:

1. Title at the first line of input is a job title.
2. Cell parameter are provide on the second line
3. The symmetry operators of the space group begin on line 3 of the input.
4. Atomic parameters for each atom. The first gives the atom's positional parameters and the second provides its thermal parameters.
5. Instruction are the commands used in drawing an illustrations to position and scale the subject for projection onto the drawing board and to utilize all available space which the commands are automatically sets the origin and drawing scale.for the instruction.

Definitions

The drawing and calculating are started NiX(NO)(P(P(C₆H₅)₃)₂ molecule at *atom designator code (ADC)* 55501 or XXXXX (NNTTTSS)where: *atom designator code(ADC)* is used to specify a particular atom in the crystal within a reasonable distance from the crystallographically defined origin are contained five-component.

$$ADC = AN*10^5 + (TA + 5)*10^4 + (TB + 5)*10^3 + (TC + 5)*10^2 + SN$$

Where: AN = *atom number* ($0 \leq AN \leq NATOM \leq 500$) - the numerical position of the atom in the input list of atoms in the asymmetric unit, which contains NATOM atoms. Atom 0 is not in the input atom list but refers to the crystal origin point (0.,0.,0.).

TA, TB, TC = *crystal lattice translation digits* – translations along cell edges a, b, and c, respectively. Each digit in an ADC can range from 1 to 9; consequently, it is possible to move up to 4 cells in any direction from the origin cell 555.

SN = *symmetry operator number* ($0 \leq SN \leq NSYM \leq 96$) – the numerical position of the symmetry operator in the input list of symmetry operators, which contains NSYM entries. Symmetry operator number 0 is not in the input list but refers to an identity operator. However, the identity operation (corresponding to position x, y, z) generally must be somewhere in the input symmetry operator list and is usually the first operator.

Example: An atom designator code of 347502 refers to atom 3 moved through symmetry operation 2, then translated –1 cell translation along a, +2 cell translations along b, and 0 cell translations along c.

An *Atom Designator Run (ADR)* is a straight run sequence of atoms that is defined using two atom designator codes with a “-“ preceding the second of the two. The run hierarchy is: first, atom number AN; second, symmetry operator number SN; third, a translation TA; fourth, b translation TB; and last, c translation TC.

Example: ADR (145502-245603) will generate the 8-atom run 145502, 245502, 145503, 245503, 145602, 245602, 145603, 245603.

The following exceptions are allowed in Org. ADRs of instructions 101, 102, 402/412, 403/413, and 404/414 only:

- The “-“ may be obtained from the second ADC.
- If the second atom in the atom designator run has the same

symmetry and translation components as the first atom, the second atom may be represented by its atom number component alone.

Example: ADR (345502-745502) may also be represented as (345502 745502) or (345502 7). ADR (355501-755501) may also be represented as (355501 755501) or (355501 7) or (3 7).

An *Atom Number Run (ANR)* is a subset of the atom designator run in which only the atom number AN changes. Normally, an ANR is entered by using only the atom number values for the first and last member of the sequence without a “-”.

Example: (1 4) will designate atoms 1, 2, 3, and 4 of the input list.

A *Vector Designator Code (VDC)* defines a vector using two atom designator codes. The vector direction is from the first to the second.

Example: 253704 263704 is a vector along the positive a director of the crystal lattice.

A *Vector Search Code* consists of two number runs and a distance range. It is used for finding interatomic distances that have a particular chemical significance, such as covalent and coordination bonds.

Example: Suppose that metal atoms are numbers 1 and 2 in the atom list, oxygen atoms are 6-12, and the interatomic distance range between metals and oxygens is 1.9 Å to 2.4 Å. The metal-to-oxygen vectors can be specified by the vector search code (1 2) (6 12) (1.9 2.4). Several variations of this basic code are used in ORTEP.

Instruction Input

1. Structure Analysis Instructions (100 Series)


This 100 series of instructions is not connected with drawing illustrations but rather with obtaining a convenient tabulation of the chemically interesting aspects of a crystal structure, including including interatomic distances and angles and principal axes of thermal motion. If the ORTEP output is omitted, these instructions do nothing.

Instructions 101 and 102

These instructions find all “target” atoms within a sphere of enclosure of radius D_{\max} about a particular “origin” atom. The instruction card has an atom designator run of one or several origin atoms (Org. ADR) and an atom number run of target atoms (Tar. ANR). The Org. ADR allows calculation of several spheres successively with a printout of results after each one.

A 101 instruction is used to obtain a tabulation of the atoms surrounding one atom or a series of several designated atoms.

Example: To obtain a list of all atoms (phosphorus and nickel) out to a distance of 12 Å about the two phosphorus P42 and P43, the following 101 instruction would be used.

101(102) 4255501 4355501 42 44 12

 (a) (b) (c)

where: (a) origin atoms 42 through 43 of symmetry operation 1,

(b) target atoms 42 through 44 of all symmetry and translation operations, and

(c) a distance D_{\max} of 12 Å.

A 102 instruction gives both interatomic distances and interatomic angles. The following instruction for example above (101) could be used to find all bonds and angles.

2. Illustration of Atoms Array Instructions (400 Series)

This series allows the user to specify which atoms are to be included in the illustration. The atom designators for the chosen atoms are stored in the ATOMS array for future use by other instructions.

Instruction 401

Group of atoms are added to the ATOMS array. The group can be denoted by atom designator runs, spheres of atoms about any center point, and boxes of atoms centered on any point. Duplicate entries of the same atomic position are prevented by program. These instructions contain:

- (a) atom designator codes for single atoms;
- (b) atom designator runs for several atoms in a run;
- (c) blank fields (except between the two entries of a run);
- (d) any combinations of (a), (b), and (c).

For example:

401 164501 -7464501 146501 -7446501

Table A.1. Crystal Data and Nonhydrogen Coordinates for Ni(NCS)(NO)(PPh₃)₂.

Cambridge Structural Database Reference Code: TPNTCN
 Compound Name: Isothiocyanato-nitrosyl-bis(triphenylphosphine) nickel
 Empirical Formula: C₃₇ H₃₀ N₄ Ni₁ O₁ P₂ S₁
 Unit Cell 12.288 13.496 9.947 91.25 86.80 95.58
 Cell Errors: 0.003 0.003 0.002 0.02 0.02 0.02
 Z: 2
 Space Group: P-1
 Symmetry Operators: +X,+Y,+Z; -X,-Y,-Z
 Atom Coordinates: (Atom Name, fractional x, fractional y, fractional z)

C11	0.56010	0.81850	0.69760
C21	0.54860	0.72320	0.74820
C31	0.44850	0.66680	0.74710
C41	0.35980	0.70580	0.69530
C51	0.37130	0.80110	0.64460
C61	0.47150	0.85750	0.64580
C12	0.65490	1.00840	0.78770
C22	0.65590	1.01420	0.92660
C32	0.62280	1.09750	0.99480
C42	0.58870	1.17500	0.92400
C52	0.58780	1.16910	0.78500
C62	0.62080	1.08580	0.71690
C13	0.72990	0.93090	0.53170
C23	0.67740	0.88830	0.42220
C33	0.71290	0.91690	0.29310
C43	0.80100	0.98800	0.27360
C53	0.85350	1.03060	0.38320
C63	0.81800	1.00210	0.51220
C14	0.97380	0.71930	0.53300
C24	0.92700	0.76870	0.43390
C34	0.98470	0.78880	0.31260
C44	1.08910	0.75950	0.29040
C54	1.13580	0.71010	0.38960
C64	1.07820	0.69000	0.51090
C15	0.98920	0.63510	0.79260
C25	1.05350	0.69250	0.88020
C35	1.13690	0.65190	0.94140
C45	1.15600	0.55390	0.91490
C55	1.09170	0.49640	0.82730
C65	1.00830	0.53700	0.76610
C16	0.78810	0.59580	0.65770
C26	0.73880	0.54260	0.76570
C36	0.65140	0.47210	0.74640
C46	0.61330	0.45470	0.61900
C56	0.66260	0.50790	0.51090
C66	0.75000	0.57850	0.53030
P1	0.69210	0.89311	0.70467
P2	0.89452	0.69582	0.69410
Ni1	0.82780	0.83008	0.81197
N1	0.75500	0.75390	0.96050
C1	0.70870	0.70900	1.04550
S1	0.64233	0.64380	1.16458
N2	0.90710	0.93080	0.85160
O1	0.93870	1.01360	0.86890

Table A.2. Calculated Hydrogen Atom Coordinates for Ni(NCS)(NO)(PPh₃)₂.

H21	0.61803	0.69274	0.78870
H31	0.43949	0.59217	0.78673
H41	0.28136	0.66167	0.69447
H51	0.30191	0.83155	0.60399
H61	0.48056	0.93214	0.60621
H22	0.68258	0.95356	0.98199
H32	0.62357	1.10206	1.10358
H42	0.56275	1.24020	0.97734
H52	0.56124	1.22975	0.72953
H62	0.61995	1.08116	0.60813
H23	0.60849	0.83255	0.43748
H33	0.67171	0.88362	0.20734
H43	0.82888	1.01032	0.17256
H53	0.92245	1.08631	0.36792
H63	0.85911	1.03547	0.59796
H24	0.84527	0.79162	0.45126
H34	0.94813	0.82749	0.23497
H44	1.13424	0.77523	0.19541
H54	1.21752	0.68716	0.37224
H64	1.11479	0.65135	0.58855
H25	1.03858	0.76927	0.90092
H35	1.18721	0.69687	1.01005
H45	1.22132	0.52215	0.96274
H55	1.10664	0.41963	0.80663
H65	0.95797	0.49203	0.69747
H26	0.76868	0.55617	0.86547
H36	0.61280	0.43052	0.83104
H46	0.54489	0.39945	0.60382
H56	0.63277	0.49428	0.41111
H66	0.78855	0.62019	0.44573

Table A.3. Crystal Data and Nonhydrogen Coordinates for NiCl(NO)(PPh₃)₂.

Cambridge Structural Database Reference Code: CLTPNN01
 Compound Name: Chloro-nitrosyl-bis(triphenylphosphine)-nickel benzene solvate
 Empirical Formula: C₃₆ H₃₀ N₁ Ni₁ O₁ P₂ (C₆ H₆)
 Unit Cell 17.399 13.136 16.954 90. 104.74 90.
 Cell Errors: 0.003 0.003 0.003 0. 0.01 0.
 Z: 4
 Space Group: Cc coordinates used from the CSD
 Symmetry Operators: +X,+Y,+Z; +X,-Y,1/2+Z; 1/2+X,1/2+Y,+Z; 1/2+X,1/2-Y,1/2+Z
 Atom Coordinates: (Atom Name, fractional x, fractional y, fractional z)

C1	0.05550	0.29180	0.26390
C2	0.09490	0.38180	0.26690
C3	0.04160	0.47590	0.25030
C4	-0.04020	0.46280	0.23460
C5	-0.07310	0.37160	0.23350
C6	-0.02240	0.28170	0.24500
C11	-0.15630	-0.23600	0.19940
C12	-0.06120	-0.21420	0.08280
C13	-0.16780	-0.04470	0.09400
C14	0.16060	-0.22630	0.30470
C15	0.05980	-0.21560	0.41590
C16	0.17240	-0.05260	0.40670
C21	-0.18810	-0.32030	0.15380
C22	-0.09090	-0.20130	-0.00040
C23	-0.24880	-0.06250	0.07070
C24	0.19670	-0.30860	0.35030
C25	0.07200	-0.18660	0.49660
C26	0.25240	-0.07670	0.42910
C31	-0.23710	-0.38610	0.18220
C32	-0.06390	-0.26230	-0.05420
C33	-0.29840	0.00440	0.01840
C34	0.24350	-0.37430	0.31880
C35	0.03810	-0.24190	0.54850
C36	0.30600	-0.01100	0.47810
C41	-0.25420	-0.36750	0.25630
C42	-0.00730	-0.33630	-0.02480
C43	-0.26690	0.08900	-0.01060
C44	0.25420	-0.35760	0.24170
C45	-0.00800	-0.32640	0.51960
C46	0.27970	0.07890	0.50470
C51	-0.22230	-0.28320	0.30190
C52	0.02240	-0.34920	0.05840
C53	-0.18590	0.10680	0.01270
C54	0.21820	-0.27530	0.19610
C55	-0.02020	-0.35550	0.43890
C56	0.19970	0.10310	0.48230
C61	-0.17340	-0.21750	0.27350
C62	-0.00460	-0.28820	0.11220
C63	-0.13640	0.03990	0.06500
C64	0.17140	-0.20960	0.22760
C65	0.01370	-0.30010	0.38710
C66	0.14600	0.03730	0.43330
Cl1	-0.06240	0.01190	0.33020
N1	0.05740	0.02230	0.18050
Ni1	0.00000	-0.05274	0.25000
O1	0.07870	-0.00610	0.12720
P1	-0.09620	-0.13830	0.15920
P2	0.09741	-0.13740	0.34290

Table A.4. Calculated Hydrogen Atom Coordinates for NiCl(NO)(PPh₃)₂.

H1	0.09088	0.22323	0.27814
H2	0.15906	0.38636	0.28004
H3	0.06700	0.55123	0.25075
H4	-0.07827	0.52924	0.22289
H5	-0.13677	0.36403	0.22418
H6	-0.04877	0.20649	0.23801
H21	-0.17465	-0.33482	0.09586
H22	-0.13529	-0.14344	-0.02339
H23	-0.27338	-0.12879	0.09339
H24	0.18833	-0.32160	0.41064
H25	0.10814	-0.12052	0.51917
H26	0.27305	-0.14706	0.40824
H31	-0.26206	-0.45210	0.14649
H32	-0.08706	-0.25213	-0.11932
H33	-0.36183	-0.00944	0.00017
H34	0.27174	-0.43876	0.35446
H35	0.04762	-0.21910	0.61164
H36	0.36863	-0.02994	0.49567
H41	-0.29255	-0.41895	0.27857
H42	0.01378	-0.38416	-0.06692
H43	-0.30570	0.14135	-0.05159
H44	0.29081	-0.40905	0.21704
H45	-0.03455	-0.36978	0.56017
H46	0.32173	0.13036	0.54307
H51	-0.23566	-0.26870	0.35988
H52	0.06679	-0.40706	0.08139
H53	-0.16129	0.17306	-0.01000
H54	0.22663	-0.26228	0.13578
H55	-0.05628	-0.42163	0.41633
H56	0.17910	0.17352	0.50310
H61	-0.14844	-0.15151	0.30922
H62	0.01856	-0.29837	0.17732
H63	-0.07298	0.05377	0.08327
H64	0.14321	-0.14510	0.19195
H65	0.00416	-0.32287	0.32395
H66	0.08335	0.05616	0.41579

Table A.5. Crystal Data and Nonhydrogen Coordinates for NiN₃(NO)(PPh₃)₂.

Cambridge Structural Database Reference Code: AZNPNI
 Compound Name: Azido-nitrosyl-bis(triphenylphosphine) nickel
 Empirical Formula: C₃₆ H₃₀ N₄ Ni₁ O₁ P₂
 Unit Cell: 13.691 19.211 12.582 90 98.13 90
 Cell Errors: 0.006 0.0010 0.005 0.0 0.03 0.0
 Z: 4
 Space Group: P2₁/n
 Symmetry Operators: +X,+Y,+Z; -X,1/2+Y,1/2-Z; -X,-Y,-Z; +X,1/2-Y,1/2+Z
 Atom Coordinates: (Atom Name, fractional x, fractional y, fractional z)

C11	-0.20980	0.41270	0.50010
C21	-0.10780	0.42230	0.51370
C31	-0.06000	0.45620	0.60480
C41	-0.11420	0.48060	0.68220
C51	-0.21610	0.47110	0.66860
C61	-0.26390	0.43710	0.57750
C12	-0.20580	0.28610	0.38230
C22	-0.18230	0.25690	0.28810
C32	-0.13250	0.19360	0.29160
C42	-0.10620	0.15940	0.38930
C52	-0.12970	0.18860	0.48350
C62	-0.17950	0.25190	0.48000
C13	-0.39520	0.35550	0.39460
C23	-0.46220	0.41000	0.37220
C33	-0.56010	0.40120	0.38700
C43	-0.59100	0.33790	0.42430
C53	-0.52400	0.28340	0.44680
C63	-0.42610	0.29220	0.43190
C14	-0.41310	0.57220	0.20550
C24	-0.48920	0.53430	0.14630
C34	-0.58680	0.55590	0.14210
C44	-0.60820	0.61550	0.19710
C54	-0.53200	0.65350	0.25630
C64	-0.43440	0.63180	0.26050
C15	-0.26010	0.57390	0.06980
C25	-0.32720	0.61440	0.00220
C35	-0.30410	0.63720	-0.09600
C45	-0.21380	0.61950	-0.12660
C55	-0.14670	0.57890	-0.05900
C65	-0.16980	0.55610	0.03920
C16	-0.21130	0.60260	0.29770
C26	-0.16240	0.66050	0.26500
C36	-0.11020	0.70450	0.34140
C46	-0.10690	0.69060	0.45040
C56	-0.15580	0.63270	0.48320
C66	-0.20800	0.58870	0.40680
N1	-0.10880	0.43340	0.22220
N2	-0.05860	0.39790	0.24420
N3	0.01270	0.35510	0.27080
N4	-0.34000	0.38190	0.13280
Ni1	-0.25629	0.42630	0.21902
O1	-0.41560	0.35390	0.10930
P1	-0.26750	0.37110	0.37510
P2	-0.28520	0.54430	0.20220

Table A.6. Calculated Hydrogen Atom Coordinates for NiN₃(NO)(PPh₃)₂.

H21	-0.06536	0.40336	0.45328
H31	0.01923	0.46340	0.61492
H41	-0.07749	0.50692	0.75289
H51	-0.25855	0.49016	0.72893
H61	-0.34312	0.42985	0.56746
H22	-0.20268	0.28332	0.21217
H32	-0.11410	0.17081	0.21824
H42	-0.06750	0.11013	0.39170
H52	-0.10932	0.16218	0.55943
H62	-0.19790	0.27469	0.55336
H23	-0.43790	0.45925	0.34323
H33	-0.61219	0.44350	0.36954
H43	-0.66727	0.33092	0.43590
H53	-0.54827	0.23418	0.47590
H63	-0.37402	0.24989	0.44928
H24	-0.47226	0.48793	0.10349
H34	-0.64571	0.52642	0.09622
H44	-0.68395	0.63252	0.19410
H54	-0.54890	0.69993	0.29900
H64	-0.37544	0.66123	0.30639
H25	-0.39754	0.62808	0.02648
H35	-0.35619	0.66858	-0.14835
H45	-0.19528	0.63718	-0.20301
H55	-0.07640	0.56517	-0.08332
H65	-0.11777	0.52467	0.09152
H26	-0.16474	0.67154	0.18027
H36	-0.07219	0.74957	0.31566
H46	-0.06641	0.72474	0.50945
H56	-0.15345	0.62169	0.56794
H66	-0.24601	0.54364	0.43255

Appendix B

Supplementary Tables of Contact Distances and Angles

Table B.1. Description of the Short Intermolecular Phosphorus-Phosphorus Contacts for Ni(NCS)(NO)(PPh₃)₂.

Pn ^A ...Pn ^S	Primed Position (Pn ^S)	Midpoint of Pn ^A ...Pn ^S	Pn ^A ...Pn ^S Distance (Å)	Ni-Pn ^A ...Pn ^S Angle (°)	Pn ^A ...Pn ^S -Ni ^S Angle (°)	Colinearity Parameter (°)
P1...P1 ^K	67602 (K)	(1/2, 1, 1/2)	7.246	173.04	173.04	173.04
P1...P1 ^J	67702 (J)	(1/2, 1, 1)	7.997	104.69	104.69	104.69
P1...P1 ^G	77602 (G)	(1, 1, 1/2)	8.660	72.53	72.53	72.53
P1...P2 ^G	77602 (G)	(0.8988, 1.0986, 0.5053)	8.096	93.84	86.00	89.92
P1...P2 ^E	45501 (E)	(0.2933, 0.7944, 0.6994)	9.909	132.15	100.08	116.12
P1...P2 ^F	77702 (F)	(0.8988, 1.0986, 1.0053)	9.424	60.63	56.44	58.54
P1...P1 ^B	55601 (B)	(0.6921, 0.8931, 1.2047)	9.947	58.73	121.27	90.00
P1...P1 ^C	55401 (C)	(0.6921, 0.8931, 0.2047)	9.947	121.27	58.73	90.00
P1...P1 ^F	77702 (F)	(1, 1, 1)	10.004	39.10	39.10	39.10
P2...P2 ^I	76602 (I)	(1, 1/2, 1/2)	7.087	176.94	176.94	176.94
P2...P1 ^G	77602 (G)	(1.1012, 0.9013, 0.4947)	8.096	86.00	93.84	89.92
P2...P2 ^H	76702 (H)	(1, 1/2, 1)	8.805	106.03	106.03	106.03
P2...P1 ^D	65501 (D)	(1.2933, 0.7944, 0.6994)	9.909	100.08	132.15	116.12
P2...P2 ^G	77602 (G)	(1, 1, 1)	9.229	66.08	66.08	66.08
P2...P1 ^F	77702 (F)	(1.1012, 0.9013, 0.9947)	9.424	56.44	60.63	58.54
P2...P2 ^B	55601 (B)	(0.8945, 0.6958, 1.1941)	9.947	62.16	117.84	90.00
P1...P2 ^L	66602 (L)	(0.3988, 0.5986, 0.5053)	11.025	112.27	118.99	115.63
P2...P1 ^L	66602 (L)	(0.3079, 0.1069, 0.2953)	11.025	118.99	112.27	115.63
P2...P2 ^C	55401 (C)	(0.8945, 0.6958, 0.1941)	9.947	117.84	62.16	90.00

Table B.2. Table of Symmetry Operations for Ni(NCS)(NO)(PPh₃)₂.

Atom Designator Code (ADC)	Coordinate of Positions	Symbol of Symmetry Operation, s	Atom Designator Code (ADC)	Coordinate of Positions	Symbol of Symmetry Operation, s
55501	x, y, z	A	77602	-x+2, -y+2, -z+1	G
55601	x, y, z+1	B	76702	-x+2, -y+1, -z+2	H
55401	x, y, z-1	C	76602	-x+2, -y+1, -z+1	I
65501	x+1, y, z	D	67702	-x+1, -y+2, -z+2	J
45501	x-1, y, z	E	67602	-x+1, -y+2, -z+1	K
77702	-x+2, -y+2, -z+2	F	66602	-x+1, -y+1, -z+1	L

Table B.3. Description of the Short Intermolecular Phosphorus-Phosphorus Contacts for NiCl(NO)(PPh₃)₂.

Pn ^A ...Pn ^S	Primed Position (Pn ^S)	Midpoint of Pn ^A ...Pn ^S	Pn ^A ...Pn ^S Distance (Å)	Ni-Pn ^A ...Pn ^S Angle (°)	Pn ^A ...Pn ^S -Ni Angle (°)	Colinearity Parameter (°)
P1...P2 ^M	44404 (M)	(-1/4, -1/4, 0)	7.163	173.77	174.53	174.15
P1...P2 ^E	55402 (E)	(0.0006, -0.0004, 0.0010)	7.900	82.23	82.84	82.54
P1...P1 ^D	55502 (D)	(-0.0962, 0.1383, 0.6592)	9.223	49.62	104.87	77.24
P1...P1 ^E	55402 (E)	(-0.0962, 0.0000, -0.0908)	9.223	104.87	49.62	77.24
P1...P2 ^I	44503 (I)	(-0.2494, -0.3878, 0.25105)	9.463	120.08	79.47	99.78
P1...P2 ^H	45503 (H)	(-0.2494, 0.11215, 0.2510)	9.479	79.18	119.43	99.30
P2...P1 ^K	54504 (K)	(1/4, -1/4, 1/2)	7.163	174.53	173.77	174.15
P2...P1 ^D	55502 (D)	(0, 0, 1/2)	7.900	82.84	82.23	82.54
P2...P2 ^D	55502 (D)	(0, 0, 1/2)	9.214	105.64	49.41	77.52
P2...P2 ^E	55402 (E)	(0.0974, 0.0000, 0.0929)	9.214	49.41	105.64	77.52
P2...P1 ^G	54503 (G)	(0.2506, -0.3878, 0.2510)	9.479	119.43	79.18	99.30
P1...P1 ^G	54503 (G)	(0.1538, -0.3883, 0.1592)	10.900	81.21	98.79	90.00
P2...P2 ^H	45503 (H)	(-0.1526, 0.1126, 0.3429)	10.900	41.88	138.12	90.00
P2...P2 ^I	44503 (I)	(-0.1526, -0.3874, 0.3429)	10.900	80.88	99.12	90.00
P2...P1 ^F	55503 (F)	(0.2506, 0.1122, 0.2510)	9.463	79.47	120.08	99.78
P2...P2 ^F	55503 (F)	(0.2500, 0.1126, 0.3429)	10.900	99.12	80.88	90.00

Table B.4. Table of Symmetry Operations for NiCl(NO)(P(C₆H₅)₃)₂.

Atom Designator Code (ADC)	Coordinate of Positions	Symbol of Symmetry Operation, s	Atom Designator Code (ADC)	Coordinate of Positions	Symbol of Symmetry Operation, s
55501	x, y, z	A	45503	x-1/2, y+1/2, z	H
56501	x, y+1, z	B	44503	x-1/2, y-1/2, z	I
54501	x, y-1, z	C	55504	x+1/2, -y+1/2, z+1/2	J
55502	x, -y, z+1/2	D	54504	x+1/2, -y-1/2, z+1/2	K
55402	x, -y, z-1/2	E	45404	x-1/2, -y+1/2, z-1/2	L
55503	x+1/2, y+1/2, z	F	44404	x-1/2, -y-1/2, z-1/2	M
54503	x+1/2, y-1/2, z	G			

Table B.5. Description of the Short Intermolecular Phosphorus-Phosphorus Contacts for NiN₃(NO)(P(C₆H₅)₃)₂.

Pn ^A ...Pn ^S	Primed Position (Pn ^S)	Midpoint of Pn ^A ...Pn ^{S*}	Pn ^A ...Pn ^S Distance (Å)	Ni- Pn ^A ...Pn ^S Angle (°)	Pn ^A ...Pn ^S -Ni ^S Angle (°)	Colinearity Parameter (°)
P1...P1 ^K	55504 (K)	(-0.2675, 0.2500, 0.6251)	7.825	170.78	64.66	117.72
P1...P2 ^F	44502 (F)	(-0.4911, 0.2077, 0.3364)	8.728	111.97	145.69	128.83
P1...P2 ^G	56603 (G)	(0.0177, 0.4134, 0.5864)	8.764	106.37	90.25	98.37
P1...P2 ^H	46603 (H)	(0.4911, 0.4134, .5864)	8.811	125.26	104.53	114.90
P1...P2 ^J	46503 (J)	(-0.4911, 0.4134, 0.1729)	8.926	48.09	109.96	79.02
P1...P1 ^H	46603 (H)	(-1/2, 1/2, 1/2)	8.978	100.62	100.62	100.62
P1...P2 ^J	55504 (J)	(-0.02764, 0.1634, 0.5386)	8.998	145.54	32.29	88.92
P1...P1 ^G	56603 (G)	(0, 1/2, 1/2)	9.030	83.98	83.89	83.89
P2...P2 ^J	46503 (J)	(-1/2, 1/2, 0)	7.411	86.93	86.93	86.93
P1...P1 ^L	55404 (L)	(-0.2675, 0.2500, 0.1251)	7.825	64.66	170.78	117.72
P2...P1 ^E	45502 (E)	(-0.5088, 0.7077, 0.1636)	8.728	145.69	111.97	128.83
P2...P1 ^G	56603 (G)	(-0.0177, 0.5866, 0.4135)	8.764	90.25	106.37	98.37
P2...P1 ^H	46603 (H)	(-0.5088, 0.5866, 0.4135)	8.811	104.53	125.26	114.90
P2...P1 ^I	46503 (I)	(-0.5088, 0.5866, -0.1729)	8.962	109.96	48.09	79.02
P2...P1 ^L	55404 (L)	(-0.2764, 0.3366, 0.0773)	8.998	32.29	145.54	88.92

Table B.6. Table of Symmetry Operations for $\text{NiN}_3(\text{NO})(\text{P}(\text{C}_6\text{H}_5)_3)_2$.

Atom Designator Code (ADC)	Coordinate of Positions	Symbol of Symmetry Operation, s	Atom Designator Code (ADC)	Coordinate of Positions	Symbol of Symmetry Operation, s
55501	x, y, z	A	56503	-x, -y+1, -z	H
55601	x, y, z+1	B	46603	-x-1, -y+1, -z+1	I
55401	x, y, z-1	C	46503	-x-1, -y+1, -z	J
54502	-x, y-1/2, -z+1/2	D	55504	x, -y+1/2, z+1/2	K
45502	-x-1, y+1/2, -z+1/2	E	56504	x, -y+1/2, z+1/2	L
44502	-x-1, y-1/2, -z+1/2	F	55404	x, -y+1/2, z-1/2	M
56603	-x, -y+1, -z+1	G	56404	x, y+1/2, z-1/2	N

Appendix C

Abstracts of Presentations of Portions of This Thesis Work

Portions of the work presented in this thesis were presented at various conferences, including two conferences for which the author received scholarships to cover the full costs of travel and meeting attendance. The abstracts of those two presentations are reproduced in this appendix.

Attendance at the fourth meeting of the Asian Crystallographic Association, AsCA'01, 15-18 November 2001, was supported by a Young Scientist Bursary Award from the conference organizers to cover travel costs to Bangalore, India, and accommodation costs at the meeting. MacScience Co. Ltd. gave a Registration Grant to cover the registration fee.

Attendance at the XIX Congress and General Assembly of the International Union of Crystallography, 6-15 August 2002, was supported by a Young Scientist Bursary Award from the IUCr to cover registration fees, travel costs to Geneva, Switzerland, and accommodation costs at the meeting.

Abstract of Presentation at the 4th Asian Crystallography Association Conference, ASCa'01, Held in Bangalore, India, 15-18 November 2001

X-RAY CRYSTAL STRUCTURE OF TWINNED BROMONITROSYL-BIS(TRIPHENYLPHOSPHINE)NICKEL

Angkana Kiatphichitpong, and *Kenneth J. Haller*, School of Chemistry, Institute of Science, Suranaree University of Technology, 111 University Avenue, Nakhon Ratchasima 30000 Thailand

The title complex was synthesized from the corresponding dibromo complex by reaction with nitrite anion as the source of the nitrosyl ligand. The diffractometer determined unit cell is triclinic containing four molecules of the complex. It was noted that the mosaicity parameter and cell parameters changed as the data reduction proceeded. Solution of the two molecule asymmetric unit was straightforward, but the two molecules appear to be nearly identical. Examination of the intensity data show the systematic condition $0kl$, $k = \text{odd}$ absent, and examination of the cell packing suggests the presence of a glide operation and a screw operation in addition to the inversion center required by the $P-1$ space group, leading to the conclusion that the true space group is $P2_1/c$. Synthetic precession photographs obtained from the frame data clearly show the twinning of the parent lattice giving rise to the apparent triclinic cell.

Crystal data: $C_{36}H_{30}NiNOP_2Br$; $M_r = 693.17$ Daltons; dark purple; 0.09 x 0.16 x 0.30 mm; hexagonal plate; triclinic; $P-1$ (No. 2), $a = 9.6411(1)$, $b = 14.8944(2)$, $c = 22.7806(4)$ Å, $\alpha = 79.5670(5)$ $\beta = 85.9471(5)$ $\gamma = 90.0044(9)$ °, $V = 3208.85(8)$ Å³ $Z = 4$, $\mu = 1.98$ mm⁻¹; $d_{calc} = 1.435$ Mg/m³, $\lambda_{MoK\alpha} = 0.71073$ Å; T = 200 K. Data collection: Nonius KappaCCD; 0.5 mm *ifg* capillary collimator; Oxford Cryosystems LT device; 53796 data collected (triclinic); 18564 unique; 12720 observed.

**Abstract of Presentation at the XIX Congress and General Assembly of
the International Union of Crystallography, Held in Geneva, Switzerland,
6-15 August 2002**

**SUPRAMOLECULAR STRUCTURES OF FOUR-COORDINATE
NICKEL BIS(TRIPHENYLPHOSPHINE) NITROSYL COMPLEXES**

Angkana Kiatphichitpong, and *Kenneth J. Haller*, School of Chemistry, Institute of Science, Suranaree University of Technology, 111 University Avenue, Nakhon Ratchasima 30000 Thailand

The multiple phenyl-phenyl edge-to-face (*ef*) C–H \cdots π attractive interactions of the concerted sextuple phenyl embrace (6PE) give a sum of interaction energy sufficient to make it a dominant supramolecular motif for triphenylphosphine (TPP) complexes (Dance & Scudder, *Chem. Comm.* 1995, 1039). The title complexes with the fourth ligand, X = isothiocyanato, azido, or chloro, while closely related have quite different supramolecular structures.

The primary extended interactions in the isothiocyanato complex are SPE between adjacent TPP occurring in parallel chains alternating; d[P–P] = 7.087 Å, colinearity = 176.9° and d[P–P] = 7.246 Å, colinearity = 173.0° 6PE. Chains are joined by four phenyl ring regions to form layers dominated by *ef* C–H \cdots π interactions. Layers are bound by nitrosyl-phenyl and phenyl-phenyl interactions.

The chloro complex contains a benzene solvate which has one end inserted into the cleft of an Ni(bis-TPP) fragment located on a pseudo 2-fold axis utilizing one complex-to-benzene *ef* and one benzene-to-complex *ef* interaction to each of the TPP ligands. Six additional *ef* interactions form the central region of the cavity and the chloro and nitrosyl ligands of another molecule cap the cavity. Thus, the benzene molecule, able to form considerably more C–H \cdots π interactions, becomes the major supramolecular link in the structure.

The shortest intermolecular P–P distances in the azido complex are 7.411 Å and 7.825 Å with colinearities of 86.9° and 117.7°, thus not 6PE. The strongest nonbond is a 2.493 Å *intramolecular* C–H \cdots N interaction to the lone pair on the N bonded to Ni destroying the pseudo three-fold symmetry of one TPP, while another strong *intramolecular* C–H \cdots N interaction to the azido ligand pi cloud involves the other TPP, thus disrupting both possibilities to form 6PEs. The azido ligand is also involved in intermolecular nonbonded interactions. Thus, as the strongest hydrogen bond acceptor, the azido ligand becomes the most important determiner of the supramolecular structure.

Presented in:

Topic: Crystallography of Organometallic, Coordination and Main Group Compounds
Subtopic: Supramolecular Coordination Complexes

Curriculum Vitae

ANGKANA KIATPHICHITPONG

Born: June 20, 1967

Citizenship: Thailand

Marital Status: Single

Education

1991 B.Sc., Chemistry
Ramkhumheang University, Bangkok, Thailand

Experience

1991-1998 Quality Control Chemist
Samukhee Cement, Ltd., Pak Chong, Thailand

Presentations

"Synthesis and Characterization of Four-Coordinate Nickel Diphosphine Complexes", (with Kenneth J. Haller), 26th Congress on Science and Technology of Thailand, Bangkok, Thailand: Abstract 18-I2P-12, 2000.

"Crystal Supramolecularity: Concerted Phenyl Embraces in Four-Coordinate Nickel Nitrosyl Bis-Triphenylphosphine Complexes", (with Kenneth J. Haller), 27th Congress on Science and Technology of Thailand, Hat Yai, Thailand, 2001.

"Synthesis and Characterization of Four-Coordinate Nickel Nitrosyl Bis-Triphenylphosphine Halide Complexes", (with Sasipron Kunapongkiti, Kittipong Chainok & Kenneth J. Haller), 27th Congress on Science and Technology of Thailand, Hat Yai, Thailand, 2001.

"X-Ray Crystal Structure of Twinned Bromonitrosyl-bis(triphenylphosphine) Nickel", (with Kenneth J. Haller), AsCA'01, 4th Asian Crystallographic Association Meeting, Bangalore, India: Abstract A4-5, 2001.

"Supramolecular Structures of Four-Coordinate Nickel Bis(Triphenylphosphine) Complexes" (with Kenneth J. Haller), 3rd National Graduate Student Symposium, Suranaree University of Technology, Nakhon Ratchasima, 2002.

"Supramolecular Structures of Four-Coordinate Nickel Bis(triphenylphosphine) Nitrosyl Complexes" (with Kenneth J. Haller), XIX Congress and General Assembly of the International Union of Crystallography, Geneva, Switzerland, 2002.

Scholarships and Honors:

AsCA Student Travel Scholarship to present paper at AsCA'01, Bangalore, India

MacScience Registration Scholarship Grant for AsCA'01, Bangalore, India

IUCr Young Scientist Grant to present paper at IUCr XIX, Geneva, Switzerland